

Scalable simulation-based inference for implicitly defined models using a metamodel for Monte Carlo log-likelihood estimator

Joonha Park

Department of Mathematics, University of Kansas, Lawrence, KS 66045 USA
(email: j.park@ku.edu)

Abstract

Models implicitly defined through a random simulator of a process have become widely used in scientific and industrial applications in recent years. However, simulation-based inference methods for such implicit models, like approximate Bayesian computation (ABC), often scale poorly as data size increases. We develop a scalable inference method for implicitly defined models using a metamodel for the Monte Carlo log-likelihood estimator derived from simulations. This metamodel characterizes both statistical and simulation-based randomness in the distribution of the log-likelihood estimator across different parameter values. Our metamodel-based method quantifies uncertainty in parameter estimation in a principled manner, leveraging the local asymptotic normality of the mean function of the log-likelihood estimator. We apply this method to construct accurate confidence intervals for parameters of partially observed Markov process models where the Monte Carlo log-likelihood estimator is obtained using the bootstrap particle filter. We numerically demonstrate that our method enables accurate and highly scalable parameter inference across several examples, including a mechanistic compartment model for infectious diseases.

keywords: parameter inference, simulation-based inference, implicitly defined model, Monte Carlo methods, particle filter

1 Introduction

A model is said to be *implicitly defined* if it is defined using a random simulator of the underlying process [12]. If the density function of an implicitly defined process cannot be evaluated, traditional likelihood-based parameter inference is generally impossible, because the likelihood function is not analytically tractable. In this paper, we develop a scalable, simulation-based parameter inference method for partially observed, implicitly defined models. Simulation models are widely used for a variety of industrial and scientific applications, precipitated by recent advances in the digital twin technology [24, 33, 34, 26].

We consider a collection of observations $Y_{1:n}$ that are conditionally independent given a realization X of the random process. For example, $Y_{1:n}$ may be noisy or partial observations of a Markov process $X_{1:n}$, where Y_i are conditionally independent observation of X_i , $i \in 1:n$. Generally, we assume that the implicitly defined process X is parameterized by $\theta \in \Theta$. If we denote the measurement density of the observed data $y = y_{1:n}$ given $X = x$ by $g(y|x; \theta)$, the likelihood is given by

$$L(\theta; y) = \int g(y|x; \theta) dP_\theta(x). \quad (1)$$

Here θ parametrizes both the law of the latent process and the measurement process, but it may consist of two separate components each governing only one of the processes. In principle, the likelihood (1) may be estimated by

$$\hat{L}(\theta; y) = \frac{1}{J} \sum_{j=1}^J g(y|X_j(\theta); \theta) \quad (2)$$

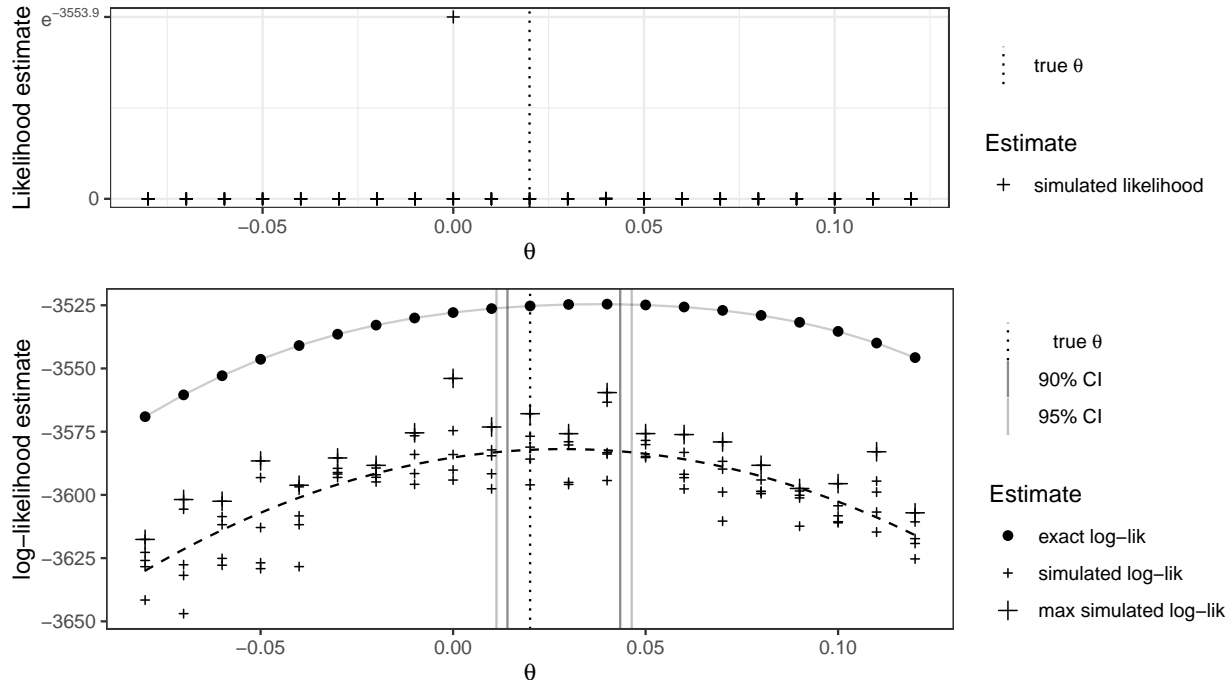


Figure 1: The top panel shows the likelihood estimates obtained by running the particle filter five times for each θ value on a natural (non-logarithmic) scale. The bottom panel shows the log of those likelihood estimates, marked by ‘+’ symbols. The maximum among the five values for each θ is indicated by a larger ‘+’ symbol. The dashed curve shows the fitted quadratic polynomial. The exact log-likelihoods computed using the Kalman filter are indicated by ‘•’. The dotted vertical line indicates the true parameter value, $\theta = 0.02$, and the gray vertical lines indicate the constructed 90% and 95% confidence intervals.

where $X_j(\theta)$, $j \in 1 : J$, are independent simulations of P_θ . Although the Monte Carlo likelihood estimator (2) is unbiased for $L(\theta; y)$, its variance grows exponentially with an increasing size of the data $y_{1:n}$. For partially observed Markov process (POMP) models, an unbiased estimator of the likelihood with substantially smaller variance than that of (2) can be obtained by running the particle filter [8, 11, 15]. In particular, when the latent Markov process is implicitly defined via a simulator, an unbiased Monte Carlo likelihood estimator can be obtained using the bootstrap particle filter [18, 19]. However, the variance of this estimator still scales exponentially with increasing n [9]. The exponentially large Monte Carlo variance in the likelihood estimator is typically realized by a very small probability of attaining relatively extremely large values. The highly skewed distribution of the likelihood estimator implies that inference based on $\hat{L}(\theta; y)$ faces a great amount of Monte Carlo variability. This phenomenon is illustrated by the top panel of Figure 1, which displays the likelihood estimates independently obtained five times for each θ value for a certain POMP model given by Example 1 below.

In order to enable simulation-based inference that is scalable to large data, methods that involve approximation of the \log -likelihood function have been developed. These methods utilize the fact that the logarithm of Monte Carlo likelihood estimators often have distributions with manageable variance and skewness. Diggle and Gratton [12] considered parameter estimation where independent and identically distributed (iid) draws from an implicit model $X_i \sim P_\theta$, $i \in 1 : n$, are observed without noise. They proposed a method where the log-likelihood function estimated using simulations and kernel density estimation is maximized by a stochastic optimization procedure such as the Nelder-Mead algorithm [27]. However, Diggle and Gratton [12] only provided a heuristic for estimating the parameter uncertainty, for situations where the Monte Carlo error is negligibly small compared to the statistical error. Such precise estimation of the log-likelihood function using a kernel method may be possible when the observations are iid and low-dimensional, but it is generally impossible for dependent or moderately high dimensional observations.

Ionides et al. [20] developed a simulation-based inference method for partially observed, implicit models producing dependent observations. They considered estimating the log-likelihood function using the log of the Monte Carlo likelihood estimates such as those obtained by the bootstrap particle filter. Both Ionides et al. [20] and the current paper consider situations where the random error in the Monte Carlo log-likelihood estimator is not small compared to the statistical error. Ionides et al. [20] used a metamodel that locally approximates the log-likelihood function with a quadratic polynomial, justified by the local asymptotic normality (LAN) of the log-likelihood function [25, 35]. Local or global metamodels are widely used for simulation-based optimization in response surface methodology [3]. Ionides et al. [20] constructed profile confidence intervals by approximating the uncertainty in parameter estimation by the sum of the Monte Carlo variance due to random simulations and the statistical variance derived from a standard asymptotic theory for maximum likelihood estimation. The Monte Carlo variance was approximately estimated by a quadratic regression and the use of the delta method. However, Ionides et al. [20] overlooked the fact that, in general, the log-likelihood function $\ell(\theta)$ and the mean function of the Monte Carlo log-likelihood estimator $\mu(\theta)$ have different curvatures and distinct statistical properties due to data randomness. This can result in misquantified uncertainty, further increasing the inference bias beyond that introduced by the delta method approximation.

In the current paper, we refine the metamodel-based uncertainty quantification approach by Ionides et al. [20]. We develop a local asymptotic normality (LAN) theory for the mean function $\mu(\theta; Y)$ of the log-likelihood estimator. This LAN property forms a basis for our metamodel describing the statistical properties of $\mu(\theta; Y)$. Our use of a carefully characterized metamodel reduces the biases in the method by Ionides et al. [20], which incorrectly relies on the observed Fisher information to quantify statistical error. In contrast, we use the observed data to quantify statistical uncertainty, assuming that the observations $y_{1:n}$ can be divided into subsets that are nearly independent of each other. This assumption is often satisfied by stochastic processes with reasonable mixing properties.

We illustrate our method through the following example.

Example 1. Consider a multivariate autoregressive process with partial observations Y_i :

$$X_i = AX_{i-1} + v_i, \quad Y_i = X_i + e_i, \quad i = 1 : 200.$$

Here $X_i, Y_i \in \mathbb{R}^{10}$, $A \in \mathbb{R}^{10 \times 10}$, $v_i \stackrel{iid}{\sim} \mathcal{N}(0, I_{10})$, and $e_i \stackrel{iid}{\sim} \mathcal{N}(0, I_{10})$. The matrix A has diagonal entries all equal to -0.3 and off-diagonal entries all equal to θ . We generate an observation sequence $y_{1:200}$ at $\theta = 0.02$. The bootstrap particle filter is run with two hundred particles five times for each parameter value $\theta \in \{-0.08, -0.07, \dots, 0.12\}$. We will refer to an estimate of the log-likelihood that is obtained through simulations as a *simulated log-likelihood*.

Figure 1 shows five simulated log-likelihoods for each θ , denoted by $\ell_k^S(\theta)$, $k \in 1 : 5$. For comparison, the exact log-likelihood for each θ is shown, obtained by running the Kalman filter [21].

We employ a metamodel in which simulated log-likelihoods are assumed to be approximately normally distributed with a locally quadratic mean function $\mu(\theta; y_{1:n})$. The function $\mu(\theta; y_{1:n})$ is estimated by fitting a quadratic polynomial through the simulated log-likelihoods. The statistical properties of $\mu(\theta; Y_{1:n})$ where the observations $Y_{1:n}$ are generated under a certain parameter value are characterized by the local asymptotic normality (LAN) of $\mu(\theta; Y_{1:n})$ (see Section 2.2 for details.) A variance parameter in the LAN statement for $\mu(\theta; Y_{1:n})$ is estimated by assuming approximate independence of contiguous subsets of $Y_{1:n}$ (Section 3.3.) Confidence intervals are constructed using the metamodel for the random function $\mu(\theta; Y_{1:n})$, incorporating both sources of randomness originating from the observations and the simulations (Section 4.) Our theory and method are developed generally for multiple parameters, unlike the approach proposed by Ionides et al. [20], which focuses on one-dimensional profile likelihoods.

Relative to other methods for simulation-based inference, our approach is highly scalable with increasing data size. Cranmer et al. [10] provide a survey of traditional and recent simulation-based inference algorithms. Approximate Bayesian computation (ABC) estimates the likelihood using the proportion of simulations in close proximity of the observed data [5]. Traditional inference methods such as ABC experience the curse of dimensionality similar to that affecting kernel density estimation in high dimensional spaces. This issue is often addressed by using summary statistics, at the expense of introducing a bias and a loss of efficiency due to the information reduction [31]. If partial observations of the implicitly defined process are available

and the density of the observations given the latent states is analytically tractable, pseudo-marginal Markov chain Monte Carlo (MCMC) methods can enable exact Bayesian inference by utilizing unbiased Monte Carlo likelihood estimators [4, 2, 1]. However, these methods are also affected by the curse of dimensionality, which is manifested by an exponentially scaling Monte Carlo variance and thus a poorly scaling sampling efficiency [30, 16].

Recent advances in machine learning have enabled training a surrogate model for the distribution of observations Y through neural density estimation techniques such as normalizing flows [13, 14, 28]. We note that these surrogate models, which approximate the distribution of Y for each given θ , differ from the metamodels we consider, which describe the log-likelihood $\ell(\theta; y)$ as a function of θ for given y . These machine learning techniques have the advantage that, once a surrogate model is trained using simulations, inference using the approximate likelihoods is straightforward. However, training a high-fidelity surrogate model for a high dimensional observation distribution requires a large number of simulations and may still involve substantial error in some parts of the observation space. Moreover, quantifying the uncertainty associated with the trained surrogate model is often challenging.

Our metamodel-based inference approach offers several advantages compared to these machine-learning-based methods. First, since Monte Carlo log-likelihood estimators often have distributions that scale linearly rather than exponentially with the size of the data $y = y_{1:n}$, our method is scalable to models that produce large amounts of data. Second, it enjoys a favorable sampling efficiency because the metamodel enables pooling the information across θ values. Third, it offers a principled method for uncertainty quantification, since the characterization of the variation in $\mu(\theta; Y)$ by the LAN property is consistent. We note that recent machine learning techniques may be combined with the metamodel-based inference framework we propose in this work by regarding the logarithm of the approximate likelihood derived from the trained surrogate model as a Monte Carlo log-likelihood estimator. However, we do not delve into this in the current paper.

The rest of the paper is organized as follows. Section 2 lays a theoretical basis for our scalable simulation-based inference approach. We develop a local asymptotic normality (LAN) property for $\mu(\theta; Y)$ and set up a simulation metamodel. Section 3 concerns fitting the metamodel to the simulated log-likelihoods via quadratic regression. Section 4 develops a procedure for uncertainty quantification and construction of confidence intervals, taking into account both simulation randomness and observation randomness. Section 5 provides numerical results showing the accuracy of our simulation-based inference method using several examples, including a mechanistic model for the population dynamics of an infectious disease. In Section 6, we numerically compare the scalability of our method and that of a pseudo-marginal MCMC method. Section 7 introduces two automatic tuning algorithms that enhance the applicability of our method. One algorithm automatically adjusts the weights associated with simulations to control the bias introduced by the quadratic approximation while maintaining high estimation efficiency. The other algorithm identifies approximately optimal points for subsequent simulations. Section 8 concludes with discussion.

2 Simulation-based inference

In this section, we define a simulation metamodel and relevant quantities. Section 2.1 outlines the difference between traditional likelihood-based inference and our metamodel-based inference. Inference using a metamodel involves estimation of what we call a *simulation-based proxy*, which is the maximizer of the mean function of the log-likelihood estimator averaged over the data distribution. Section 2.2 develops the local asymptotic normality (LAN) for the mean function of the log-likelihood estimator. Section 2.3 defines a metamodel for the log-likelihood estimator, based on the LAN property. Section 2.4 discusses application to partially observed Markov process (POMP) models in the case where the simulation-based log-likelihood estimator is obtained using the bootstrap particle filter. Section 2.5 discusses the bias introduced by a simulation metamodel.

2.1 Simulation-based proxy

We denote the marginal density of the observation $Y = y$ under parameter θ by

$$p_\theta^Y(y) = \frac{dP_\theta^Y}{dy} = \int g(y|x; \theta) dP_\theta(x).$$

If we simulate the underlying process and obtain a draw X from P_θ , we may consider $\log g(y|X; \theta)$ as an estimate of the log-likelihood $\ell(\theta; y) = \log p_\theta^Y(y)$. We will refer to an estimate of the log-likelihood obtained via simulation of the underlying process as a *simulated log-likelihood*. The simulated log-likelihood will be denoted by $\ell^S(\theta; y)$ or $\ell^S(\theta)$, or in some cases by $\ell^S(X, y)$ when emphasizing the fact that it is a function of the simulated draw X . We define the *expected simulated log-likelihood* as

$$\mu(\theta; y) := \mathbb{E} \ell^S(\theta; y) = \int \ell^S(x, y) dP_\theta(x).$$

If the simulated log-likelihood $\ell^S(\theta; y)$ is given by the logarithm of an unbiased likelihood estimator $\hat{L}(\theta; y)$, such as $g(y|X; \theta)$ where X is a draw from P_θ , then $\mu(\theta; y)$ is less than or equal to the exact log-likelihood $\ell(\theta; y)$ due to Jensen's inequality:

$$\mu(\theta; y) = \mathbb{E} \ell^S(\theta; y) \leq \log \mathbb{E} \hat{L}(\theta; y) = \ell(\theta; y).$$

The Jensen bias can be written as

$$\ell(\theta; y) - \mu(\theta; y) = \sum_{j \geq 2} \frac{\kappa_j(\theta; y)}{j!} \quad (3)$$

where $\kappa_j(\theta; y)$ is the j -th order cumulant of the distribution of the simulated log-likelihood $\ell^S(\theta; y)$ for given y (see the supplementary text, Section S3.1 for more details.) Since the Jensen bias depends on higher-order cumulants of $\ell^S(\theta; y)$, or the tail distribution of $\ell^S(\theta; y)$, estimating this bias involves high Monte Carlo variability.

For a given set of observations $y = y_{1:n}$, the maximizer of the expected simulated log-likelihood $\mu(\theta; y)$ will be referred to as the *maximum expected simulated log-likelihood estimator (MESLE)*.

Definition 1 (MESLE). Given the observations $y_{1:n}$, the maximum expected simulated log-likelihood estimate (MESLE) is defined as

$$\theta_{MESLE}(y_{1:n}) := \arg \max_{\theta} \mu(\theta; y_{1:n}). \quad (4)$$

The MESLE substitutes the role of the the maximum likelihood estimator (MLE) for traditional likelihood-based inference. Since $\mu(\theta; y)$ is not known analytically and is instead estimated through the simulated log-likelihoods, the MESLE must also be estimated via simulations. If the Jensen bias $\ell(\theta; y) - \mu(\theta; y)$ varies as a function of θ , the MESLE may differ from the MLE.

If the observed data Y are generated under θ_0 , the *data-averaged expected simulated log-likelihood* is defined as

$$U(\theta_0, \theta) := \mathbb{E}_{\theta_0} \mu(\theta; Y) = \int \mu(\theta; y) p_{\theta_0}^Y(y) dy. \quad (5)$$

The parameter value θ that maximizes $U(\theta_0, \theta)$ will be referred to as the *simulation-based proxy* for θ_0 .

Definition 2 (Simulation-based proxy). The *simulation-based proxy* for θ_0 , denoted by $\mathcal{R}(\theta_0)$, is defined as the maximizer of the data-averaged expected simulated log-likelihood $U(\theta_0, \theta)$:

$$\mathcal{R}(\theta_0) = \arg \max_{\theta} U(\theta_0, \theta).$$

For simplicity, $\mathcal{R}(\theta_0)$ will sometimes be denoted by θ_* .

The MESLE converges in probability to the simulation-based proxy as the data size increases, under certain regularity conditions for M-estimation [35].

If the Jensen bias $\ell(\theta; Y_{1:n}) - \mu(\theta; Y_{1:n})$ is constant as a function of θ for every $Y_{1:n}$, then $U(\theta_0, \theta)$ will have a constant difference with respect to $\mathbb{E}_{\theta_0} \ell(\theta; Y)$, which is maximized at $\theta = \theta_0$. Thus the inference bias, $\|\mathcal{R}(\theta_0) - \theta_0\|$, will be equal to zero. However, $\mathcal{R}(\theta_0)$ can be different from θ_0 in general (see supplementary Section S1.1 for concrete examples.) Any simulation-based inference method that estimates a response surface for $\ell(\theta)$ using a metamodel inherently involves the possibility of nonzero inference bias, although the method may be scalable. In contrast, methods like ABC or pseudo-marginal MCMC, which estimate the likelihood $L(\theta)$ separately for each θ without relying on a metamodel, may be asymptotically exact as the number of simulation increases but are not scalable. When the data size is large, the latter class of methods is unlikely to yield smaller inference errors than the methods that use a metamodel. A numerical comparison between our method and a pseudo-marginal MCMC method, presented in Section 6, supports this.

2.2 Local asymptotic normality for $\mu(\theta; y_{1:n})$

We develop the local asymptotic normality (LAN) for the mean function $\mu(\theta; y_{1:n})$ of the simulated log-likelihood $\ell^S(\theta; y_{1:n})$ under several assumptions. First, we assume that $\ell^S(\theta; y_{1:n})$ can be expressed as the sum of log-likelihood estimates for individual observation pieces y_i , $i \in 1:n$.

Assumption 1. *A log-likelihood estimator $\ell_i^S(\theta; y_i)$ is available for each observation y_i , $i \in 1:n$. These individual simulated log-likelihoods sum to the simulated log-likelihood for the entire data $y_{1:n}$:*

$$\ell^S(\theta; y_{1:n}) = \sum_{i=1}^n \ell_i^S(\theta; y_i).$$

For example, Assumption 1 is satisfied if y_i , $i \in 1:n$, are conditionally independent given X with measurement density $g(y_{1:n}|X) = \prod_{i=1}^n g_i(y_i|X)$ and if the simulated log-likelihood is given by

$$\ell^S(\theta; y_{1:n}) = \log g(y_{1:n}|X) = \sum_{i=1}^n \log g_i(y_i|X), \quad X \sim P_\theta,$$

where we let $\ell_i^S(\theta; y_i) = \log g_i(y_i|X)$. Assumption 1 is also satisfied when the simulated log-likelihood is obtained through the bootstrap particle filter for POMP models. See Section 2.4 for details. Under Assumption 1, we let $\mu_i(\theta; y_i) = \mathbb{E} \ell_i^S(\theta; y_i)$ such that expected simulated log-likelihood can be expressed as

$$\mu(\theta; y_{1:n}) = \sum_{i=1}^n \mu_i(\theta; y_i).$$

We make the following additional assumptions. Recall that when the true parameter is θ_0 , the simulation-based proxy is denoted by $\mathcal{R}(\theta_0) = \theta_*$.

Assumption 2. *The parameter space Θ is a subset of \mathbb{R}^d , and the individual expected simulated log-likelihood $\mu_i(\theta; y_i)$ is three times continuously differentiable with respect to $\theta = (\theta_{(1)}, \dots, \theta_{(d)})$ for every y_i , $i \in 1:n$.*

Assumption 3. *There exists a positive definite matrix $K_1(\theta_0) \in \mathbb{R}^{d \times d}$ such that as $n \rightarrow \infty$,*

$$\frac{1}{\sqrt{n}} \sum_{i=1}^n \frac{\partial \mu_i}{\partial \theta}(\theta_*; Y_i) \xrightarrow{Y_{1:n} \sim P_{\theta_0}^Y} \mathcal{N}(0, K_1(\theta_0)),$$

where \Rightarrow indicates convergence in distribution.

Assumption 4. *There exists a positive definite matrix $K_2(\theta_0) \in \mathbb{R}^{d \times d}$ such that*

$$\frac{1}{n} \sum_{i=1}^n \frac{\partial^2 \mu_i}{\partial \theta^2}(\theta_*; Y_i) \xrightarrow{Y_{1:n} \sim P_{\theta_0}^Y} -K_2(\theta_0),$$

where $\xrightarrow{i.P.}$ indicates convergence in probability.

Assumption 5. *There exists an open ball B_0 containing θ_* and a constant C such that for every i ,*

$$\mathbb{E} \sup_{\theta \in B_0} \max_{k_1, k_2, k_3 \in 1:d} \left\| \frac{\partial^3 \mu_i}{\partial \theta_{(k_1)} \partial \theta_{(k_2)} \partial \theta_{(k_3)}}(\theta; Y_i) \right\| \leq C.$$

Assumptions 3 and 4 are satisfied under mild conditions when $\ell_i^S(\theta; Y_i)$ are marginally independent, due to the central limit theorem and the law of large numbers, respectively. The observations $Y_{1:n}$ are marginally independent, for example, when the components of $X = (X_1, \dots, X_n)$ are independent and Y_i only depends on X_i , for $i \in 1:n$. However, Assumptions 3 and 4 may still be satisfied for marginally dependent Y_i if X satisfies certain mixing conditions, as discussed in Supplementary Section S2.1.

Under Assumptions 1-5, we obtain the following LAN result for $\mu(\theta; Y_{1:n})$.

Algorithm 1 Simulation-based parameter inference using a metamodel for $\ell^S(\theta; y)$

- 1: **Input:** observations $y_{1:n} = (y_1, \dots, y_n)$; collection of parameter values $\{\theta_m; m \in 1:M\}$ at which the process X is simulated to obtain log-likelihood estimates
 - 2: **Output:** p-values for hypothesis tests on the simulation-based proxy θ_*
 - 3: For each $m \in 1:M$, simulate X under P_{θ_m} to obtain a simulated log-likelihood $\ell^S(\theta_m; y_{1:n})$
 - 4: Fit a quadratic polynomial to the points $\{(\theta_m, \ell^S(\theta_m, y_{1:n})); m \in 1:M\}$ with weights w_m
 - 5: Estimate $K_1(\theta_0)$ as described in Algorithm 3
 - 6: Carry out a metamodel likelihood ratio test as described in Section 4 using the fitted quadratic polynomial and the estimate \hat{K}_1
-

Proposition 1 (Local asymptotic normality (LAN) for $\mu(\theta; Y_{1:n})$). *Suppose that Assumptions 1-5 hold where $Y_{1:n} \sim P_{\theta_0}^Y$. Let*

$$S_n := \frac{1}{\sqrt{n}} \sum_{i=1}^n \frac{\partial \mu_i}{\partial \theta}(\theta_*; Y_i).$$

Then S_n converges in distribution to $\mathcal{N}(0, K_1(\theta_0))$ and

$$\mu(\theta_* + \frac{t}{\sqrt{n}}; Y_{1:n}) - \mu(\theta_*; Y_{1:n}) - S_n^\top t + \frac{1}{2} t^\top K_2(\theta_0) t \quad (6)$$

converges in probability to zero uniformly for $t \in B$ as $n \rightarrow \infty$ for every bounded set B containing 0.

The proof of Proposition 1 is given in the supplementary text, Section S2.2. Proposition 1 can be compared to the original LAN for the log-likelihood function $\ell(\theta)$, which states that there exists a sequence of random variables $\{S'_n; n \geq 1\}$ that converges in probability to $\mathcal{N}(0, \mathcal{I}(\theta_0))$ and such that

$$\ell(\theta_0 + \frac{t}{\sqrt{n}}; Y_{1:n}) - \ell(\theta_0; Y_{1:n}) = S_n'^\top t - \frac{1}{2} t^\top \mathcal{I}(\theta_0) t + o_p(1)$$

as $n \rightarrow \infty$ for every t [25]. Iid observations $Y_{1:n}$ satisfy this LAN property under certain regularity conditions with $\mathcal{I}(\theta_0)$ equal to the Fisher information [35]. We summarize the differences between the original LAN and Proposition 1 as follows:

1. Proposition 1 suggests an asymptotically quadratic approximation for the expected simulated log-likelihood $\mu(\theta; Y_{1:n})$, not for the log-likelihood function $\ell(\theta; Y_{1:n})$.
2. Whereas the original LAN for $\ell(\theta; Y_{1:n})$ has both the scaled asymptotic negative curvature and the asymptotic covariance for the random slope equal to the Fisher information, that is,

$$\lim_{n \rightarrow \infty} -\mathbb{E} \frac{1}{n} \frac{\partial^2 \ell(\theta; Y_{1:n})}{\partial \theta^2} = \lim_{n \rightarrow \infty} \frac{1}{n} \text{Var} \left(\frac{\partial \ell(\theta; Y_{1:n})}{\partial \theta} \right) = \mathcal{I}(\theta_0),$$

the LAN for $\mu(\theta; Y_{1:n})$ has distinct values of $K_1(\theta_0)$ and $K_2(\theta_0)$.

3. Proposition 1 considers a local approximation around the simulation-based proxy $\theta_* = \mathcal{R}(\theta_0)$.

Ionides et al. [20] overlooked these differences, thereby introducing bias and misspecifying uncertainty. This paper properly addresses these issues by using a metamodel constructed based on Proposition 1.

2.3 Simulation metamodel

Proposition 1 states the local asymptotic property for $\mu(\theta; Y_{1:n}) = \mathbb{E} \ell^S(\theta; Y_{1:n})$ due to the randomness in $Y_{1:n}$ under $P_{\theta_0}^Y$. We will additionally assume that for given observations $y_{1:n}$, the simulated log-likelihood $\ell^S(\theta; y_{1:n})$ is approximately normally distributed. The approximate normality of $\ell^S(\theta; y_{1:n})$ can be obtained as a consequence of the central limit theorem when $\ell_i^S(\theta; y_i)$ are independent or weakly dependent. Mixing conditions similar to those discussed in Section S2.1 justifying Assumption 3 can also justify the asymptotic normality of $\ell^S(\theta; y_{1:n})$.

Assumption 6. For a given sequence of observations $\{y_i; i \geq 1\}$, the simulated log-likelihoods $\ell^S(\theta; y_{1:n})$ satisfy

$$\frac{\ell^S(\theta; y_{1:n}) - \mu(\theta; y_{1:n})}{\sigma(\theta; y_{1:n})} \Rightarrow \mathcal{N}(0, 1)$$

for every θ in a neighborhood of θ_* where $\sigma^2(\theta; y_{1:n}) = \text{Var}\{\ell^S(\theta; y_{1:n})\}$.

Assuming that the LAN for $\mu(\theta; Y_{1:n})$ and Assumption 6 hold, the simulated log-likelihood $\ell^S(\theta; y_{1:n})$ is approximately normally distributed with a quadratic mean function. We formulate these facts as our metamodel, consisting of two parts. The first part states the normality of $\ell^S(\theta; y_{1:n})$ and the quadraticity of $\mu(\theta; y_{1:n})$ for given observations $y_{1:n}$. This will be referred to as the *conditional simulation metamodel* given the data.

Definition 3 (Conditional simulation metamodel given data). Given observations $y_{1:n}$, the simulated log-likelihood is distributed as

$$\ell^S(\theta; y_{1:n}) \sim \mathcal{N}\left\{a + b^\top \theta + \theta^\top c \theta, \frac{\sigma^2(y_{1:n})}{w(\theta)}\right\} \quad (7)$$

for some $a \in \mathbb{R}$, $b \in \mathbb{R}^d$, $c \in \mathbb{R}^{d \times d}$, $\sigma^2 \in \mathbb{R}$, and a positive function $w(\theta)$, for all θ in a neighborhood of θ_* .

Here $w(\theta)$ represents the precision of the simulated log-likelihood $\ell^S(\theta; y_{1:n})$, often signifying the amount of Monte Carlo efforts to obtain $\ell^S(\theta; y_{1:n})$. For instance, the log of the likelihood estimator obtained through the particle filter has a variance that scales inversely proportional to the number of particles used [7]. In this case, $w(\theta)$ is equal to the number of particles. Section 2.4 discusses more on the use of the particle filter for POMP models. Thus we assume that $w(\theta)$ is known at each θ where simulations are performed, whereas $\sigma^2(y_{1:n})$ is an unknown quantity that will be estimated via simulations.

The second part of our metamodel describes the statistical properties of the coefficients of the quadratic mean function $\mu(\theta; Y_i)$ explained by the LAN. Comparing (6) and (7), we see that

$$\begin{aligned} & \mu\left(\theta_* + \frac{t}{\sqrt{n}}; Y_{1:n}\right) - \mu(\theta_*; Y_{1:n}) \\ &= b^\top \left(\theta_* + \frac{t}{\sqrt{n}}\right) + \left(\theta_* + \frac{t}{\sqrt{n}}\right)^\top c \left(\theta_* + \frac{t}{\sqrt{n}}\right) - b^\top \theta_* - \theta_*^\top c \theta_* \\ &= b^\top \frac{t}{\sqrt{n}} + \frac{1}{n} t^\top c t + \frac{2}{\sqrt{n}} \theta_*^\top c t = S_n^\top t - \frac{1}{2} t^\top K_2(\theta_0) t + o_p(1) \end{aligned}$$

as $n \rightarrow \infty$ under $Y_{1:n} \sim P_{\theta_0}^Y$. Thus we have

$$\begin{aligned} \frac{1}{n} c &= -\frac{1}{2} K_2(\theta_0) + o_p(1), \\ \frac{1}{\sqrt{n}} b &= S_n - \frac{2}{\sqrt{n}} c \theta_* + o_p(1) = S_n + \sqrt{n} K_2(\theta_0) \theta_* + o_p(1). \end{aligned} \quad (8)$$

An asymptotic approximation given by (8) will be referred to as a *marginal simulation metamodel*.

Definition 4 (Marginal simulation metamodel). The linear and quadratic coefficients b and c for the mean function of the conditional metamodel (Definition 3) are given by

$$c(Y_{1:n}) = -\frac{n}{2} K_2(\theta_0), \quad b(Y_{1:n}) \sim \mathcal{N}\{n K_2(\theta_0) \theta_*, n K_1(\theta_0)\}, \quad (9)$$

where $Y_{1:n} \sim P_{\theta_0}^Y$.

We note that we do not make any assumption about the distribution of the constant term $a(Y_{1:n})$. Since the LAN property concerns the relative difference $\mu(\theta + \frac{t}{\sqrt{n}}; Y_{1:n}) - \mu(\theta; Y_{1:n})$, it enables estimation of $\mathcal{R}(\theta_0)$ without any knowledge on the constant term.

Algorithm 1 gives an outline of our simulation-based parameter inference method using the metamodel. For inference, we simulate the process X under M parameter values θ_m , $m \in 1 : M$, and obtain simulated log-likelihoods $\ell^S(\theta_m; y_{1:n})$. The metamodel parameters a , b , c , and σ^2 can be estimated by fitting a quadratic

polynomial to the points $\{(\theta_m, \ell^S(\theta_m; y_{1:n})); m \in 1:M\}$ through standard weighted regression with weights $w(\theta_m)$. If the regression estimates are given by $(\hat{a}, \hat{b}, \hat{c})$, we obtain a point estimate for the MESLE by

$$\arg \max_{\theta} \hat{a} + \hat{b}^\top \theta + \theta^\top \hat{c} \theta = -\frac{1}{2} \hat{c}^{-1} \hat{b}.$$

We note that the metamodel parameters (a, b, c) and σ^2 may not be estimated unless $M \geq \frac{d(d+1)}{2} + d + 1$ where d is the dimension of the parameter vector.

We remark on the appropriate number of simulations M . In order for the MESLE to be identifiable, the information on the location of θ_* given by the curvature of the quadratic mean function in (7) should be at least comparable to the uncertainty in the estimated mean function. This condition can be approximately stated as

$$(\delta\theta)^\top c(y_{1:n})(\delta\theta) \gtrsim \frac{\sigma(y_{1:n})}{\sqrt{M}}, \quad (10)$$

where $\delta\theta$ is the half-width of the window of parameter values $\{\theta_1, \dots, \theta_M\}$ in which the simulations are carried out. Since $c(y_{1:n}) = -\frac{n}{2} K_2(\theta_0)$ often scales as $\mathcal{O}(n)$ and $\sigma(y_{1:n}) = \text{Var}^{1/2}\{\ell^S(\theta; y_{1:n})\}$ as $\mathcal{O}(\sqrt{n})$, Equation (10) implies that θ_{MESLE} can be estimated at a scale $\|\delta\theta\| = \mathcal{O}(n^{-1/2})$ that is comparable to the statistical uncertainty $\|\theta_{MESLE}(y_{1:n}) - \theta_*\| = \mathcal{O}(n^{-1/2})$ provided that $M \gtrsim \mathcal{O}(n)$. If $M \ll n$, the simulation-based uncertainty swamps the statistical uncertainty.

On the other hand, in order for the quadratic approximation of $\mu(\theta; y_{1:n})$ to be valid on the given interval, the third order term in the Taylor expansion of $\mu(\theta; y_{1:n})$ should be negligible relative to the simulation-based uncertainty of order $\mathcal{O}(\sigma(y_{1:n}) \cdot M^{-1/2}) = \mathcal{O}(n^{1/2} M^{-1/2})$. Since the third order term scales as $\mathcal{O}(n \cdot \|\delta\theta\|^3)$, the quadratic approximation is valid at a scale $\|\delta\theta\| = \mathcal{O}(n^{-1/2})$ if $\mathcal{O}(n \cdot \|\delta\theta\|^3) = \mathcal{O}(n^{-1/2}) \ll \mathcal{O}(n^{1/2} M^{-1/2})$, or $M \ll \mathcal{O}(n^2)$. In Section 7.1, we introduce an algorithm that automatically reduces the weights of simulations performed at points far from the estimated parameter, ensuring that the cubic term in the approximation is statistically insignificant and maintaining the validity of the LAN approximation.

2.4 Application to partially observed Markov processes (POMPs)

The particle filter is a class of recursive Monte Carlo algorithms for making inference for hidden Markov models. The bootstrap particle filter runs by simulating the latent Markov process successively from one observation time to the next, without evaluating the Markov transition density. An unbiased estimator of the likelihood $L(\theta; y_{1:n})$ can be obtained from the collections of simulated particles. Thus the bootstrap particle filter can enable inference for implicitly defined, partially observed, Markov processes. Algorithm 2 gives a pseudocode for the bootstrap particle filter, with expressions for the unbiased likelihood estimator $\hat{L}(\theta)$ and for the estimators $\hat{L}_i(\theta)$ of the conditional densities $p(y_i | y_{1:i-1}; \theta)$, $i \in 1:n$.

We use the log of the unbiased likelihood estimator as the simulated log-likelihood $\ell^S(\theta; y_{1:n}) = \log \hat{L}(\theta; y_{1:n})$ and use the individual simulated log-likelihoods given by $\ell_i^S(\theta; y_i) = \log \hat{L}_i(\theta)$. By construction, we have $\ell^S(\theta) = \sum_{i=1}^n \ell_i^S(\theta)$, which is Assumption 1. Bérard et al. [7] showed that the log of the unbiased likelihood estimator minus the exact log-likelihood converges to a Gaussian limit under certain regularity conditions if the number of particles J increases linearly with the time length n :

$$\ell^S(\theta; y_{1:n}) - \ell(\theta; y_{1:n}) \xrightarrow[n \rightarrow \infty]{\text{in probability}} \mathcal{N}\left(-\frac{1}{2}\sigma^2, \sigma^2\right), \quad (11)$$

where $\sigma^2 > 0$ is a constant that depends on the model, the observed data, and $\lim_{n \rightarrow \infty} \frac{n}{J}$. This result justifies the asymptotic normality of $\ell^S(\theta; y_{1:n})$ described by the conditional metamodel (Definition 3) for POMP models.

2.5 Bias in simulation-based inference

The Jensen bias $B(\theta; y_{1:n}) = \ell(\theta; y_{1:n}) - \mu(\theta; y_{1:n})$ depends on the tail distribution of the simulated log-likelihood $\ell^S(\theta; y_{1:n})$, as Equation (3) suggests. Thus if $\ell^S(\theta; y_{1:n})$ has a heavy right tail, then the Jensen

Algorithm 2 The bootstrap particle filter for partially observed Markov processes

- 1: **Input:** observations $y_{1:n} = (y_1, \dots, y_n)$; parameter value θ ; simulator of the distribution of X_1 under P_θ ; simulator of the conditional distribution of $X_i|X_{i-1}$ for $i \in 2:n$ under P_θ ; number of particles J
- 2: **Output:** particle approximations to the filtering distributions $X_i|y_{1:i}$ for $i \in 1:n$; unbiased likelihood estimator $\hat{L}(\theta; y_{1:n})$
- 3: **for** $i \in 1:n$ **do**
- 4: **if** $i = 1$ **then**
- 5: Simulate J iid particles X_i^j , $j \in 1:J$, from the distribution of X_1 under P_θ
- 6: **else**
- 7: Simulate X_i^j from $X_i|(X_{i-1} = \tilde{X}_{i-1}^j)$ for $j \in 1:J$ under P_θ
- 8: **end if**
- 9: Compute an estimate of the conditional density $p(y_i|y_{1:i-1}; \theta)$ by

$$\hat{L}_i(\theta) = \frac{1}{J} \sum_{j=1}^J g_i(y_i|X_i^j; \theta)$$

- 10: Compute resampling weights

$$w_i^j = g_i(y_i|X_i^j; \theta) / \{J \hat{L}_i(\theta)\}, \quad j \in 1:J$$

- 11: Resample particles by letting $\tilde{X}_i^j = X_i^{a_i^j}$ where

$$a_i^j \sim \text{Categorical}(\{1, \dots, J\}, \{w_i^1, \dots, w_i^J\})$$

- 12: **end for**

- 13: Compute an unbiased likelihood estimator $\hat{L}(\theta; y_{1:n}) = \prod_{i=1}^n \hat{L}_i(\theta)$
-

bias can be large and hard to estimate. However, a bound on the Jensen bias can be obtained when $\ell^S(\theta; y_{1:n})$ has a light, sub-Gaussian right tail. Specifically, if

$$\mathbb{P}[\ell^S(\theta) - \mu(\theta) \geq t] \leq \frac{C'}{\sqrt{2\pi C}} e^{-\frac{t^2}{2C^2}}$$

for every $t \geq 0$ for some $C, C' > 0$, then the Jensen bias is upper bounded by $\frac{C^2}{2} + \log(1 + C')$. Another case where the Jensen bias can be bounded is when each individual simulated log-likelihood $\ell_i^S(\theta)$ is bounded within an interval of width $s_i(\theta)$. Then the Jensen bias is upper bounded by $\sum_{i=1}^n s_i(\theta)$. This may be useful if the observation space is compact. Section S3.2 in the supplementary text gives proofs for these results.

We develop a bound on the inference bias $\|\mathcal{R}(\theta_0) - \theta_0\|$ as follows. Consider the cross entropy $H(\theta_0, \theta) := -\mathbb{E}_{\theta_0} \{\log p_\theta^Y(Y)\}$ and its second order Taylor approximation around $\theta = \theta_0$, given by

$$q_{-H}(\theta) := -H(\theta_0, \theta_0) - \frac{1}{2}(\theta - \theta_0)^\top \mathcal{I}(\theta_0)(\theta - \theta_0). \quad (12)$$

Here $\mathcal{I}(\theta_0) = \left[\frac{\partial^2}{\partial \theta^2} H(\theta_0, \theta) \right]_{\theta=\theta_0}$ denotes the Fisher information at θ_0 . Similarly, consider a second order approximation to $U(\theta_0, \theta)$ around $\theta = \theta_*$ given by

$$q_U(\theta) := U(\theta_0, \theta_*) - \frac{1}{2}(\theta - \theta_*)^\top \mathcal{J}(\theta_0, \theta_*)(\theta - \theta_*), \quad (13)$$

where $\mathcal{J}(\theta_0, \theta_*) := -\left[\frac{\partial^2}{\partial \theta^2} U(\theta_0, \theta) \right]_{\theta=\theta_*}$. Provided that $\ell^S(\theta)$ is given by the logarithm of an unbiased likelihood estimator, we obtain the following result.

Proposition 2. *Suppose that the quadratic approximations $q_{-H}(\theta)$ and $q_U(\theta)$ given by (12)–(13) are ϵ -accurate on a δ -neighborhood of $\mathcal{R}(\theta_0) = \theta_*$, that is,*

$$| -H(\theta_0, \theta) - q_{-H}(\theta) | \leq \epsilon, \quad | U(\theta_0, \theta) - q_U(\theta) | \leq \epsilon,$$

for every θ such that $\|\theta - \theta_*\| \leq \delta$. Suppose further that both the Fisher information $\mathcal{I}(\theta_0)$ and $\mathcal{J}(\theta_0, \theta_*)$ are positive definite and that

$$\bar{B} := \sup_{\theta; \|\theta - \theta_*\| \leq \delta} \mathbb{E}_{Y_{1:n} \sim P_{\theta_0}^Y} B(\theta; Y_{1:n})$$

is finite. If the smallest eigenvalue λ of $\mathcal{J}(\theta_0, \theta_*)$ satisfies $\lambda \delta^2 \geq 2(\bar{B} + 2\epsilon)$, then we have

$$\|\theta_0 - \theta_*\| \leq 2\delta^{-1}\lambda^{-1}(\bar{B} + 2\epsilon).$$

The proof is provided in Section S3.3 of the supplementary text. When n is large, $\mathcal{J}(\theta_0, \theta_*)$, and consequently λ , can be approximately estimated by $-2\hat{c}$, where \hat{c} is the quadratic coefficient of the quadratic polynomial fitted to $\{(\theta_m, \ell^S(\theta_m)); m \in 1:M\}$.

A similar bound on the difference between the MESLE and the MLE can be established.

Proposition 3. Consider a given observation sequence $y_{1:n}$. Suppose that for every θ such that $\|\theta - \theta_{MESLE}\| \leq \delta$, the following quadratic approximations are ϵ -accurate:

$$\begin{aligned} \left| \ell(\theta) - \ell(\theta_{MLE}) - \frac{1}{2}(\theta - \theta_{MLE})^\top \frac{\partial^2 \ell}{\partial \theta^2}(\theta_{MLE})(\theta - \theta_{MLE}) \right| &\leq \epsilon, \\ \left| \mu(\theta) - \mu(\theta_{MESLE}) - \frac{1}{2}(\theta - \theta_{MESLE})^\top \frac{\partial^2 \mu}{\partial \theta^2}(\theta_{MESLE})(\theta - \theta_{MESLE}) \right| &\leq \epsilon. \end{aligned}$$

Suppose further that both $-\frac{\partial^2 \ell}{\partial \theta^2}(\theta_{MLE})$ and $-\frac{\partial^2 \mu}{\partial \theta^2}(\theta_{MESLE})$ are positive definite and that $\bar{B}' := \sup_{\theta; \|\theta - \theta_{MESLE}\| \leq \delta} B(\theta; y_{1:n})$ is finite. If the smallest eigenvalue λ' of $-\frac{\partial^2 \mu}{\partial \theta^2}(\theta_{MESLE})$ satisfies $\lambda' \delta^2 \geq 2(\bar{B}' + 2\epsilon)$, then we have

$$\|\theta_{MLE} - \theta_{MESLE}\| \leq 2\delta^{-1}\lambda'^{-1}(\bar{B}' + 2\epsilon).$$

3 Estimation of θ_{MESLE} and $K_1(\theta_0)$

3.1 Estimation of the metamodel parameters

For our normal, locally quadratic metamodel

$$\ell^S(\theta; y_{1:n}) \sim \mathcal{N} \left\{ a + b^\top \theta + \theta^\top c \theta, \frac{\sigma^2(y_{1:n})}{w(\theta)} \right\},$$

the mean function $a + b^\top \theta + \theta^\top c \theta$ can be estimated by weighted least square regression. We will write $A = (a, b^\top, \text{vech}(c)^\top)^\top$ where $\text{vech}(c)$ is the half-vectorization of the symmetric matrix $c = (c_{ij})_{i \in 1:d, j \in 1:d}$, given by

$$\text{vech}(c) = (c_{11}, c_{21}, \dots, c_{d1}, c_{22}, \dots, c_{d2}, \dots, c_{dd})^\top \in \mathbb{R}^{\frac{d(d+1)}{2}}.$$

We will write $\theta = (\theta_{(1)}, \dots, \theta_{(d)})^\top$ and denote by θ^2 the $d \times d$ matrix whose k -th diagonal entry is $\theta_{(k)}^2$ and whose (k, l) -th entry is $2\theta_{(k)}\theta_{(l)}$ for $k \neq l$. We can then write

$$\theta^\top c \theta = \text{vech}(\theta^2)^\top \text{vech}(c)$$

and the mean function as

$$\mu(\theta; A) := a + b^\top \theta + \theta^\top c \theta = (1, \theta^\top, \text{vech}(\theta^2)^\top) A =: \theta^{0:2^\top} A$$

where $\theta^{0:2} = (1, \theta^\top, \text{vech}(\theta^2)^\top)^\top \in \mathbb{R}^{\frac{d^2+3d+2}{2}}$. We will write

$$\theta_{1:M}^{0:2} = \begin{pmatrix} \theta_1^{0:2^\top} \\ \vdots \\ \theta_M^{0:2^\top} \end{pmatrix} \in \mathbb{R}^{M \times \left(\frac{d^2+3d+2}{2}\right)}.$$

The log-likelihood for A and σ^2 under our conditional metamodel is given by

$$\log p_{\text{meta}}(\ell^S(\theta_{1:M})|A, \sigma^2) = \sum_m -\frac{1}{2} \log \left(2\pi \frac{\sigma^2}{w_m} \right) - \frac{(\ell^S(\theta_m) - \mu(\theta_m; A))^2}{2\sigma^2/w_m}$$

where $w_m := w(\theta_m)$. Maximizing this metamodel log-likelihood is equivalent to a quadratic regression with weights w_m , $m \in 1:M$. We will write $\ell_m^S := \ell^S(\theta_m)$ and denote by W be the diagonal matrix with diagonal entries w_1, \dots, w_M . We assume that $\theta_{1:M}^{0:2} \in \mathbb{R}^{M \times (\frac{d^2+3d+2}{2})}$ has rank $\frac{d^2+3d+2}{2}$. We use the notation $\|v\|_W^2 := v^\top W v$ such that

$$\sum_{m=1}^M w_m \cdot (\ell^S(\theta_m) - \mu(\theta_m; A))^2 = \|\ell_{1:M}^S - \theta_{1:M}^{0:2 \top} A\|_W^2$$

where $\ell_{1:M}^S := (\ell^S(\theta_1), \dots, \ell^S(\theta_M))^\top$. The maximum metamodel likelihood estimates for A and $\sigma^2 = \sigma^2(y_{1:n})$ are given by

$$\hat{A} = (\hat{a}, \hat{b}^\top, \text{vech}(\hat{c})^\top)^\top = \{\theta_{1:M}^{0:2 \top} W \theta_{1:M}^{0:2}\}^{-1} \theta_{1:M}^{0:2 \top} W \ell_{1:M}^S, \quad (14)$$

$$\hat{\sigma}^2 = \frac{1}{M} \|\ell_{1:M}^S - \theta_{1:M}^{0:2} \hat{A}\|_W^2. \quad (15)$$

For the test of hypotheses

$$H_0 : A = A_0 = (a_0, b_0^\top, \text{vech}(c_0)^\top)^\top, \quad \sigma^2 = \sigma_0^2, \quad H_1 : \text{not } H_0,$$

the metamodel log-likelihood ratio statistic is given by

$$MLLR_{A_0, \sigma_0^2} := \frac{\log p_{\text{meta}}(\ell_{1:M}^S | A_0, \sigma_0^2)}{\sup_{A, \sigma^2} \log p_{\text{meta}}(\ell_{1:M}^S | A, \sigma^2)} = \frac{M}{2} \log \frac{\hat{\sigma}^2}{\sigma_0^2} - \frac{\|\ell_{1:M}^S - \theta_{1:M}^{0:2} A_0\|_W^2}{2\sigma_0^2} + \frac{M}{2}. \quad (16)$$

As the number of simulation M grows, $-2 \cdot MLLR_{A_0, \sigma_0^2}$ converges in distribution to $\chi_{\frac{d^2+3d+4}{2}}^2$ under the null hypothesis $H_0 : A = A_0, \sigma^2 = \sigma_0^2$. The degrees of freedom $\frac{d^2+3d+4}{2}$ equals the number of scalar metamodel parameters, namely a , d entries of b , $\frac{d^2+d}{2}$ diagonal and lower triangular entries of c , and σ^2 . The finite sample distribution of the $MLLR_{A_0, \sigma_0^2}$ statistic under the null hypothesis is characterized in supplementary Section S4.1.

3.2 Estimation and uncertainty quantification for the MESLE

The maximum metamodel likelihood estimator for θ_{MESLE} is given by

$$\hat{\theta}_{\text{MESLE}} = -\frac{1}{2} \hat{c}^{-1} \hat{b},$$

where \hat{b} and \hat{c} are obtained by quadratic regression, (14). The variance of $\hat{\theta}_{\text{MESLE}}$ scales as $\mathcal{O}(M^{-1}n^{-1})$. This can be seen by using the delta method as follows [35]. From (14), we can show that

$$\text{Var}(\hat{A}) = \sigma^2 \{\theta_{1:M}^{0:2 \top} W \theta_{1:M}^{0:2}\}^{-1} \quad (17)$$

and

$$\sqrt{M}(\hat{\theta}_{\text{MESLE}} - \theta_{\text{MESLE}}) \Rightarrow \mathcal{N}(0, \Sigma_{\text{MESLE}}),$$

where

$$\Sigma_{\text{MESLE}} = \sigma^2 \cdot \left(\frac{\partial(-\frac{1}{2}c^{-1}b)}{\partial(a, b, c)} \right) \left(\lim_{M \rightarrow \infty} M \{\theta_{1:M}^{0:2 \top} W \theta_{1:M}^{0:2}\}^{-1} \right) \left(\frac{\partial(-\frac{1}{2}c^{-1}b)}{\partial(a, b, c)} \right)^\top.$$

According to our marginal metamodel, b and c scale as $\mathcal{O}(n)$, and we often have $\sigma^2 = \mathcal{O}(n)$. We also have $\theta_{1:M}^{0:2 \top} W \theta_{1:M}^{0:2} = \mathcal{O}(M)$. Hence, we have $\text{Var}(\hat{\theta}_{\text{MESLE}}) = M^{-1} \cdot \mathcal{O}(n^{-2}\sigma^2) = \mathcal{O}(M^{-1}n^{-1})$.

If the quadratic coefficient in (21) is negative and the discriminant of the left hand side is nonnegative, then the constructed confidence interval will be of the form $(-\infty, \text{LB}) \cup (\text{UB}, \infty)$ where $-\infty < \text{LB} < \text{UB} < \infty$. This situation arises roughly when $\hat{c}^2 \lesssim \hat{\sigma}^2/M$. To see this, we note that for $d = 1$ we have

$$V = \begin{pmatrix} V_{bb} & V_{bc} \\ V_{bc} & V_{cc} \end{pmatrix} = \left(\sum_m w_m \right) \begin{pmatrix} \overline{\theta^2} - (\overline{\theta})^2 & \overline{\theta^3} - \overline{\theta} \cdot \overline{\theta^2} \\ \overline{\theta^3} - \overline{\theta} \cdot \overline{\theta^2} & \overline{\theta^4} - (\overline{\theta^2})^2 \end{pmatrix}$$

where $\overline{\theta^j} = (\sum_m w_m \theta_m^j) / (\sum_m w_m)$, $j \in 1:4$, and thus $\det V = V_{bb}V_{cc} - V_{bc}^2 = \mathcal{O}(M) \cdot V_{bb}$. The coefficient for θ^2 in (21) may be negative if $\hat{c}^2 \lesssim \hat{\sigma}^2/M$. This implies that the MESLE may not be estimated if the signal to noise ratio is too small. If the discriminant of the quadratic polynomial in (21) is negative, the confidence interval is the entire real line $(-\infty, \infty)$, and the MESLE may not be estimated either.

The p-value and the confidence interval developed in this section can be numerically found using the `ht` and `ci` functions in R package `sbim` (<https://CRAN.R-project.org/package=sbim>).

3.3 Estimation of $K_1(\theta_0)$

The marginal metamodel (Definition 4) implies that $K_2(\theta_0)$ can be estimated by $-\frac{2}{n}\hat{c}$, where \hat{c} is given by (14). Estimation of $K_1(\theta_0)$ is more complicated, because it involves estimating the variability in $\frac{\partial \mu}{\partial \theta}(\theta_*; Y_{1:n})$, where only a single set of observations $y_{1:n}$ is available. One possible method for estimating $K_1(\theta_0)$ is to use parametric bootstrap, where we generate n_{boot} sets of observations $y_{1:n}^{\text{boot},k}$ at $\theta = \hat{\theta}_{\text{MESLE}}$ for $k \in 1:n_{\text{boot}}$ and compute the sample covariance matrix of $\frac{\partial \hat{\mu}}{\partial \theta}(\hat{\theta}_{\text{MESLE}}; y_{1:n}^{\text{boot},k})$ for those bootstrap samples. However, this approach has two major disadvantages. First, for each bootstrap sample, simulated log-likelihoods $\ell^S(\theta_m; y_{1:n}^{\text{boot},k})$ need to be obtained in order to estimate $\frac{\partial \hat{\mu}}{\partial \theta}(\hat{\theta}_{\text{MESLE}}; y_{1:n}^{\text{boot},k})$, which increases the computational complexity by a factor of n_{boot} . Another disadvantage is that if our simulator P_θ is misspecified, the sample variance of $\frac{\partial \hat{\mu}}{\partial \theta}(\hat{\theta}_{\text{MESLE}}; y_{1:n}^{\text{boot},k})$ may have a non-negligible bias.

Here we propose a method where $K_1(\theta_0)$ is estimated using the given data $y_{1:n}$. We divide the observations $y_{1:n}$ into blocks and assume that these blocks of observations are approximately independent of each other and identically distributed, marginally over the law of X . This assumption may hold if the process X is approximately stationary and possesses a mixing property. Since the derivative of the mean function evaluated at θ_* is given by

$$\frac{\partial \mu}{\partial \theta}(\theta_*; A) = b + 2c\theta_* = (\mathbf{0}_d, I_d, 2\theta_{*,\text{mat}})A,$$

where $\mathbf{0}_d \in \mathbb{R}^d$ is a column vector of zeros, the derivative of the mean function at θ_* can be estimated by

$$\widehat{\frac{\partial \mu}{\partial \theta}}(\theta_*; Y_{1:n}) = \frac{\partial \hat{\mu}}{\partial \theta}(\theta_*; \hat{A}) = \hat{b} + 2\hat{c}\theta = (\mathbf{0}_d, I_d, 2\theta_{*,\text{mat}})\hat{A}.$$

where $\hat{A} = (\hat{a}, \hat{b}, \hat{c})$ is given by Equation (14). Since \hat{A} is unbiased for A , we have

$$\mathbb{E} \left(\widehat{\frac{\partial \mu}{\partial \theta}}(\theta_*; Y_{1:n}) \middle| Y_{1:n} \right) = b + 2c\theta_* = \frac{\partial \mu}{\partial \theta}(\theta_*; Y_{1:n}).$$

We can estimate $K_1(\theta_0) = \lim_{n \rightarrow \infty} \frac{1}{n} \text{Var}_{Y_{1:n} \sim P_{\theta_0}^Y} \frac{\partial \mu}{\partial \theta}(\theta_*; Y_{1:n})$ using the expression

$$\begin{aligned} & \frac{1}{n} \text{Var}_{Y_{1:n} \sim P_{\theta_0}^Y} \left\{ \mathbb{E} \left(\widehat{\frac{\partial \mu}{\partial \theta}}(\theta_*; Y_{1:n}) \middle| Y_{1:n} \right) \right\} \\ &= \frac{1}{n} \text{Var}_{Y_{1:n} \sim P_{\theta_0}^Y} \left\{ \widehat{\frac{\partial \mu}{\partial \theta}}(\theta_*; Y_{1:n}) \right\} - \frac{1}{n} \mathbb{E}_{Y_{1:n} \sim P_{\theta_0}^Y} \left\{ \text{Var} \left(\widehat{\frac{\partial \mu}{\partial \theta}}(\theta_*; Y_{1:n}) \middle| Y_{1:n} \right) \right\}, \quad (22) \end{aligned}$$

The steps for estimating $K_1(\theta_0)$ are summarized in Algorithm 3. The conditional variance in the second term on the right hand side of (22) is given by

$$\text{Var} \left(\widehat{\frac{\partial \mu}{\partial \theta}}(\theta_*; Y_{1:n}) \middle| Y_{1:n} \right) = (\mathbf{0}_d, I_d, 2\theta_{*,\text{mat}}) \text{Var}(\hat{A} | Y_{1:n}) (\mathbf{0}_d, I_d, 2\theta_{*,\text{mat}})^\top,$$

Algorithm 3 Estimation of $K_1(\theta_0)$ using block partitioning

- 1: Choose ϑ , an approximate guess for θ_* , such as the average of $\{\theta_m; m \in 1 : M\}$
 - 2: Fit a quadratic polynomial to $\{(\theta_m, \ell^S(\theta_m; y_{1:n})); m \in 1 : M\}$ and let $\widehat{\frac{\partial \mu}{\partial \theta}}(\vartheta; y_{1:n})$ be the slope of the fitted quadratic polynomial at ϑ
 - 3: Obtain an estimate of $\frac{1}{n} \mathbb{E} \left\{ \text{Var} \left(\widehat{\frac{\partial \mu}{\partial \theta}}(\vartheta; Y_{1:n}) \middle| Y_{1:n} \right) \right\}$ via (23)
 - 4: Partition $\{1, \dots, n\}$ into blocks B_1, \dots, B_K such that $(Y_i; i \in B_k)$ are approximately independent of each other
 - 5: **for** $k \in 1 : K$ **do**
 - 6: Fit a quadratic polynomial to $\{(\theta_m, \sum_{i \in B_k} \ell_i^S(\theta_m; y_i)); m \in 1 : M\}$
 - 7: Let $\widehat{\frac{\partial \mu_{B_k}}{\partial \theta}}(\vartheta; y_{B_k})$ denote the slope of the fitted quadratic polynomial at ϑ
 - 8: **end for**
 - 9: Let $\frac{1}{n} \widehat{\text{Var}}_{Y_{1:n} \sim P_{\theta_0}^Y} \left\{ \widehat{\frac{\partial \mu}{\partial \theta}}(\vartheta; Y_{1:n}) \right\}$ be the (weighted) sample variance of $\left\{ \widehat{\frac{\partial \mu_{B_k}}{\partial \theta}}(\vartheta; y_{B_k}); k \in 1 : K \right\}$ as given by (24)
 - 10: Let $\hat{K}_1(\theta_0)$ be (24) minus (23)
-

where we have

$$\text{Var}(\hat{A}|Y_{1:n}) = (\theta_{1:M}^{0:2 \top} W \theta_{1:M}^{0:2})^{-1} \sigma^2(Y_{1:n}).$$

Thus, the second term on the right hand side of (22) can be approximated by

$$\frac{\hat{\sigma}^2(Y_{1:n})}{n} (\mathbf{0}_d, I_d, 2\vartheta_{\text{mat}}) \{ \theta_{1:M}^{0:2 \top} W \theta_{1:M}^{0:2} \}^{-1} (\mathbf{0}_d, I_d, 2\vartheta_{\text{mat}})^\top, \quad (23)$$

where ϑ is a reasonable guess for θ_* , such as the average of $\theta_1, \dots, \theta_M$, and $\hat{\sigma}^2(Y_{1:n})$ is given by (15).

The first term on the right hand side of (22), $\frac{1}{n} \text{Var}_{Y_{1:n} \sim P_{\theta_0}^Y} \left\{ \widehat{\frac{\partial \mu}{\partial \theta}}(\theta_*; Y_{1:n}) \right\}$ can be estimated as follows. Let B_1, \dots, B_K be contiguous, non-overlapping blocks partitioning the set $\{1, \dots, n\}$ chosen such that $\{Y_i; i \in B_k\}$, $k \in 1 : K$, are approximately independent of each other. A quadratic polynomial is fitted to $\{(\theta_m, \sum_{i \in B_k} \ell_i^S(\theta_m; y_i)); m \in 1 : M\}$ for each block $k \in 1 : K$. Let the estimated slope of the fitted quadratic polynomial for the k -th block evaluated at ϑ be denoted by $\widehat{\frac{\partial \mu_{B_k}}{\partial \theta}}(\vartheta)$. Then the first term on the right hand side of (22) can be estimated by the weighted sample variance of $\left\{ \widehat{\frac{\partial \mu_{B_k}}{\partial \theta}}(\vartheta); k \in 1 : K \right\}$, given by

$$\frac{1}{K-1} \sum_{k=1}^K |B_k| \left(\frac{1}{|B_k|} \widehat{\frac{\partial \mu_{B_k}}{\partial \theta}}(\vartheta) - \frac{1}{n} \sum_{k=1}^K \widehat{\frac{\partial \mu_{B_k}}{\partial \theta}}(\vartheta) \right) \left(\frac{1}{|B_k|} \widehat{\frac{\partial \mu_{B_k}}{\partial \theta}}(\vartheta) - \frac{1}{n} \sum_{k=1}^K \widehat{\frac{\partial \mu_{B_k}}{\partial \theta}}(\vartheta) \right)^\top \quad (24)$$

where $|B_k|$ denotes the size of B_k . An estimate of $K_1(\theta_0)$ is obtained by subtracting (23) from (24). The standard error of this estimate scales as $\mathcal{O}(n^{-1/2})$.

4 Estimation and uncertainty quantification for the simulation-based proxy θ_*

In this section, we develop a hypothesis testing procedure for the simulation-based proxy $\mathcal{R}(\theta_0) =: \theta_*$. We assume that the variance $\sigma^2(\theta; y_{1:n})$ of $\ell^S(\theta; y_{1:n})$ is constant in the local neighborhood of θ_* where simulations are carried out. Our approach differs from the method proposed by Ionides et al. [20] in two key ways: (a) we account for the difference between the local asymptotic normality for the log-likelihood function $\ell(\theta; Y)$ and that of the expected simulated log-likelihood function $\mu(\theta; Y)$, and (b) we avoid using the delta method approximation.

We employ a restricted maximum likelihood (REML) approach, using the relative differences $\ell(\theta_m; Y_{1:n}) - \ell(\theta_1; Y_{1:n})$, for $m \in 2 : M$, to eliminate the dependence on $a(Y_{1:n})$, which often has an intractable distribution.

The reference point is chosen to θ_1 without loss of generality. The conditional metamodel (Definition 3) gives that

$$\mu(\theta_m; Y_{1:n}) - \mu(\theta_1; Y_{1:n}) = b^\top (\theta_m - \theta_1) + \theta_m^\top c \theta_m - \theta_1^\top c \theta_1 = (\theta_m^{1:2} - \theta_1^{1:2})^\top \begin{pmatrix} b \\ \text{vech}(c) \end{pmatrix},$$

where $\theta_m^{1:2} = (\theta_m^\top, \text{vech}(\theta_m^2)^\top)^\top \in \mathbb{R}^{M \times \frac{d^2+3d}{2}}$. We will denote the relative differences by $(\ell_2^S - \ell_1^S, \dots, \ell_M^S - \ell_1^S)^\top = C \ell_{1:M}^S$, where $C := (-\mathbf{1}_{M-1}, I_{M-1}) \in \mathbb{R}^{(M-1) \times M}$. The distribution of $C \ell_{1:M}^S$ conditional on the observations $Y_{1:n}$ is given by

$$C \ell_{1:M}^S | Y_{1:n} \sim \mathcal{N} \left(C \theta_{1:M}^{1:2} \begin{pmatrix} b \\ \text{vech}(c) \end{pmatrix}, \sigma^2 C W^{-1} C^\top \right). \quad (25)$$

We will assume that $C \theta_{1:M}^{1:2}$ has a full column rank. The marginal metamodel (Definition 4) states that

$$c(Y_{1:n}) = -\frac{n}{2} K_2(\theta_0), \quad b(Y_{1:n}) \sim \mathcal{N} \{ n K_2(\theta_0) \theta_*, n K_1(\theta_0) \} = \mathcal{N} \{ -2c \theta_*, n K_1(\theta_0) \}.$$

We will assume that $b(Y_{1:n})$ and $\sigma^2(Y_{1:n})$ are independent. Under this assumption, we have

$$C \ell_{1:M}^S | \sigma^2 \sim \mathcal{N} \left(C \theta_{1:M}^{1:2} \begin{pmatrix} -2c \theta_* \\ \text{vech}(c) \end{pmatrix}, \sigma^2 C W^{-1} C^\top + C \theta_{1:M} n K_1 \theta_{1:M}^\top C^\top \right). \quad (26)$$

The density of (26) evaluated for $C \ell_{1:M}^S$ will be referred to as the marginal metamodel likelihood and denoted by p_{meta} . Mathematical details for this section are given in the supplementary text Section S5. By maximizing this marginal metamodel likelihood using the plug-in estimates $\hat{\sigma}^2$ given by (15) and \hat{K}_1 obtained via Algorithm 3, we obtain point estimators $\hat{\theta}_*$ and \hat{c} satisfying

$$\begin{pmatrix} -2\hat{c} \hat{\theta}_* \\ \text{vech}(\hat{c}) \end{pmatrix} = \left\{ \theta_{1:M}^{1:2 \top} \hat{P} \theta_{1:M}^{1:2} \right\}^{-1} \theta_{1:M}^{1:2 \top} \hat{P} \ell_{1:M}^S, \quad (27)$$

where

$$\hat{P} := C^\top \{ C W^{-1} C^\top + \hat{\sigma}^{-2} C \theta_{1:M} n \hat{K}_1 \theta_{1:M}^\top C^\top \}^{-1} C.$$

The estimate $\hat{\theta}_*$ was very close to $\hat{\theta}_{\text{MESLE}}$ for all numerical examples we considered in Section 5. We also obtain a second-stage estimate estimate for the variance σ^2 , given by

$$\hat{\sigma}_{2\text{nd}}^2 := \frac{1}{M-1} \left\| \ell_{1:M}^S - \theta_{1:M}^{1:2} \left\{ \theta_{1:M}^{1:2 \top} \hat{P} \theta_{1:M}^{1:2} \right\}^{-1} \theta_{1:M}^{1:2 \top} \hat{P} \ell_{1:M}^S \right\|_{\hat{P}}^2. \quad (28)$$

We carry out a test on the simulation-based proxy

$$H_0 : \theta_* = \theta_{*,0}, \quad H_1 : \theta_* \neq \theta_{*,0}$$

using the marginal metamodel log likelihood ratio defined as

$$MLLR_{\theta_{*,0}} = \log \frac{\sup_{c, \sigma^2} p_{\text{meta}}(C \ell_{1:M}^S | \theta_{*,0}, c, \sigma^2)}{\sup_{\theta_*, c, \sigma^2} p_{\text{meta}}(C \ell_{1:M}^S | \theta_*, c, \sigma^2)}.$$

The distribution of $MLLR_{\theta_{*,0}}$ under H_0 is described by Proposition 5.

Proposition 5. Let $T(\theta_{*,0}) = \theta_{1:M}^{1:2} \begin{pmatrix} \theta_{*,0, \text{mat}} \\ -\frac{1}{2} I_{\frac{d^2+d}{2}} \end{pmatrix}$ and

$$S(\theta_{*,0}) = T(\theta_{*,0}) \{ T(\theta_{*,0})^\top \hat{P} T(\theta_{*,0}) \}^{-1} T(\theta_{*,0})^\top.$$

Then the metamodel log-likelihood ratio $MLLR_{\theta_{*,0}}$ is given by

$$MLLR_{\theta_{*,0}} = -\frac{M-1}{2} \log \frac{\| \{ I_{M-1} - S(\theta_{*,0}) \hat{P} \} \ell_{1:M}^S \|_{\hat{P}}^2}{\hat{\sigma}_{2\text{nd}}^2}.$$

Furthermore, if Assumptions 1-6 hold,

$$\frac{M - \frac{d^2+3d+2}{2}}{d} \left\{ \frac{\| \{I_{M-1} - S(\theta_{*,0})\hat{P}\} \ell_{1:M}^S \|^2_{\hat{P}}}{(M-1)\hat{\sigma}_{2nd}^2} - 1 \right\} \sim F_{d, M - \frac{d^2+3d+2}{2}} \quad (29)$$

under $H_0 : \theta_* = \theta_{*,0}$, provided that $\hat{\sigma}^2 = \sigma^2$ and $\hat{K}_1 = K_1$.

Proposition 5 suggests that we reject $H_0 : \theta_* = \theta_{*,0}$ when

$$\left\| \{I_{M-1} - S(\theta_{*,0})\hat{P}\} \ell_{1:M}^S \right\|_{\hat{P}}^2 > (M-1)\hat{\sigma}_{2nd}^2 \left(\frac{d \cdot F_{d, M - \frac{d^2+3d+2}{2}, \alpha}}{M - \frac{d^2+3d+2}{2}} + 1 \right) \quad (30)$$

to achieve an approximate significance level α . If we denote the left hand side of (29) by F , then an approximate p-value is given by $P[F_{d, M - \frac{d^2+3d+2}{2}} > F]$.

When $d = 1$, an approximate level $1 - \alpha$ confidence interval for θ_* can be obtained by inverting the hypothesis test.

Corollary 2. Assume that the parameter space is one dimensional (i.e., $\Theta \subseteq \mathbb{R}$). Write $\theta_{1:M}^{1:2 \top} \hat{P} \theta_{1:M}^{1:2} = \begin{pmatrix} \rho_{11} & \rho_{12} \\ \rho_{12} & \rho_{22} \end{pmatrix}$ and

$$\zeta_0 = \left\| \ell_{1:M}^S \right\|_{\hat{P}}^2 - (M-1)\hat{\sigma}_{2nd}^2 \left(\frac{F_{1, M-3, \alpha}}{M-3} + 1 \right), \quad \begin{pmatrix} \zeta_1 \\ \zeta_2 \end{pmatrix} = \theta_{1:M}^{1:2 \top} \hat{P} \ell_{1:M}^S.$$

Then under Assumptions 1-6, an approximate level $1 - \alpha$ confidence interval for θ_* is given by

$$\left\{ \theta_{*,0}; (\zeta_0 \rho_{11} - \zeta_1^2) \theta_{*,0}^2 + (\zeta_1 \zeta_2 - \zeta_0 \rho_{12}) \theta_{*,0} + \frac{1}{4} (\rho_{22} \zeta_0 - \zeta_2^2) < 0 \right\}. \quad (31)$$

The approximate p-value and the approximate confidence interval developed in this section can be numerically found using the `ht` and `ci` functions in R package `sbim`.

There is a bias-variance trade-off in the choice of the simulation points $\{\theta_m; m \in 1:M\}$. If the simulation points are chosen within a narrow range, the quadratic approximation to $\mu(\theta)$ will be relatively accurate in that range, resulting in a smaller inference bias. However, the regression estimates will exhibit greater variance, leading to wider confidence intervals. In practice, a balance can be achieved by considering both the statistical significance of the third-order term in the Taylor expansion approximation of $\mu(\theta)$ and the size of the constructed confidence region, as demonstrated in Section 5.

5 Numerical results

We numerically test the simulation-based parameter inference methods developed in Sections 3 and 4. Hypothesis tests and construction of confidence intervals were carried out using the `ht` and `ci` functions in R package `sbim` (available at <https://CRAN.R-project.org/package=sbim>). Additional numerical results are provided in Supplementary Section S7.

5.1 Gamma process with Poisson observations

We first consider independent, gamma distributed draws $X_{1:n} \stackrel{iid}{\sim} \Gamma(\gamma, \lambda)$ and conditionally independent Poisson observations Y_i of X_i , for $i \in 1:n$. We consider estimating λ , assuming that γ is known. We generate $n = 1000$ observations $y_{1:n}$ for $\gamma = 1$, $\lambda = 1$. Simulations $X_{1:n} \stackrel{iid}{\sim} \Gamma(1, \lambda)$ are carried out at $\lambda = 1.0 \pm 0.001 \times k$, $k = 0, \dots, 200$ ($M = 401$). Example S1 in the supplementary text shows that the MESLE is given by $(n\gamma) / \sum_{i=1}^n y_i$ and that the simulation-based proxy λ_* is equal to the true parameter value $\lambda = 1$. Additionally, it shows that $K_1(\lambda) = 2$ and $K_2(\lambda) = 1$ are different, and both differ from the Fisher information $\mathcal{I}(\lambda) = \frac{1}{2}$.

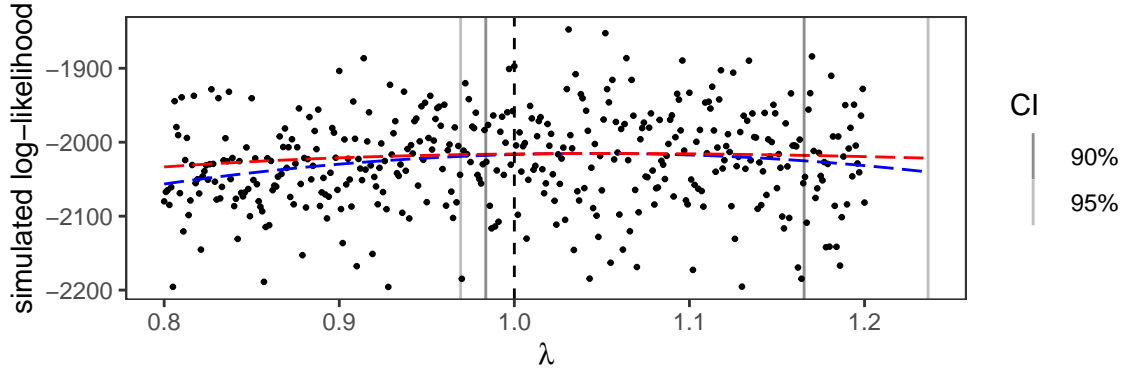


Figure 2: Simulated log-likelihoods for the gamma-Poisson process. The 90% and 95% confidence intervals constructed for the simulation-based proxy λ_* are marked by gray vertical lines. The true value of λ is marked by the vertical dashed line. The blue dashed curve indicates the fitted quadratic polynomial, and the red dashed curve the exact log-likelihood function, with a vertical shift for better visual comparison.

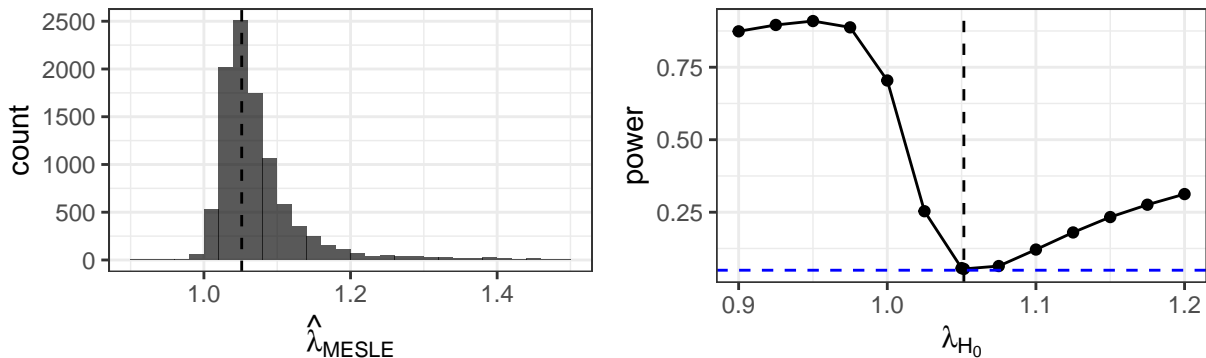


Figure 3: The left panel shows the distribution of the estimate $\hat{\lambda}_{MESLE}$ over 10000 replications of simulation-based estimation. The exact value of λ_{MESLE} is marked by the vertical dashed line. A small number of $\hat{\lambda}_{MESLE}$ that were outside the displayed range were omitted from the plot. The right plot shows the estimated rejection probabilities for $H_0 : \lambda_{MESLE} = \lambda_{H_0}$ at a 5% significance level for varied null values λ_{H_0} . The blue horizontal line indicates the significance level.

Figure 2 shows the simulated log-likelihoods and 90% and 95% confidence intervals constructed for the simulation-based proxy λ_* , marked by pairs of gray vertical lines. The fitted quadratic polynomial is indicated by the blue curve, and the exact log-likelihood by the red curve with a vertical shift for easier comparison with the fitted polynomial. These curves show that the second order derivative of the fitted quadratic function is different than that of the log-likelihood function, aligning with the fact that $K_2(\lambda) = 1$ is not equal to the Fisher information $\mathcal{I}(\lambda) = \frac{1}{2}$. Hence, using the approximate method by Ionides et al. [20] would lead to misquantified parameter uncertainty.

For the given data $y_{1:n}$, we estimated λ_{MESLE} by simulating $X_{1:n}$ at varied λ values and applying the method introduced in Section 3.2. We replicated this experiment ten thousand times. For each replication, a hypothesis test for the MESLE, $H_0 : \lambda_{MESLE} = \lambda_{H_0}$, $H_1 : \lambda_{MESLE} \neq \lambda_{H_0}$, was carried out. The left panel of Figure 3 shows the distribution of the point estimates for λ_{MESLE} . These estimates are centered around the exact value with an interquartile range of approximately 0.05. The right panel in Figure 3 shows the proportion of the hypothesis tests where the null hypothesis for varied λ_{H_0} is rejected at a 5% significance level. This plot shows that the empirical significance level aligns with the nominal level and that the test has reasonably high power when the difference between λ_{MESLE} and the null value λ_{H_0} is greater than approximately 0.1.

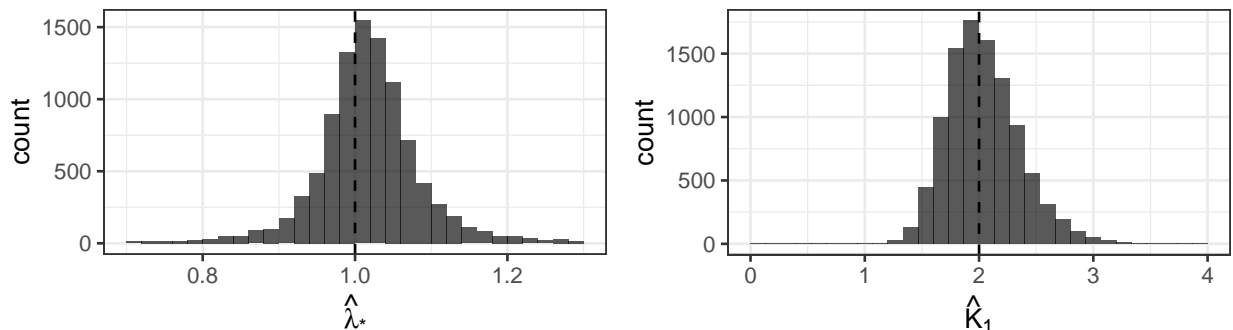


Figure 4: The distribution of the estimates for the simulation-based proxy λ_* (left) and the estimates for K_1 (right). The dashed lines indicate the true values of λ and K_1 .

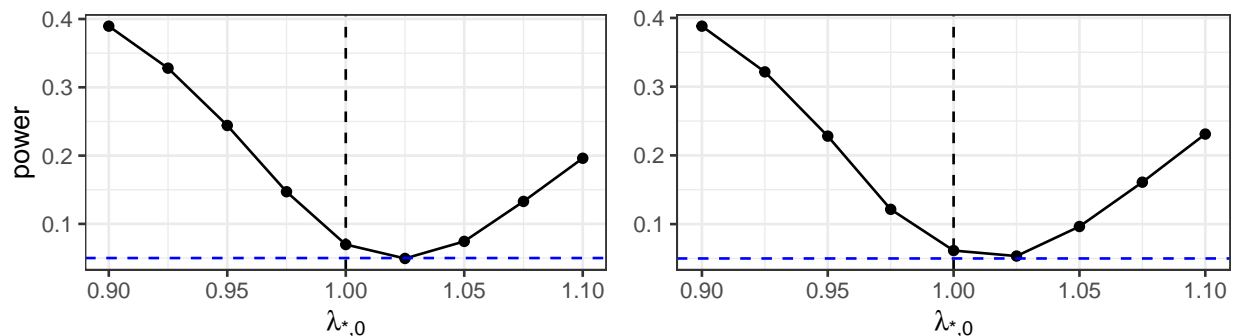


Figure 5: The left panel shows the probability of rejecting the null hypothesis $H_0 : \lambda_* = \lambda_{*,0}$ at a 5% significance level for varied null values $\lambda_{*,0}$. The right panel shows the probability of rejecting the null hypothesis when the exact value of $K_1(\lambda_0)$ is used instead of an estimated value.

method	Nominal confidence level (%)		
	80	90	95
metamodel-based	77.6 (0.8)	87.8 (0.7)	93.2 (0.5)
Ionides et al. [20]	45.3 (1.0)	54.9 (1.0)	63.0 (1.0)

Table 1: Percentages of confidence intervals encompassing the true parameter $\lambda_0 = 1$ using our metamodel-based method (first row) and the method proposed by Ionides et al. [20] (second row) in ten thousand replications. The numbers in parentheses represent twice the standard errors.

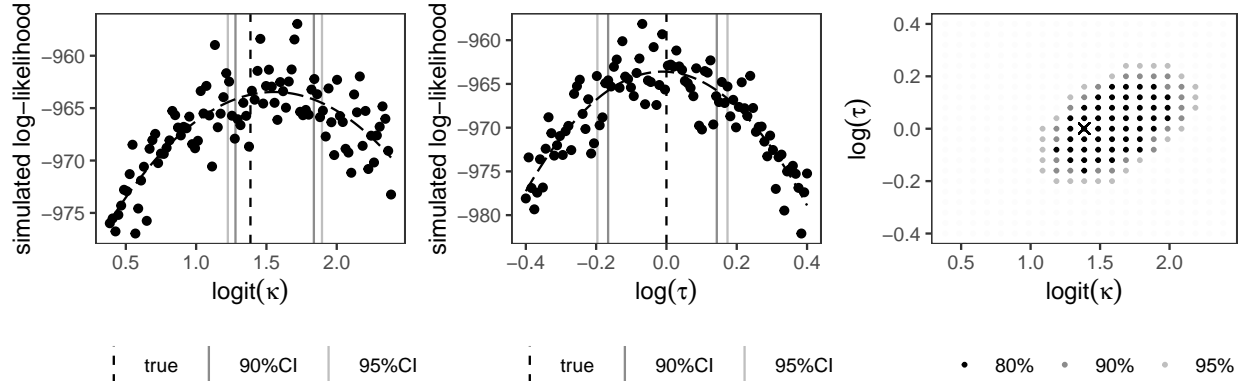


Figure 6: Left: Simulated log-likelihoods and constructed confidence intervals for $\text{logit}(\kappa)$ in the stochastic volatility model. Middle: Simulated log-likelihoods and confidence intervals for $\log(\tau)$. Right: Constructed confidence regions for (κ, τ) at 95%, 90%, and 80% confidence levels. The true parameter values are marked by with an ‘X’.

We independently generated data $y_{1:n}$ ten thousand times at $\lambda_0 = 1$ and estimated the simulation based proxy λ_* using the method developed in Section 4. Tests on the simulation-based proxy, $H_0 : \lambda_* = \lambda_{*,0}$, $H_1 : \lambda_* \neq \lambda_{*,0}$ were carried out for varied null values $\lambda_{*,0}$. The left panel of Figure 4 shows the distribution of the point estimates λ_* , which was approximately centered at the true parameter value. The right panel of Figure 4 shows the distribution of the estimates for $K_1(\lambda_0)$, estimated using Algorithm 3. The distribution of \hat{K}_1 is centered at the exact value of $K_1(\lambda_0) = 2$.

The left panel in Figure 5 shows the empirical proportions where $H_0 : \lambda_* = \lambda_{*,0}$ is rejected at a 5% significance level for varied $\lambda_{*,0}$. The empirical rejection probability was 0.07 at the true null value $\lambda_{*,0} = 1$. The rejection probability was closest to the significance level 0.05 approximately at $\lambda_{*,0} = 1.025$. One of the reasons for this bias is the variability in the estimated values of $K_1(\lambda_0)$ obtained by Algorithm 3. If we instead use the exact value $K_1(\lambda_0)$ for the hypothesis tests, the power curve has a smaller bias, as shown by the right plot of Figure 5. However, there is still a bias when the exact $K_1(\lambda_0)$ is used; this is possibly due to the metamodel not being exact or the violation of the assumption that $S_n(Y_{1:n})$ and $\sigma^2(Y_{1:n})$ are independent.

We constructed confidence intervals for λ_* using Eq. (31) ten thousand times. For comparison, we constructed Monte Carlo confidence intervals using the method of Ionides et al. [20], utilizing the `mcap` function from the `pomp` package [23, 22]. Table 1 reports the probabilities that the 80%, 90%, and 95% confidence intervals constructed by both methods encompass the true parameter value $\lambda_0 = 1$. These results demonstrate that our method constructs confidence intervals that are significantly more accurate than those produced by the method of Ionides et al. [20]. The latter exhibits bias because the curvature of the quadratic polynomial fitted to the simulated log-likelihoods generally differs from the Fisher information.

5.2 Stochastic volatility model

We consider a stochastic volatility model, where the distribution of the log rate of return r_i of a stock at time i is described by

$$r_i = e^{s_i} W_i, \quad W_i \stackrel{iid}{\sim} t_5,$$

where s_i denotes the volatility at time i and t_5 the t distribution with five degrees of freedom. The distribution of the stochastic volatility process $\{s_i\}$ is described by

$$s_i = \kappa s_{i-1} + \tau \sqrt{1 - \kappa^2} V_i \quad \text{for } i > 1, \quad s_1 = \tau V_1, \quad V_i \stackrel{iid}{\sim} \mathcal{N}(0, 1).$$

The rates of return r_i are observed for $i \in 1:n$ where $n = 500$. We simulate the stochastic volatility process for $\kappa = 0.8, \tau = 1$ and generate an observed data sequence $r_{1:n}$.

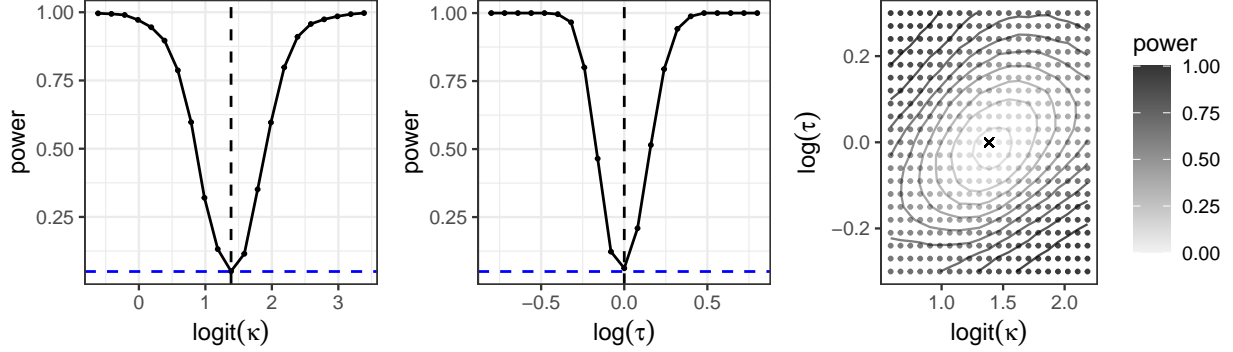


Figure 7: Left: Probability of rejecting the null hypothesis $H_0 : \kappa_* = \kappa_{*,0}$ for varied null values. Middle: Probabilities of rejecting $H_0 : \tau_* = \tau_{*,0}$ for varied null values. Right: Probabilities of rejecting $H_0 : (\kappa_*, \tau_*) = (\kappa_{*,0}, \tau_{*,0})$ for varied null value pairs, with level sets indicated. The true parameter values are marked by an ‘X’. All tests were carried out using a 5% significance level.

parameter	# particles	method	Nominal confidence level (%)		
			80	90	95
κ	10	metamodel-based	79.3 (2.6)	90.4 (1.9)	95.4 (1.3)
		Ionides et al. [20]	63.1 (3.1)	76.2 (2.7)	84.8 (2.3)
	100	metamodel-based	79.2 (2.6)	89.3 (2.0)	94.7 (1.4)
		Ionides et al. [20]	76.7 (2.7)	88.2 (2.0)	94.3 (1.5)
τ	10	metamodel-based	76.6 (2.7)	86.5 (2.2)	92.4 (1.7)
		Ionides et al. [20]	60.5 (3.1)	75.5 (2.7)	83.5 (2.3)
	100	metamodel-based	77.3 (2.6)	90.1 (1.9)	94.9 (1.4)
		Ionides et al. [20]	76.8 (2.7)	88.5 (2.0)	94.6 (1.4)

Table 2: Percentages of confidence intervals encompassing the true parameter values for κ and τ using our metamodel-based method (first row) and the method of Ionides et al. [20] (second row). The confidence intervals are constructed one thousand times by running the particle filter with ten or one hundred particles. The numbers in parentheses represent twice the standard errors.

The bootstrap particle filter was run at varied parameter values $\theta = (\kappa, \tau)$ to obtain likelihood estimates using the R package `pomp` [23, 22]. Figure 6 shows the logarithm of the likelihood estimates using one hundred particles. The left and the middle plots respectively show the confidence intervals for $\text{logit}(\kappa)$ and $\text{log}(\tau)$ where the other parameter was fixed at its true value. The right plot shows the 80%, 90%, and 95% confidence regions constructed by carrying out the hypothesis tests jointly for both parameters, $H_0 : (\kappa_*, \tau_*) = (\kappa_{*,0}, \tau_{*,0})$, $H_1 : (\kappa_*, \tau_*) = (\kappa_{*,0}, \tau_{*,0})$, for varied null value pairs and marking those for which the p-value is greater than 20%, 10%, and 5%, respectively. All three constructed confidence regions encompass the true parameter value.

Hypothesis tests were replicated one thousand times, each time generating a new observation sequence under $\kappa = 0.8$ and $\tau = 1$ and estimating the likelihood using one hundred particles. Figure 7 shows the estimated probabilities of rejecting the null hypothesis at a 5% significance level for varied null values. For tests on either parameter, the empirically estimated significance levels were close to the nominal significance level of 0.05, and the power increased as the null values diverged from the true values. The right plot of Figure 7 shows the rejection probability for the simultaneous test on both parameters. The empirical significance level was approximately 7.3%, and the rejection probability increased as $(\kappa_{*,0}, \tau_{*,0})$ moved farther from the true values.

Table 2 shows the percentages of the confidence intervals constructed for κ and τ that encompass the true

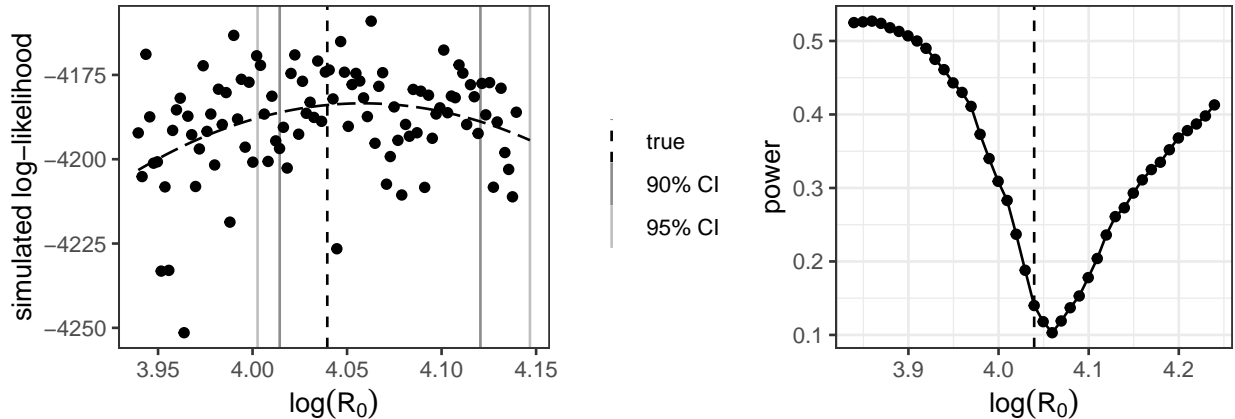


Figure 8: Left: Simulated log-likelihoods and the constructed 90% and 95% confidence intervals for $\log(R_0)$. Right: Probability of rejecting the null hypothesis for varied null values of R_0 at a 5% significance level. The true value is indicated by the dashed vertical line.

values. The likelihood estimates were obtained using either ten or one hundred particles. The confidence intervals constructed using our method include the true parameter values with probabilities close to the nominal confidence levels in both cases. However, the confidence intervals constructed using the method proposed by Ionides et al. [20] exhibit significantly lower coverage probabilities when a small number of particles are used for likelihood estimation. As the Monte Carlo variance of the log-likelihood estimate increases with fewer particles, the fitted quadratic polynomial may deviate significantly from the exact log-likelihood function. This leads to a misquantification of parameter uncertainty in the method of Ionides et al. [20]. In contrast, our method correctly distinguishes between K_1 and K_2 in the LAN of the simulated log-likelihoods (Proposition 1), maintaining accuracy even when weak or imprecise Monte Carlo likelihood estimators are used.

5.3 Stochastic SEIR model for population dynamics of measles transmission

We demonstrate our parameter inference procedure applied to a mechanistic model describing the population dynamics of measles transmission in England and Wales between 1950 and 1964. Weekly reported case data for twenty cities were analyzed by He et al. [19] using a stochastic compartment model consisting of the susceptible (S), exposed (E), infectious (I), and recovered (R) compartments. Partial observations of the compartment sizes are given by weekly reported case numbers, which are random fractions of weekly aggregate transitions from the infectious to the recovered compartment. We carried out parameter inference for the basic reproduction number R_0 . Model details as well as additional parameter inference results are given in the supplementary text Section S7.3.

We simulated the SEIR model at a suitably chosen parameter vector and generated a sequence of weekly reported cases data. Unbiased likelihood estimate for the observed data sequence were obtained for varied parameters using the bootstrap particle filter via the R package `pomp`. The left plot of Figure 8 shows the simulated log-likelihoods for varied $\log(R_0)$ and the constructed 90% and 95% confidence intervals. Simulations were carried out at $M = 100$ points uniformly placed between the exact value ± 0.1 on the log scale. We replicated simulation-based inference for R_0 one thousand times. The right plot of Figure 8 shows the probability of rejecting the null hypothesis at a 5% significance level for varied null values of R_0 . The empirical significance level was somewhat higher than the nominal significance level. However, the rejection probability was minimized near the true parameter value, indicating a reasonably small bias in parameter inference.

method	Number of simulations					
	100	1000	3000	10^4	3×10^4	10^5
pseudo-marginal MCMC	0.17	0.21	0.25	0.30	0.36	0.40
metamodel-based	0.54	18	58	190	600	1800

Table 3: Effective sample sizes for pseudo-marginal MCMC and corresponding efficiency measures for our metamodel-based method, with varying numbers of simulations.

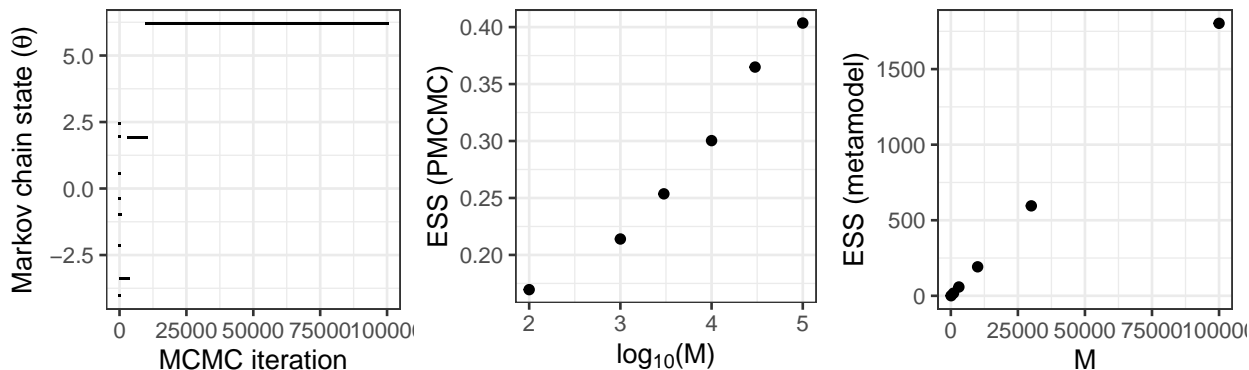


Figure 9: Left: Trace plot of a pseudo-marginal MCMC run with length $M = 10^5$ for Example 2. Middle: The effective sample size of pseudo-marginal MCMC scales approximately logarithmically with the length of the Markov chain. Right: The corresponding efficiency measure for our metamodel-based method scales linearly with the number of simulations.

6 Comparison with pseudo-marginal MCMC

We compare our metamodel-based inference method to a pseudo-marginal Markov chain Monte Carlo method in terms of sampling efficiency. For a metamodel-based method, the condition for parameter identifiability (10),

$$(\delta\theta)^\top c(y_{1:n})(\delta\theta) \gtrsim \frac{\sigma(y_{1:n})}{\sqrt{M}}$$

implies that for given data $y_{1:n}$, the standard error of our metamodel-based parameter estimator scales approximately as $\|\delta\theta\| = \mathcal{O}(M^{-1/4})$ as the number of simulation M increases. We will demonstrate that pseudo-marginal MCMC methods scale much more poorly, with the rate of $\|\delta\theta\|$ scaling as $\mathcal{O}((\log M)^{-1/4})$, which is significantly worse than our metamodel-based method.

Pseudo-marginal Markov chain Monte Carlo enables Bayesian inference where an unbiased estimator $\hat{L}(\theta; y_{1:n})$ of the likelihood $L(\theta; y_{1:n})$ is available [2]. When the unbiased likelihood estimator is obtained for a POMP model using the particle filter, the method is referred to as particle Markov chain Monte Carlo (PMCMC) [1]. Pseudo-marginal MCMC constructs a Markov chain having the posterior density

$$\pi(\theta|y_{1:n}) \propto h(\theta) \cdot L(\theta; y_{1:n})$$

as a stationary distribution, where $h(\theta)$ denotes the density of a prior distribution. Suppose that at a certain point, the current state of the constructed Markov chain is θ and an unbiased likelihood estimate $\hat{L}(\theta; y_{1:n})$ has been obtained. A candidate θ' for the next state of the Markov chain is proposed using a proposal kernel with density $q(\theta'|\theta)$. If we denote by $\hat{L}(\theta'; y_{1:n})$ a new Monte Carlo likelihood estimate obtained by running simulations under θ' , the proposed candidate θ' is accepted with probability

$$\min \left(1, \frac{h(\theta')\hat{L}(\theta'; y_{1:n})q(\theta|\theta')}{h(\theta)\hat{L}(\theta; y_{1:n})q(\theta'|\theta)} \right). \quad (32)$$

The elements of the constructed Markov chain are considered as approximate draws from the target posterior distribution.

We numerically compare pseudo-marginal MCMC with our method using the following example.

Example 2. Consider $X_{1:n} \stackrel{iid}{\sim} \mathcal{N}(\theta, \tau^2)$ and conditionally independent observations $Y_i|X_i \sim \mathcal{N}(X_i, 1)$, $i \in 1:n$, where $\tau = 30$ is known. Suppose that observations $y_{1:n}$ are available with $n = 200$. Independent simulations $X_{1:n}$ are drawn from the $\mathcal{N}(\theta, \tau^2)$ distribution, and the simulated log-likelihood is given by $\ell^S(\theta) = -\frac{1}{2} \sum_{i=1}^n (X_i - y_i)^2 - \frac{n}{2} \log(2\pi)$. The exact MLE is given by the sample mean, $\bar{y} = \frac{1}{n} \sum_{i=1}^n y_i$. Marginally, $Y_i \stackrel{iid}{\sim} \mathcal{N}(\theta, \tau^2 + 1)$, and the exact 95% confidence interval for θ is given by $\bar{y} \pm z_{0.025} \cdot \sqrt{(\tau^2 + 1)/n}$ where $P[\mathcal{N}(0, 1) > z_{0.025}] \approx 1.96 = 0.025$. For Bayesian inference, we consider a flat prior $h(\theta) \equiv 1$. The posterior distribution is given by $\theta|y_{1:n} \sim \mathcal{N}(\bar{y}, \frac{\tau^2+1}{n})$, and the 95% Bayesian credible interval is identical to the 95% confidence interval, $\bar{y} \pm z_{0.025} \cdot \sqrt{(\tau^2 + 1)/n}$. In this section, pseudo-marginal MCMC was run with proposal kernel $\theta' \sim \mathcal{N}(\theta, 3^2)$.

Consider a Markov chain of length M constructed by pseudo-marginal MCMC. This chain uses the same number of simulations as a metamodel-based method that employs M simulated log-likelihoods. In a pseudo-marginal MCMC, a proposed value θ is accepted if the associated simulated log-likelihood $\ell^S(\theta)$ is relatively large compared to the previous values in the chain. However, if the data size n is large, the Monte Carlo standard deviation σ of the simulated log-likelihoods scales as $\mathcal{O}(\sqrt{n})$ and thus dominates the difference in the log-likelihood function, which remains $\mathcal{O}(1)$ over the range of the exact Bayesian credible interval. Thus, whether a proposed value is accepted is almost entirely dependent on chance variation in $\ell^S(\theta)$, and the probability that the Markov chain changes value at the m -th step is approximately m^{-1} . Hence, the total number of updates in a chain of length M scales as $\sum_{m=1}^M m^{-1} \approx \log M$. The left plot of Figure 9 shows a trace plot of a pseudo-marginal MCMC chain of length $M = 10^5$ for Example 2. This chain remains at the same value for approximately 90% of its length. The MCMC parameter estimate $\hat{\theta}_{MCMC}^M$, obtained by averaging the values in the chain, has variability comparable to that of a single draw from the posterior. The efficiency of MCMC can be assessed using the effective sample size (ESS), defined as

$$\text{ESS} = \frac{\text{Var}_{\pi}(\theta)}{\text{Var}(\hat{\theta}_{MCMC}^M)}, \quad (33)$$

where the numerator represents the variance of the target posterior distribution for θ , and the denominator represents the Monte Carlo variance of the MCMC estimator $\hat{\theta}_{MCMC}^M$.

We estimated the ESS for pseudo-marginal MCMC by computing the Monte Carlo variance $\text{Var}(\hat{\theta}_{MCMC}^M)$ using one thousand independently constructed Markov chains. For each chain, MCMC estimates for θ were obtained by taking the running average at steps $M = 100, 1000, 3000, 10^4, 3 \times 10^4$, and 10^5 after discarding the first one hundred iterations as burn-in. The effective sample sizes were then calculated by substituting the sample variance of these one thousand MCMC estimates into the denominator of (33). The exact value of the numerator was given by $(\tau^2 + 1)/n$. For comparison, we estimated the parameter θ using our metamodel-based method with the same range of simulation counts M . A corresponding efficiency measure was computed using Equation 33, replacing the denominator with the sample variance of the parameter estimates across one thousand replications. Table 3 presents the ESS values for both methods. For pseudo-marginal MCMC, the effective sample size grew very slowly and remained extremely low even at $M = 10^5$. The fact that the ESS was less than one suggests that the chains had not yet effectively explored the target posterior distribution and that the MCMC estimate $\hat{\theta}_{MCMC}^M$ was essentially determined by a single best simulation outcome, similar to what was demonstrated in the top panel of Figure 1. The middle plot of Figure 9 shows that these ESS values scaled logarithmically with the chain length M . In contrast, the equivalent ESS values for our metamodel-based method were dramatically higher than those for pseudo-marginal MCMC. The right plot of Figure 9 shows that the ESS scaled linearly with the number of simulations M , indicating no diminishing returns.

Next, we constructed Monte Carlo interval estimates for θ using both methods. The left plot of Figure 10 shows a 95% credible interval constructed using $M = 1000$ pseudo-marginal MCMC draws, after discarding the first one hundred iterations as burn-in. This interval estimate exhibits a substantial bias relative to the exact credible interval, as the constructed chain remains outside the exact 95% credible interval for most of

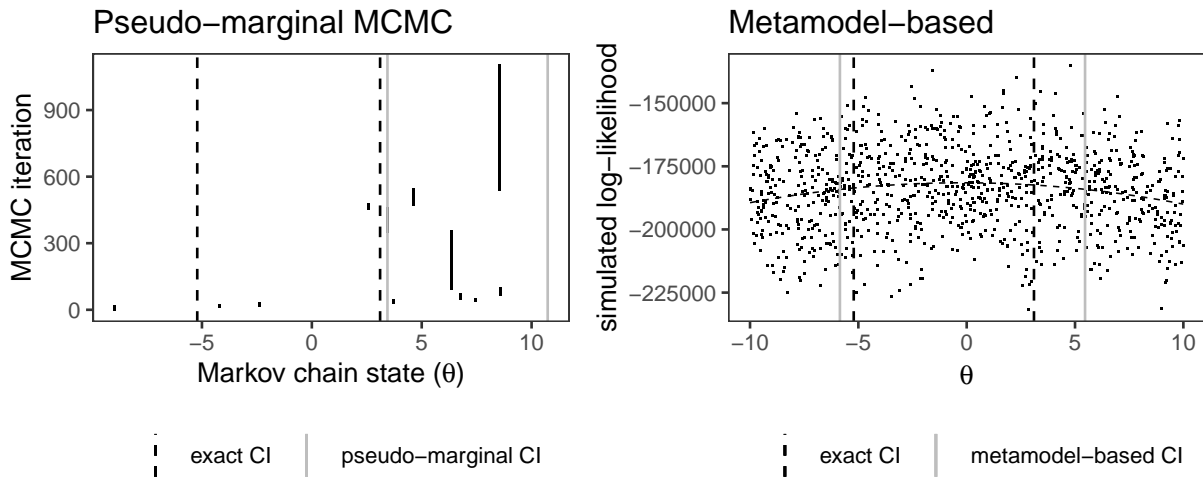


Figure 10: Left: Trace plot of a Markov chain of length 1100 using pseudo-marginal MCMC for Example 2. The exact 95% credible interval is marked by two vertical dashed lines. The 95% credible interval constructed from the MCMC draws, after discarding the first one hundred as burn-in, is marked by vertical gray lines. Right: A 95% confidence interval for θ generated using our metamodel-based method with $M = 1000$ simulations, marked by gray vertical lines. The exact 95% confidence interval, indicated by dashed vertical lines, is identical to the exact 95% credible interval in the left panel.

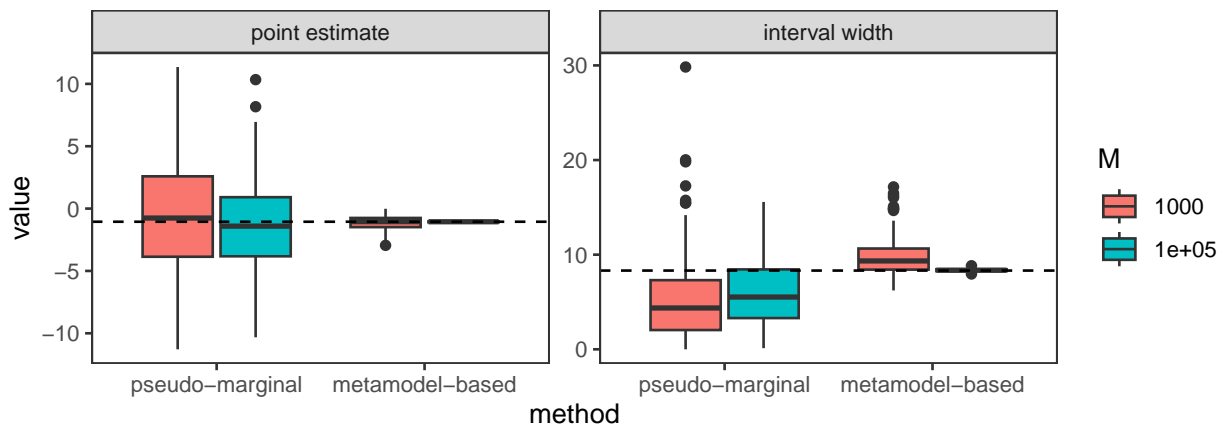


Figure 11: Left: Distribution of point estimates for θ obtained by pseudo-marginal MCMC and our metamodel-based method using $M = 10^3$ and 10^5 simulations. The exact MLE ($= \bar{y}$) is indicated by the horizontal line. Right: Distribution of the widths of the constructed 95% credible intervals for pseudo-marginal MCMC and the 95% confidence intervals constructed using our metamodel-based method. The width of the exact 95% credible and confidence intervals is indicated by the horizontal line.

its run. In contrast, the right panel of Figure 10 shows that a 95% confidence interval constructed using our metamodel-based method is reasonably close to the exact confidence interval, with a moderately greater width due to simulation randomness.

Figure 11 shows the distribution of point estimates and the widths of constructed 95% credible and confidence intervals for two hundred replications of each method. The number of simulations were either $M = 10^3$ or 10^5 . The left panel illustrates that the point estimates derived from pseudo-marginal MCMC exhibit significantly higher variation than those obtained by our metamodel-based method. For pseudo-marginal MCMC, the variation decreases only marginally when the number of iterations M increases from 10^3 to 10^5 . In contrast, point estimates obtained by our metamodel-based method have both high precision and high accuracy. The right panel of Figure 11 shows that the widths of the 95% credible intervals constructed using pseudo-marginal MCMC present substantial variation and a significant downward bias relative to the exact 95% credible interval, indicating an underestimation of parameter uncertainty. In contrast, the 95% confidence intervals constructed using our metamodel-based method show only moderate upward bias and variation when $M = 1000$. With $M = 10^5$ simulations, the simulation-based uncertainty is nearly eliminated, yielding Monte Carlo confidence intervals that closely match the exact confidence interval.

The fact that the ESS of pseudo-marginal MCMC scales logarithmically with M implies that a desired level of precision in parameter estimation may not be achieved in practice. Specifically, in the supplementary text, Section S8.1, we argue that parameter estimates obtained by pseudo-marginal MCMC have standard errors approximately given by

$$\text{standard error of } \hat{\theta}_{MCMC}^M \approx \|c\|^{-1/2} \sigma^{1/2} (\log M)^{-1/4}, \quad (34)$$

where c indicates the curvature of the expected simulated log-likelihood $\mu(\theta)$ and σ the standard deviation of the simulated log-likelihoods. This result is numerically supported by Figure 11, which shows a slight reduction in the variability of parameter estimates from pseudo-marginal MCMC when M increases from 10^3 to 10^5 . Hence, to achieve a standard error of $\mathcal{O}(1/\sqrt{n})$, one must have

$$\log M = \mathcal{O}(\sigma^2),$$

given that $\|c\| = \mathcal{O}(n)$. These results align with the findings of Pitt et al. [29] and Doucet et al. [16], which suggest that the computational budget is optimally allocated when a sufficiently large amount of Monte Carlo effort is invested to ensure that the Monte Carlo variance of the log-likelihood estimator, σ^2 , is close to one.

When the particle filter is used for likelihood estimation with J particles, Bérard et al. [7] establish in a central limit theorem-type result that σ^2 asymptotically scales as $\mathcal{O}(n/J)$ under certain regularity conditions. This suggests that choosing $J = \mathcal{O}(n)$ particles may achieve optimal efficiency for pseudo-marginal MCMC. However, this result has practical implications only when each observation y_i , $i \in 1:n$, is low dimensional. The claimed asymptotic normality of ℓ^S is not attained unless J is exponentially large in the dimension of y_i , due to the highly skewed distribution of the measurement density $g_i(y_i|X_i)$. The requirement for the number of particles to increase exponentially with the space dimension is well known in the particle filter literature and is often referred to as the curse of dimensionality [6, 32]. If the dimension k of each y_i is at least moderately large, the distribution of the simulated log-likelihood ℓ_i^S can be approximated as

$$\hat{\ell}_i^S = \log \left\{ \frac{1}{J} \sum_{j=1}^J g_i(y_i|X_i^j) \right\} \approx \max_{j \in 1:J} \log g_i(y_i|X_i^j) - \log J. \quad (35)$$

However, the variance of the right-hand side of (35) scales as $\mathcal{O}(k/\log J)$, provided that the distribution of $\log g_i(y_i|X_i^j)$ is approximately normal. See the supplementary text (Section S8.2) for numerical justification. This suggests that, to achieve $\sigma^2 \approx 1$ for optimal efficiency in pseudo-marginal MCMC, $J = \mathcal{O}(e^k)$ particles should be used for likelihood estimation at each MCMC iteration. In contrast, our metamodel-based inference method enables robust and accurate parameter inference even when σ^2 is large, as the required number of simulations scales linearly with σ^2 .

We compared the coverage probabilities of interval estimates and the effective sample sizes of pseudo-marginal MCMC and our proposed method as the data size n varied among 10, 50, 200, and 1000. The left plot of Figure 12 presents the proportion of 95% credible and confidence intervals that contain the true

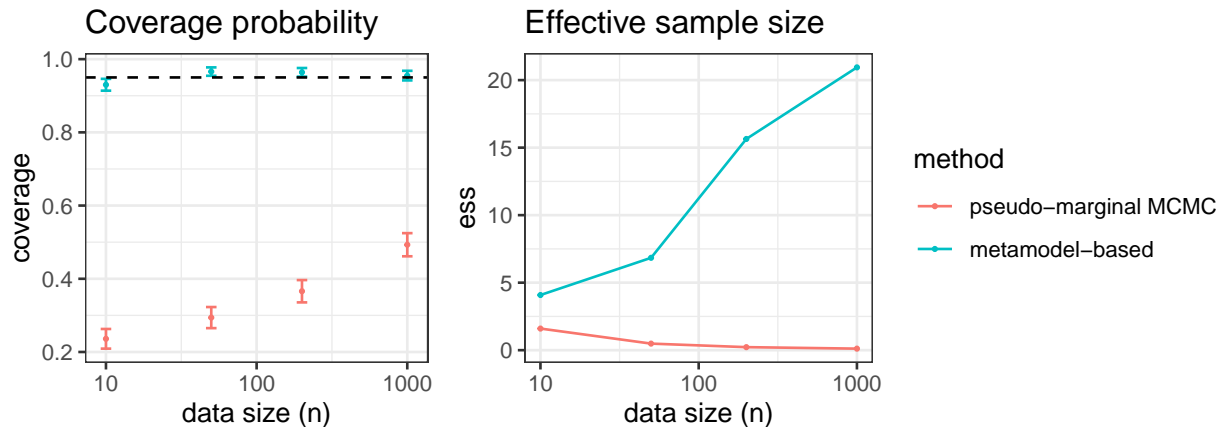


Figure 12: Left: Coverage probabilities of the 95% credible intervals constructed using pseudo-marginal MCMC and the 95% confidence intervals constructed using our metamodel-based method, with data size ranging from ten to one thousand. The nominal 95% level is indicated by a horizontal dashed line, and the error bars represent plus or minus two standard errors. Right: Effective sample sizes for pseudo-marginal MCMC and our metamodel-based method, averaged over one hundred generated datasets, for varying data sizes.

parameter value, $\theta = 0$. The credible intervals were constructed using $M = 1000$ samples from pseudo-marginal MCMC after discarding the first 100 burn-in cycles. The confidence intervals for our metamodel-based method were constructed using the same number of simulations ($M = 1000$). Approximately 95% of the intervals constructed by our metamodel-based approach contained the true parameter value. In contrast, the credible intervals obtained from pseudo-marginal MCMC exhibited notably lower coverage. The underestimation of parameter uncertainty in pseudo-marginal MCMC is due to its very low effective sample size.

The right plot of Figure 12 shows the average effective sample sizes (ESS) for pseudo-marginal MCMC and our metamodel-based method across the same range of n . The estimated ESS values were averaged over 100 generated datasets. For each dataset, the ESS was computed by comparing the sample standard deviation of the parameter estimates with the exact posterior standard deviation using Equation 33. The ESS for pseudo-marginal MCMC decreases as the data size increases due to the increasing variability and skewness in the distribution of the Monte Carlo likelihood estimator. In contrast, the ESS for the metamodel-based method is significantly higher and increases with n , as the improved signal-to-noise ratio of the simulated log-likelihoods enables precise parameter estimation using the metamodel. Both plots in Figure 12 demonstrate that the metamodel-based approach scales significantly better with increasing data size than pseudo-marginal MCMC.

7 Automatic tuning algorithms

In this section, we introduce two automatic tuning algorithms that enhance the applicability of the inference methods developed in this paper. The first algorithm automatically adjusts the weights assigned to simulated outcomes, ensuring that the quadratic approximation to the simulated log-likelihoods introduces little bias. Specifically, the weights of the parameter points far from the estimated MESLE are discounted so that the third order term in a cubic regression becomes statistically insignificant. This automatic weight adjustment scheme can be incorporated into Algorithm 1 to improve hypothesis testing and confidence interval construction. The second algorithm proposes the next simulation point to achieve near-optimal efficiency. This point is selected to minimize the Monte Carlo variance of the parameter estimate while ensuring that the quadratic approximation to the simulated log-likelihoods remain valid. Both of these algorithms are implemented in the R package `sbim`. Further details on these algorithms are provided in the supplementary text (Section S9.)

Algorithm 4 Automatic weight adjustments for bias reduction

```
1: Fit a quadratic polynomial to  $(\theta_m, \ell^S(\theta_m))$  with weights  $w_m, m \in 1 : M$ , to obtain a first-stage quadratic
   approximation  $q_2(\theta) = \hat{a} + \hat{b}^\top \theta + \theta^\top \hat{c} \theta$ 
2: Let  $\hat{\theta}_{MESLE} = -\frac{1}{2} \hat{c}^{-1} \hat{b} = \arg \max_{\theta} q_2(\theta)$  be the estimated MESLE
3: Let  $g \leftarrow \infty$ 
4: loop
5:   Weight adjustments:  $w_m^{adj} = w_m \cdot \exp(-\{q_2(\hat{\theta}_{MESLE}) - q_2(\theta_m)\}/g)$ 
6:   Update  $q_2$  and  $\hat{\theta}_{MESLE}$  using the adjusted weights
7:   Fit a cubic polynomial to  $(\theta_m, \ell^S(\theta_m))$  with weights  $w_m^{adj}, m \in 1 : M$ 
8:   Let  $p_{cubic}$  be the p-value for the significance of the cubic term
9:   if  $p_{cubic} < 0.01$  then ▷ cubic term is significant, decrease  $g$ 
10:     if  $g = \infty$  then
11:       Let  $g \leftarrow q_2(\hat{\theta}_{MESLE}) - \min_{m \in 1 : M} q_2(\theta_m)$ 
12:     else
13:       Let  $g \leftarrow g/1.8$ 
14:     end if
15:   else if  $p_{cubic} > 0.3$  then ▷ cubic term is not significant, increase  $g$  for efficiency
16:     Let  $g \leftarrow 1.3 \cdot g$ 
17:   else
18:     Break from loop
19:   end if
20: end loop
```

7.1 Automatic weight adjustments for bias reduction

Obtaining simulated log-likelihoods across a wide range of parameter values increases estimation efficiency but also introduces bias due to the approximation error of a quadratic polynomial. We develop an algorithm that automatically balances efficiency and accuracy by adjusting the weights w_m assigned to the parameter value θ_m . Denoting by $q_2(\theta)$ the quadratic polynomial fitted to $(\theta_m, \ell^S(\theta_m))$ with weights w_m , the weight for the m -th point is adjusted as

$$w_m^{adj} \leftarrow w_m \cdot \exp\left(-\frac{q_2(\hat{\theta}_{MESLE}) - q_2(\theta_m)}{g}\right),$$

ensuring that points far from the estimated MESLE, $\hat{\theta}_{MESLE}$, have more heavily discounted weights. The scalar g is tuned using an iterative procedure as follows. Let p_{cubic} be the p-value indicating the significance of the cubic term when a cubic polynomial is fitted to $(\theta_m, \ell^S(\theta_m))$ with the adjusted weights w_m^{adj} for $m \in 1 : M$.

- If the cubic term is highly statistically significant (e.g., $p_{cubic} < 0.01$), the quadratic approximation q_2 is likely introducing significant error. In this case, we decrease g to narrow the range of parameter values that effectively contribute to parameter estimation.
- Conversely, If the cubic term is insignificant (e.g., $p_{cubic} > 0.3$), the quadratic approximation q_2 is sufficiently accurate, allowing for broader exploration of the parameter space to improve estimation efficiency. In this case, we increase g .

The value of g is iteratively adjusted until p_{cubic} suggests a reasonable balance between efficiency and accuracy. Algorithm 4 summarizes this procedure. The functions `ht` and `ci` in the `sbim` package include an option to automatically adjust the weights before performing hypothesis testing or constructing confidence intervals.

Algorithm 5 Near-optimal selection of the next simulation point

- 1: **Input:** simulation points $\{\theta_m; m \in 1:M\}$; simulated log-likelihoods $\{\ell^S(\theta_m); m \in 1:M\}$; weights $\{w_m; m \in 1:M\}$
 - 2: **Output:** a proposal for the next simulation point θ_{M+1}
 - 3: Adjust weights w_m to reduce the bias due to quadratic approximation (Algorithm 4)
 - 4: Fit a quadratic polynomial to $(\theta_m, \ell^S(\theta_m))$ with the adjusted weights w_m^{adj} , $m \in 1:M$ and let $\hat{A} = (\hat{a}, \hat{b}^\top, \text{vech}(\hat{c})^\top)^\top$ be the estimated coefficients.
 - 5: Define STV by (36) as a function of θ_{M+1}
 - 6: Find $\arg \min_{\theta_{M+1}} STV(\theta_{M+1})$ using a gradient-based numerical optimization algorithm such as BFGS and return the minimizer
-

7.2 Selecting the next simulation point for near-optimal efficiency

Given the costs associated with simulations, efficiently selecting simulation points is practically important. In particular, experiments should be designed to minimize the Monte Carlo variability of parameter estimates for a given number of simulations. We develop an algorithm that sequentially proposes the next simulation point to achieve near-optimal efficiency.

Suppose that currently there are M simulated log-likelihoods available, obtained at θ_m , $m \in 1:M$. Let $\hat{A} = (\hat{a}, \hat{b}^\top, \text{vech}(\hat{c})^\top)^\top$ be the coefficients of the fitted quadratic polynomial with weights adjusted as described in Section 7.1. We see from (17) that the Monte Carlo variance of \hat{A} is given by

$$\text{Var}(\hat{A}) = \sigma^2 \{\theta_{1:M}^{0:2 \top} W^{adj} \theta_{1:M}^{0:2}\}^{-1}$$

where W^{adj} is the diagonal matrix having the adjusted weights w_m^{adj} as its diagonal entries. Applying the delta method, we can approximate the Monte Carlo variance of the estimated MESLE, $\hat{\theta}_{MESLE} = -\frac{1}{2}\hat{c}^{-1}\hat{b}$, by

$$\text{Var}(\hat{\theta}_{MESLE}) \approx \sigma^2 \left(\frac{\partial \hat{\theta}_{MESLE}}{\partial \hat{A}} \right) \{\theta_{1:M}^{0:2 \top} W^{adj} \theta_{1:M}^{0:2}\}^{-1} \left(\frac{\partial \hat{\theta}_{MESLE}}{\partial \hat{A}} \right)^\top.$$

After a new simulation is performed at θ_{M+1} , the variance of $\hat{\theta}_{MESLE}$ decreases to

$$\sigma^2 \left(\frac{\partial \hat{\theta}_{MESLE}}{\partial \hat{A}} \right) \{\theta_{1:M}^{0:2 \top} W^{adj} \theta_{1:M}^{0:2} + w_{M+1}^{adj} \theta_{M+1}^{0:2} \theta_{M+1}^{0:2 \top}\}^{-1} \left(\frac{\partial \hat{\theta}_{MESLE}}{\partial \hat{A}} \right)^\top$$

where w_{M+1}^{adj} is the adjusted weight for the new simulation point. We select the next simulation point that minimizes a scaled total variation of $\hat{\theta}_{MESLE}$, defined as

$$\text{STV} := \text{Tr} \left\{ -\hat{c}^{-1} \left(\frac{\partial \hat{\theta}_{MESLE}}{\partial \hat{A}} \right) \{\theta_{1:M}^{0:2 \top} W^{adj} \theta_{1:M}^{0:2} + w_{M+1}^{adj} \theta_{M+1}^{0:2} \theta_{M+1}^{0:2 \top}\}^{-1} \left(\frac{\partial \hat{\theta}_{MESLE}}{\partial \hat{A}} \right)^\top \right\}. \quad (36)$$

Here Tr denotes the trace of a matrix and $-\hat{c}$ is the curvature of the fitted quadratic function before the addition of the new simulation point. The scaled total variation (STV) of the parameter estimator incorporates inferential connections between parameter components and their relative scales by multiplying the approximated Monte Carlo variance by $-\hat{c}^{-1}$. Algorithm 5 summarizes the automatic design point selection procedure. The next simulation point, θ_{M+1} , can be determined using standard numerical optimization routines such as the Broyden–Fletcher–Goldfarb–Shanno (BFGS) algorithm [17]. Section S9 of the supplementary text provides numerical demonstrations and additional details on this algorithm. The method is implemented in the `optDesign` function of the `sbim` package.

8 Discussion

We developed a scalable inference method for models implicitly defined using simulators. Implicitly defined, mechanistic models for the processes of interest can enable interpretable inference and accurate prediction.

However, exact simulation-based inference for these models is often impossible due to exponentially scaling Monte Carlo errors. Our method employs a metamodel for the Monte Carlo log-likelihood estimator, enabling highly scalable inference. We propose a principled approach to uncertainty quantification, which is often not addressed by recent methods using machine learning techniques that train surrogate models approximating the distribution of observations. Our metamodel-based approach also differs from the synthetic likelihood method proposed by Wood [36], in that our metamodel describes the distribution of the log-likelihood estimator rather than that of summary statistics selected using domain knowledge.

We leave a few ideas that stem from the current work for future projects. First, the assumptions in our metamodel may be relaxed to account for heteroskedasticity of log-likelihood estimators. The extended model is likely to pose challenges in parameter estimation and uncertainty quantification, which might be addressed using suitable computational Bayesian methods. Second, our inference framework using a metamodel for the log-likelihood estimator may be applied to likelihood estimates obtained from recently developed tools such as normalizing flows. This application may benefit from a semiparametric extension of the metamodel, incorporating Gaussian-process-valued fluctuations around the quadratic approximation of the mean function.

The parameter inference methods developed in this paper are implemented in the R package `sbim` (<https://CRAN.R-project.org/package=sbim>).

Acknowledgments

The author is grateful to Edward Ionides for his comments on early drafts of this manuscript.

References

- [1] C. Andrieu, A. Doucet, and R. Holenstein. Particle Markov chain Monte Carlo methods. *J. R. Stat. Soc. Ser. B. Stat. Methodol.*, 72(3):269–342, 2010.
- [2] C. Andrieu and G. O. Roberts. The pseudo-marginal approach for efficient Monte Carlo computations. *Ann. Statist.*, 37(2):697–725, 2009.
- [3] R. R. Barton and M. Meckesheimer. Metamodel-based simulation optimization. *Handbooks in operations research and management science*, 13:535–574, 2006.
- [4] M. A. Beaumont. Estimation of population growth or decline in genetically monitored populations. *Genetics*, 164(3):1139–1160, 2003.
- [5] M. A. Beaumont, W. Zhang, and D. J. Balding. Approximate Bayesian computation in population genetics. *Genetics*, 162(4):2025–2035, 2002.
- [6] T. Bengtsson, P. Bickel, and B. Li. Curse-of-dimensionality revisited: collapse of the particle filter in very large scale systems. In *Probability and Statistics: Essays in Honor of David A. Freedman*, pages 316–334. Institute of Mathematical Statistics, 2008.
- [7] J. Bérard, P. Del Moral, and A. Doucet. A lognormal central limit theorem for particle approximations of normalizing constants. *Electron. J. Probab.*, 19(94):1–28, 2014.
- [8] O. Cappé, S. J. Godsill, and E. Moulines. An overview of existing methods and recent advances in sequential Monte Carlo. *Proceedings of the IEEE*, 95(5):899–924, 2007.
- [9] F. Cérou, P. Del Moral, and A. Guyader. A nonasymptotic theorem for unnormalized feynman–kac particle models. *Ann. Inst. Henri Poincaré Probab. Stat.*, 47(3):629–649, 2011.
- [10] K. Cranmer, J. Brehmer, and G. Louppe. The frontier of simulation-based inference. *Proc. Natl. Acad. Sci. USA*, 117(48):30055–30062, 2020.
- [11] P. Del Moral. *Feynman-Kac Formulae: Genealogical and Interacting Particle Systems with Applications*. Springer, New York, 2004.

- [12] P. J. Diggle and R. J. Gratton. Monte Carlo methods of inference for implicit statistical models. *J. R. Stat. Soc. Ser. B. Stat. Methodol.*, pages 193–227, 1984.
- [13] L. Dinh, D. Krueger, and Y. Bengio. NICE: Non-linear independent components estimation. 2014.
- [14] L. Dinh, J. Sohl-Dickstein, and S. Bengio. Density estimation using real NVP. In *International Conference on Learning Representations*, 2017.
- [15] A. Doucet, N. De Freitas, and N. Gordon. An introduction to sequential Monte Carlo methods. In A. Doucet, N. De Freitas, and N. Gordon, editors, *Sequential Monte Carlo methods in practice*, chapter 1, pages 3–14. Springer, 2001.
- [16] A. Doucet, M. Pitt, G. Deligiannidis, and R. Kohn. Efficient implementation of Markov chain Monte Carlo when using an unbiased likelihood estimator. *Biometrika*, 102(2):295–313, 2015.
- [17] R. Fletcher. *Practical methods of optimization*. John Wiley & Sons, second edition, 1987.
- [18] N. J. Gordon, D. J. Salmond, and A. F. Smith. Novel approach to nonlinear/non-Gaussian Bayesian state estimation. *IEE Proceedings F (Radar and Signal Processing)*, 140(2):107–113, 1993.
- [19] D. He, E. L. Ionides, and A. A. King. Plug-and-play inference for disease dynamics: measles in large and small populations as a case study. *Journal of the Royal Society Interface*, 7(43):271–283, 2009.
- [20] E. L. Ionides, C. Breto, J. Park, R. A. Smith, and A. A. King. Monte Carlo profile confidence intervals for dynamic systems. *Journal of The Royal Society Interface*, 14(132):20170126, 2017.
- [21] R. E. Kalman. A new approach to linear filtering and prediction problems. *Journal of Basic Engineering*, 82(1):35–45, 1960.
- [22] A. A. King, E. L. Ionides, C. M. Bretó, S. P. Ellner, M. J. Ferrari, S. Funk, S. G. Johnson, B. E. Kendall, M. Lavine, D. Nguyen, E. B. O’Dea, D. C. Reuman, H. Wearing, and S. N. Wood. *pomp: Statistical Inference for Partially Observed Markov Processes*, 2023. R package, version 5.4.
- [23] A. A. King, D. Nguyen, and E. L. Ionides. Statistical inference for partially observed Markov processes via the R package pomp. *Journal of Statistical Software*, 69(12):1–43, 2016.
- [24] R. Laubenbacher, J. P. Sluka, and J. A. Glazier. Using digital twins in viral infection. *Science*, 371(6534):1105–1106, 2021.
- [25] L. Le Cam and G. L. Yang. *Asymptotics in statistics: some basic concepts*. Springer-Verlag New York, Inc., 2000.
- [26] National Academies of Sciences, Engineering, and Medicine (NASEM). *Foundational Research Gaps and Future Directions for Digital Twins*. The National Academies Press, Washington, DC, 2024.
- [27] J. A. Nelder and R. Mead. A simplex method for function minimization. *Comput. J.*, 7(4):308–313, 1965.
- [28] G. Papamakarios, T. Pavlakou, and I. Murray. Masked autoregressive flow for density estimation. *Advances in neural information processing systems*, 30, 2017.
- [29] M. K. Pitt, R. dos Santos Silva, P. Giordani, and R. Kohn. On some properties of Markov chain Monte Carlo simulation methods based on the particle filter. *J. Econometrics*, 171(2):134–151, 2012. Bayesian Models, Methods and Applications.
- [30] C. Sherlock, A. H. Thiery, G. O. Roberts, and J. S. Rosenthal. On the efficiency of pseudo-marginal random walk Metropolis algorithms. *Ann. Statist.*, 43(1):238 – 275, 2015.
- [31] S. A. Sisson, Y. Fan, and M. Beaumont. *Handbook of approximate Bayesian computation*. CRC press, 2018.

- [32] C. Snyder, T. Bengtsson, P. Bickel, and J. Anderson. Obstacles to high-dimensional particle filtering. *Monthly Weather Review*, 136(12):4629–4640, 2008.
- [33] R. Subramanian, Q. He, and M. Pascual. Quantifying asymptomatic infection and transmission of covid-19 in new york city using observed cases, serology, and testing capacity. *Proc. Natl. Acad. Sci. USA*, 118(9):e2019716118, 2021.
- [34] F. Tao and Q. Qi. Make more digital twins. *Nature*, 573(7775):490–491, 2019.
- [35] A. W. Van der Vaart. *Asymptotic statistics*. Cambridge university press, 1998.
- [36] S. N. Wood. Statistical inference for noisy nonlinear ecological dynamic systems. *Nature*, 466(7310):1102–1104, 2010.

Supplementary text for *Scalable simulation-based inference for implicitly defined models using a metamodel for Monte Carlo log-likelihood estimator*

Joonha Park

Department of Mathematics, University of Kansas, Lawrence, KS 66045 USA
(email: j.park@ku.edu)

S1 Further details on the simulation-based proxy $\mathcal{R}(\theta_0)$ and inference bias

S1.1 Simulation-based proxy and MESLE for several iid examples

In this section, we compute the MESLE and the simulation-based proxy for several examples.

Example S1. Suppose that the latent process is given by n iid copies of Gamma random variables $X_1, \dots, X_n \sim \Gamma(\gamma, \lambda)$ with shape parameter γ and rate parameter λ . Partial observations Y_1, \dots, Y_n are given by $Y_i | X_i \sim \text{Pois}(X_i)$. Since $X_i = G_i / \lambda$ for $G_i \sim \Gamma(\gamma, 1)$, the expected simulated log-likelihood at λ is given by

$$\mu(\lambda; y_i) = \mathbb{E}[-X_i + y_i \log X_i + \text{const.}] = -\gamma \lambda^{-1} - y_i \log \lambda + \text{const.}$$

where the constant terms do not depend on λ . The expected simulated log-likelihood for n observations $y_{1:n}$ is given by

$$\mu(\lambda; y_{1:n}) = -n\gamma \lambda^{-1} - \sum_i y_i \cdot \log \lambda + \text{const.}$$

and the MESLE is given by $\lambda_{MESLE} = n\gamma / \sum_i y_i$. Each Y_i marginally follows the negative binomial distribution with probability mass function

$$p_\lambda^Y(y) = \frac{\Gamma(y + \gamma)}{\Gamma(y + 1)\Gamma(\gamma)} \left(\frac{1}{1 + \lambda}\right)^y \left(\frac{\lambda}{1 + \lambda}\right)^\gamma.$$

Thus it can be checked that MLE for λ is equal to the MESLE for this model.

The data-averaged expected simulated log-likelihood for n observations is given by

$$U(\lambda_0, \lambda) = \mathbb{E}_{Y_{1:n} \stackrel{iid}{\sim} P_{\lambda_0}^Y} \mu(\lambda; Y_{1:n}) = -n\gamma \lambda^{-1} - n\gamma \lambda_0^{-1} \log \lambda + \text{const.},$$

since the marginal mean of Y is equal to $\gamma \lambda_0^{-1}$. The simulation-based proxy $\mathcal{R}(\lambda_0)$ is thus equal to λ_0 .

The matrix $K_1(\lambda_0)$ is given by

$$K_1(\lambda_0) = \frac{1}{n} \text{Var}_{\lambda_0} \left[\frac{\partial \mu}{\partial \lambda}(\lambda_*; Y_{1:n}) \right] = \frac{1}{n} \lambda_*^{-2} \text{Var} \left(\sum_i Y_i \right) = \lambda_*^{-2} \gamma (1 + \lambda_0) \lambda_0^{-2} = \gamma \lambda_0^{-4} (1 + \lambda_0).$$

The matrix $K_2(\lambda_0)$ is given by

$$K_2(\lambda_0) = -\frac{1}{n} \mathbb{E} \frac{\partial^2}{\partial \lambda^2} \mu(\lambda_*; Y_{1:n}) = -\mathbb{E} [-2\gamma \lambda_*^{-3} + (\sum_i Y_i) \lambda_*^{-2}] = 2\gamma \lambda_*^{-3} - \lambda_*^{-2} \cdot \gamma \lambda_0^{-1} = \gamma \lambda_0^{-3}.$$

Note that this $K_2(\lambda_0)$ differs from the Fisher information for the marginal distribution of Y , which is given by

$$\mathcal{I}(\lambda_0) = \gamma(1 + \lambda_0)^{-1}\lambda_0^{-2}.$$

For the parameter values $\gamma = 1$ and $\lambda_0 = 1$ used in Section 5.1, $K_1(\lambda_0) = 2$, $K_2(\lambda_0) = 1$ and $\mathcal{I}(\lambda_0) = \frac{1}{2}$. Note that $K_1(\lambda_0)$ and $K_2(\lambda_0)$ are different. Additionally, the fact that $K_2(\lambda_0)$ differs from $\mathcal{I}(\lambda_0)$ aligns with the observation from Figure 2 that the second derivative of the estimated μ function (blue dashed curve) was greater in magnitude than that of the log-likelihood function (red dashed curve).

Example S2. Consider a normal model $X_1, \dots, X_n \stackrel{iid}{\sim} \mathcal{N}(\theta, I_d)$ where $\theta \in \mathbb{R}^d$. Partial observations are given by $Y_i|X_i \sim \mathcal{N}(X_i, I_d)$. Marginally, we have $Y_i \sim \mathcal{N}(\theta, 2I_d)$. The expected simulated log-likelihood for n observations $y_{1:n}$ is given by

$$\mu(\theta; y_{1:n}) = -\frac{1}{2} \sum_{i=1}^n \|y_i - \theta\|^2 + \text{const.} = -\frac{1}{2} \left(\sum_{i=1}^n \|y_i - \bar{y}\|^2 + n\|\bar{y} - \theta\|^2 \right) + \text{const.}$$

where $\bar{y} := \frac{1}{n} \sum_{i=1}^n y_i$. The MESLE is given by $\theta_{MESLE} = \bar{y}$, which is equal to the MLE. The data-averaged expected simulated log-likelihood for n observations is given by

$$U(\theta_0, \theta) = \mathbb{E}_{Y_{1:n} \stackrel{iid}{\sim} \mathcal{N}(\theta_0, 2I_d)} \mu(\theta; Y_{1:n}) = -\frac{n}{2} \|\theta - \theta_0\|^2 + \text{const.}$$

Therefore the simulation-based proxy $\mathcal{R}(\theta_0)$ is equal to θ_0 .

Example S3. Consider the normal model $X_1, \dots, X_n \stackrel{iid}{\sim} \mathcal{N}(0, \Sigma)$ and $Y_i|X_i \sim \mathcal{N}(X_i, \Psi)$, where Ψ is known and Σ is the unknown parameter. The expected simulated log-likelihood is given by

$$\mu(\Sigma; y_{1:n}) = -\frac{1}{2} \left\{ \sum_{i=1}^n y_i^\top \Psi^{-1} y_i + n \text{Tr}(\Psi^{-1} \Sigma) \right\} - \frac{n}{2} \log \det \Psi + \text{const.}$$

Therefore the MESLE is given by $\Sigma_{MESLE} = 0$. However, the MLE is given by $\Sigma_{MLE} = \frac{1}{n} \sum_i y_i y_i^\top - \Psi$. It can be seen that the simulation-based proxy $\mathcal{R}(\Sigma_0)$ is the zero matrix, thus again different from the true value Σ_0 .

Example S4. Consider the same model $X_1, \dots, X_n \stackrel{iid}{\sim} \mathcal{N}(0, \Sigma)$ and $Y_i|X_i \sim \mathcal{N}(X_i, \Psi)$ as in Example S3, but suppose that Σ is known and Ψ is the unknown parameter. It can be checked that the MESLE is given by $\Psi_{MESLE} = \frac{1}{n} \sum_i y_i y_i^\top + \Sigma$. However, the MLE for Ψ is given by $\hat{\Psi}_{MLE} = \frac{1}{n} \sum_{i=1}^n y_i y_i^\top - \Sigma$. The data-averaged expected simulated log-likelihood is given by

$$U(\Psi_0, \Psi) = -\frac{n}{2} \text{Tr}\{\Psi^{-1}(2\Sigma + \Psi_0)\} - \frac{n}{2} \log \det \Psi + \text{const.},$$

and the simulation-based proxy is given by $\mathcal{R}(\Psi_0) = 2\Sigma + \Psi_0$. Thus both the MESLE and the simulation-based proxy have a bias of 2Σ .

S1.2 Simulation-based proxy from an information theoretic perspective

In the case where the simulated log-likelihood is given by $\log g(y|X; \theta)$, the simulation-based proxy $\mathcal{R}(\theta_0)$ may be interpreted from an information-theoretic perspective as follows (see Proposition S1). The KL divergence between two distributions P and Q with densities p and q , respectively, will be denoted by

$$D_{KL}(P||Q) = \int \log \frac{dP}{dQ} dP = D_{KL}(p||q) = \int \log \frac{p(y)}{q(y)} p(y) dy.$$

In our parameterized setting we define the expected Kullback-Leibler divergence between P_{θ_0} and P_θ as

$$EKL(\theta_0||\theta) := \int D_{KL}(g_{x', \theta_0} || g_{x, \theta}) dP_{\theta_0}(x') dP_\theta(x),$$

where we write $g_{x, \theta}(y) \equiv g(y|x; \theta)$. The simulation-based proxy minimizes the expected KL divergence between $P_{\theta_0}^Y$ and $g_{X, \theta}$ as well as that between g_{X', θ_0} and $g_{X, \theta}$ where $X' \sim P_{\theta_0}$ is independent of $X \sim P_\theta$.

Proposition S1. *If the simulated log-likelihood $\ell^S(\theta; y)$ is given by $\log g(y|X; \theta)$ where X is a draw from P_θ , the simulation-based proxy satisfies*

$$\mathcal{R}(\theta_0) = \arg \min_{\theta \in \Theta} \mathbb{E}_{X \sim P_\theta} D_{KL}(p_{\theta_0}^Y || g_{X, \theta}) = \arg \min_{\theta \in \Theta} EKL(\theta_0 || \theta).$$

Proof of Proposition S1. This follows from Proposition S1, because the first terms in (S1) and (S2) do not depend on θ . \square

Lemma S1. *Let the Shannon entropy of a density p be given by $H(p) = -\int \log p(y) \cdot p(y) dy$. If the simulated log-likelihood $\ell^S(\theta; y)$ is given by $\log g(y|X, \theta)$ where X is a draw from P_θ , the data-averaged simulated log-likelihood satisfies*

$$U(\theta_0, \theta) = -H(p_{\theta_0}^Y) - \mathbb{E}_{X \sim P_\theta} D_{KL}(p_{\theta_0}^Y || g_{X, \theta}) \quad (\text{S1})$$

$$= -\mathbb{E}_{X \sim P_{\theta_0}} H(g_{X, \theta_0}) - EKL(\theta_0 || \theta) \quad (\text{S2})$$

Proof of Lemma S1.

$$\begin{aligned} U(\theta_0, \theta) &= \int \log g_{x, \theta}(y) dP_\theta(x) dP_{\theta_0}^Y(y) \\ &= \int \left[\log p_{\theta_0}^Y(y) - \log \frac{p_{\theta_0}^Y(y)}{g_{x, \theta}(y)} \right] dP_\theta(x) dP_{\theta_0}^Y(y) \\ &= -H(p_{\theta_0}^Y) - \mathbb{E}_{X \sim P_\theta} D_{KL}(p_{\theta_0}^Y || g_{X, \theta}). \end{aligned}$$

On the other hand,

$$\begin{aligned} \int \log g_{x, \theta}(y) \cdot g_{x', \theta_0}(y) dy &= - \int \log \frac{g_{x', \theta_0}(y)}{g_{x, \theta}(y)} g_{x', \theta_0}(y) dy + \int \log g_{x', \theta_0}(y) \cdot g_{x', \theta_0}(y) dy \\ &= -D_{KL}(g_{x', \theta_0} || g_{x, \theta}) - H(g_{x', \theta_0}). \end{aligned}$$

Integrating the above display with respect to $dP_{\theta_0}(x') dP_\theta(x)$, we obtain (S2). \square

S2 Further mathematical details on Section 2

S2.1 Sufficient conditions for Assumption 3 for marginally dependent $Y_{1:n}$

If $Y_{1:n}$ are marginally independent, then Assumption 3 is satisfied under suitable conditions on the moments by the Lindeberg-Feller central limit theorem [5]. Here we consider some cases where $Y_{1:n}$ are marginally dependent but where Assumption 3 is still satisfied.

Example S5. Let $X = \{X_i; 1 \leq i \leq n\}$ be a k -dependent stochastic process for some $k \geq 1$, meaning that the σ -algebra $\mathcal{F}_i = \sigma(X_j; j \leq i)$ is independent of $\mathcal{F}'_{i+k} = \sigma(X_j; j > i+k)$ for all i . Let $Y = \{Y_i; 1 \leq i \leq n\}$ be a collection of *local* observations of X . That is, Y_i depends only on $\{X_j; j \in \mathcal{N}(i)\}$ where $\mathcal{N}(i) \subseteq \{\max(i-b, 1), \dots, \min(i+b, n)\}$ for some fixed $b \geq 1$, such that $g_i(Y_i|X) = g_i(Y_i|X_{\mathcal{N}(i)})$. Then Y_i and $Y_{i+2b+k+1}$ are independent, since $X_{\mathcal{N}(i)} \in \mathcal{F}_{i+b}$ and $X_{\mathcal{N}(i+2b+k+1)} \in \mathcal{F}'_{i+b+k}$ are independent. It follows that the sequence $\{\frac{\partial \mu_i}{\partial \theta}(\theta_*; Y_i); i \geq 1\}$ is $2b+k$ -dependent. If $\{\frac{\partial \mu_i}{\partial \theta}(\theta_*; Y_i); i \geq 1\}$ are uniformly bounded and satisfy $\text{Var}\{\sum_{i=1}^n \frac{\partial \mu_i}{\partial \theta}(\theta_*; Y_i)\} / n^{2/3} \rightarrow \infty$ as $n \rightarrow \infty$, the central limit theorem holds for the sequence $\{\frac{\partial \mu_i}{\partial \theta}(\theta_*; Y_i); i \geq 1\}$ by Chung [5, Theorem 7.3.1].

Example S6. Suppose that $X = \{X_i; i \geq 1\}$ is a strictly stationary and strongly mixing process. A process is strongly mixing if the strong mixing coefficient

$$\alpha_k := \sup\{|\text{P}(A \cap B) - \text{P}(A)\text{P}(B)|; A \in \mathcal{F}_i, B \in \mathcal{F}'_{i+k-1}\}$$

converges to zero as $k \rightarrow \infty$. If the observations Y_i are local in the sense described in Example S5 and X is strongly mixing, then the sequence $\{\frac{\partial \mu_i}{\partial \theta}(\theta_*; Y_i); i \geq 1\}$ is also strongly mixing. Suppose that the sequence $\{\frac{\partial \mu_i}{\partial \theta}(\theta_*; Y_i); i \geq 1\}$ is strictly stationary and satisfies

$$\int_0^1 \alpha^{-1}(u) Q(u)^2 du < \infty \quad (\text{S3})$$

where $\alpha^{-1}(u) = \inf\{k; \alpha_k \leq u\}$ and $Q(u) = \inf\{t; \mathbb{P}[\|\frac{\partial \mu_1}{\partial \theta}(\theta_*; Y_1)\| > t] \leq u\}$. Then according to Doukhan et al. [6, Theorem 1], the central limit theorem holds for the sequence $\{\frac{\partial \mu_i}{\partial \theta}(\theta_*; Y_i); i \geq 1\}$. For the special case where this sequence is k -dependent for some $k \geq 1$, the condition (S3) reduces to $\mathbb{E} \left\| \frac{\partial \mu_i}{\partial \theta}(\theta_*; Y_i) \right\|^2 < \infty$.

We note that the mixing conditions for X mentioned in Examples S5 and S6 can also be used to justify the asymptotic normality of simulated log-likelihoods $\ell^S(\theta; y_{1:n})$ for a given set of observations $y_{1:n}$ (Assumption 6). Specifically, if the individual simulated log-likelihoods $\ell_i^S(\theta; y_i)$ depend locally on the simulated draw X in the sense described in Example S5, then the central limit theorem applies to $\ell^S(\theta; y_{1:n})$ provided that $\ell_i^S(\theta; y_i)$ satisfy the same conditions on $\frac{\partial \mu_i}{\partial \theta}(\theta_*; Y_i)$ stated in Examples S5 or S6.

S2.2 Proofs for Section 2.2

Proof of Proposition 1. Using Taylor's expansion with an integral remainder term, for $f : \mathbb{R} \rightarrow \mathbb{R}$ that is three times continuously differentiable at a , we have

$$f(x) = f(a) + f'(a)(x - a) + \frac{1}{2} f''(a)(x - a)^2 + \int_a^x f'''(t) \frac{(x - t)^2}{2} dt. \quad (\text{S4})$$

Consider a bounded set B containing zero. Applying this result to three times differentiable function $\tau \mapsto \mu_i(\theta_* + \tau \frac{t}{\sqrt{n}})$ where $t \in B$, we obtain

$$\begin{aligned} \mu_i(\theta_* + \frac{t}{\sqrt{n}}; Y_i) &= \mu_i(\theta_*; Y_i) + \frac{\partial \mu_i}{\partial \theta}(\theta_*; Y_i) \frac{t}{\sqrt{n}} + \frac{1}{2n} t^\top \frac{\partial^2 \mu_i}{\partial \theta^2}(\theta_*; Y_i) t \\ &\quad + \frac{1}{2n^{3/2}} \int_0^1 \frac{\partial^3 \mu_i}{\partial \theta^3}(\theta_* + \tau \frac{t}{\sqrt{n}}; Y_i)(t, t, t)(1 - \tau)^2 d\tau \end{aligned}$$

where $\frac{\partial^3 \mu_i}{\partial \theta^3}(\theta_*; Y_i) : \mathbb{R}^{3d} \rightarrow \mathbb{R}$ is a trilinear form given by

$$\frac{\partial^3 \mu_i}{\partial \theta^3}(\theta_*; Y_i)(t, s, r) = \sum_{k_1, k_2, k_3 \in 1:d} \frac{\partial^3 \mu_i}{\partial \theta_{(k_1)} \partial \theta_{(k_2)} \partial \theta_{(k_3)}}(\theta_*; Y_i) t_{k_1} s_{k_2} r_{k_3}, \quad \forall t, s, r \in \mathbb{R}^d.$$

By Assumption 3,

$$S_n = \frac{1}{\sqrt{n}} \sum_{i=1}^n \frac{\partial \mu_i}{\partial \theta}(\theta_*; Y_i)$$

converges in distribution to $\mathcal{N}(0, K_1(\theta_0))$, and by Assumption 4,

$$\frac{1}{n} \sum_{i=1}^n \frac{\partial^2 \mu_i}{\partial \theta^2}(\theta_*; Y_i)$$

converges in probability to $-K_2(\theta_0)$. The absolute value of the integral remainder term is bounded by

$$\begin{aligned} &\left| \int_0^1 \frac{\partial^3 \mu_i}{\partial \theta^3}(\theta_* + \tau \frac{t}{\sqrt{n}}; Y_i)(t, t, t)(1 - \tau)^2 d\tau \right| \\ &\leq \sup_{\tau \in [0,1]} \max_{k_1, k_2, k_3 \in 1:d} \left\| \frac{\partial^3 \mu_i}{\partial \theta_{(k_1)} \partial \theta_{(k_2)} \partial \theta_{(k_3)}}(\theta_* + \tau \frac{t}{\sqrt{n}}; Y_i) \right\| d^3 \|t\|_\infty^3 \int_0^1 (1 - \tau)^2 d\tau. \end{aligned}$$

For sufficiently large n , $\{\theta_* + \tau \frac{t}{\sqrt{n}}; t \in B, \tau \in [0, 1]\}$ is contained in B_0 defined in Assumption 5. Therefore, we have

$$\sum_{i=1}^n \left[\mu_i(\theta_* + \frac{t}{\sqrt{n}}; Y_i) - \mu_i(\theta_*; Y_i) \right] = S_n^\top t - \frac{1}{2} t^\top K_2(\theta_0) t + R_n(t) + o_p(1)$$

where $o_p(1)$ signifies a term that is independent of t and converges in probability to zero and where the remainder term $R_n(t)$ satisfies

$$\mathbb{E} \sup_{t \in B} |R_n(t)| \leq \frac{1}{6n^{1/2}} C d^3 \|t\|_\infty^3.$$

Thus by Markov's inequality, $R_n(t)$ converges in probability to zero uniformly for $t \in B$. \square

S3 Further details on Section 2.5 Bias in simulation-based inference

The simulation-based inference procedure outlined in Section 2 and developed in detail in Sections 3–4 may have a bias in general due to the use of a metamodel for the log-likelihood estimator. In this section, we examine the bias and develop bounds on the inference bias under certain conditions.

S3.1 Power series expression for Jensen bias using the cumulants of simulated log-likelihood

We refer to the difference $B(\theta) = \ell(\theta) - \mu(\theta)$ as the Jensen bias, which is always nonnegative when the simulated log-likelihood is given by the log of an unbiased likelihood estimator. For hidden Markov models, an unbiased simulation likelihood can be obtained by running the bootstrap particle filter, as described by Algorithm 2. Berard et al. [4] showed that under certain conditions, the logarithm of this estimator, which we denote by $\ell^S(\theta)$, approximately follows

$$\ell^S(\theta) \approx \mathcal{N} \left(\ell(\theta) - \frac{1}{2} \sigma^2(\theta), \sigma^2(\theta) \right)$$

(see (11)). In this case, the Jensen bias can be approximated by half the variance in the simulated log-likelihood.

More generally, we will consider the situation where the simulation likelihood $e^{\ell^S(\theta)}$ is unbiased for the likelihood $L(\theta)$. This happens in all examples we consider in this paper, whether $\ell^S(\theta)$ is given by the log-measurement density $g_{1:n}(y_{1:n}|X)$ or by the log-likelihood estimate produced by the bootstrap particle filter. Provided that the simulation likelihood is unbiased for the likelihood, the log-likelihood can be expressed as

$$\ell(\theta) = \log \mathbb{E} e^{\ell^S(\theta)}. \tag{S5}$$

The cumulant generating function, or the second characteristic function, $\psi(z)$ of a random variable X is defined as the principal branch of the logarithm of its characteristic function [9, 11],

$$\psi(z) := \log \mathbb{E} e^{izX}.$$

The cumulant generating function is uniquely continuously defined on real intervals containing zero on which $\phi_X(s)$ is nonzero. If we denote by $\psi(z)$ the cumulant generating function for the simulated log-likelihood $\ell^S(\theta)$, we may express $\ell(\theta)$ as

$$\ell(\theta) = \log \mathbb{E} e^{\ell^S(\theta)} = \psi(-i), \tag{S6}$$

provided that $\psi(z)$ can be extended to a complex domain $|z| < R$ for some $R > 1$. Conditions under which an analytic extension of $\psi(z)$ is possible is discussed below. Under those conditions, $\psi(z)$ can be expressed as an absolutely convergent power series,

$$\psi(z) = \sum_{n=1}^{\infty} \frac{i^n \kappa_n(\theta)}{n!} z^n, \quad |z| < R. \tag{S7}$$

The number $\kappa_n(\theta)$ is the n -th order cumulant of $\ell^S(\theta)$. The first two cumulants corresponding to $n = 1, 2$ are equal to the mean and the variance of the random variable. The log-likelihood $\ell(\theta)$ can thus be expressed as

$$\ell(\theta) = \sum_{j=1}^{\infty} \frac{\kappa_j(\theta)}{j!}. \quad (\text{S8})$$

The expected simulated log-likelihood $\mu(\theta)$ can be considered as a first order approximation to (S8), since $\mu(\theta) = \kappa_1(\theta)$. The Jensen bias is given by

$$B(\theta) = \ell(\theta) - \mu(\theta) = \sum_{j \geq 2} \frac{\kappa_j(\theta)}{j!}. \quad (\text{S9})$$

In the special case where $\ell^S(\theta)$ exactly follows the normal distribution with mean $\mu(\theta)$ and variance $\sigma^2(\theta)$, the analytic characteristic function is given by $\exp(i\mu(\theta)z - \frac{\sigma^2(\theta)z^2}{2})$, which is nowhere equal to zero. Thus the cumulant generating function is defined and analytic on the entire complex plane, and the log-likelihood is given by

$$\ell(\theta) = \psi(-i; \theta) = \kappa_1(\theta) + \frac{\kappa_2(\theta)}{2} = \mu(\theta) + \frac{\sigma^2(\theta)}{2}. \quad (\text{S10})$$

The Jensen bias is equal to $B(\theta) = \sigma^2(\theta)/2$. We note, however, that even when the centered and scaled simulated log-likelihood $\frac{\ell^S(\theta; y_{1:n}) - \mu(\theta; y_{1:n})}{\sigma(\theta; y_{1:n})}$ converges to the normal distribution as $n \rightarrow \infty$ (Assumption 6), the higher order terms ($j \geq 3$) in (S9) do not approach zero in general. For instance, if the simulated log-likelihoods for the observation pieces $\{\ell^S(\theta; y_i); i \in 1:n\}$ are independent of each other, we have

$$\ell(\theta; y_{1:n}) = \log \mathbb{E} e^{\sum_{i=1}^n \ell^S(\theta; y_i)} = \sum_{i=1}^n \log \mathbb{E} e^{\ell^S(\theta; y_i)} = \sum_{j \geq 1} \frac{\sum_{i=1}^n \kappa_j(\theta; y_i)}{j!},$$

and thus all cumulants $\kappa_j(\theta; y_{1:n})$, $j \geq 1$, scale linearly with n .

We will now discuss the conditions for analytic extensions of the characteristic function and the cumulant generating function. A characteristic function $\phi(s)$ is called an analytic characteristic function if there is an analytic function on a complex circle $|z| < \rho$ (where $\rho > 0$) that agrees with $\phi(s)$ on some real neighborhood of zero, say $(-\epsilon, \epsilon)$ [11]. The extended function defined on a complex domain will also be called the analytic characteristic function and denoted by $\phi(z)$. The extended analytic characteristic function has a Maclaurin series expansion about zero.

Theorem S1. *Suppose that a random variable with cumulative distribution function (cdf) F has an analytic characteristic function $\phi(z)$. The Maclaurin series of the analytic characteristic function*

$$\phi(z) = \sum_{n=0}^{\infty} \frac{i^n \alpha_n}{n!} z^n \quad (\text{S11})$$

is absolutely convergent on a complex disk $|z| < R$ for some positive R if and only if the relation

$$1 - F(x) + F(-x) = o(e^{-rx}) \quad \text{as } x \rightarrow \infty$$

holds for all positive $r < R$. Then the n -th moment of the random variable is given by $\alpha_n = i^{-n} \phi^{(n)}(0)$, where $\phi^{(n)}$ denotes the n -th derivative of ϕ .

Proof. This follows from Theorem 7.1.1, Corollary to Theorem 7.1.1, and Theorem 7.2.1 of Lukacs [11] and Chapter 5, Theorem 3 of Ahlfors [3]. \square

Theorem S1 implies that the Maclaurin series (S11) for $\phi(z)$ converges at $z = -i$ if both $1 - F(x)$ and $F(-x)$ decays faster than e^{-rx} as $x \rightarrow \infty$ for all $r < R$ for some $R > 1$. The first condition that $1 - F(x)$ decays faster than e^{-rx} is almost satisfied if the likelihood $L(\theta)$ is finite. If we denote the cumulative distribution function of $\ell^S(\theta)$ by F , we have

$$\infty > L(\theta) = \mathbb{E} e^{\ell^S(\theta)} = \int_{-\infty}^{\infty} e^x dF(x) \geq e^c (1 - F(c)) \quad \text{for all } c.$$

Therefore, $1 - F(x) = o(-rx)$ for all $r < 1$. However, this result is weaker than the required condition that $1 - F(x) = o(e^{-rx})$ for all $r < R$ for some $R > 1$.

The condition regarding the other tail, $F(-x) = o(e^{-rx})$ for $r < R$, can be readily satisfied if we truncate the simulated log-likelihood $\ell^S(\theta)$ from below, say at $-C$ for some large C . If $\ell^S(\theta) \geq -C_0$ with probability at least p for some C_0 , then we have

$$\begin{aligned} \log \mathbb{E} e^{\max(\ell^S, -C)} - \ell &\leq \log \frac{\mathbb{E} e^{\ell^S} \mathbf{1}[\ell^S \geq -C] + e^{-C} \mathbf{P}[\ell^S < -C]}{\mathbb{E} e^{\ell^S} \mathbf{1}[\ell^S \geq -C]} \\ &\leq \frac{e^{-C} \mathbf{P}[\ell^S < -C]}{\mathbb{E} e^{\ell^S} \mathbf{1}[\ell^S \geq -C]} \leq \frac{e^{-C}}{pe^{-C_0}} = p^{-1} e^{C_0 - C}, \end{aligned}$$

and this truncation error can be bounded by an arbitrarily small number by taking C sufficiently large.

If the analytic extension of the characteristic function $\phi(z)$ is nonzero anywhere in a disk $|z| < R$, then the cumulant generating function can be extended analytically to the same complex disk. For an analytic, nonzero function on $|z| < R$, an analytic, single-branched logarithm can be defined in that disk (see e.g., Chapter 4, Corollary to Theorem 16 in Ahlfors [3].) Here, that the logarithm is single-branched means that its value at any given point z is defined as a single number, not up to integer multiples of $2\pi i$. We define an extended cumulative generating function $\psi(z)$ on the complex disk $|z| < R$ as the single-branched logarithm of $\phi(z)$ which is equal to zero at $z = 0$. Since this $\psi(z)$ is analytic on $|z| < R$, an absolutely convergent power series expansion of $\psi(z)$ about $z = 0$ is available, giving (S7).

We note that the preceding analysis suggests consideration of a higher order MESLE and a higher order simulation-based proxy defined as follows.

Definition S1. Let $\kappa_j(\theta; y_{1:n})$ be the j -th order cumulant of the simulated log-likelihood $\ell^S(\theta; y_{1:n})$ for $j \geq 1$. The k -th order maximum expected simulated log-likelihood (MESLE) for $k \geq 1$ is defined as

$$\hat{\theta}_{[k]}(y_{1:n}) := \arg \max_{\theta} \sum_{j=1}^k \frac{\kappa_j(\theta; y_{1:n})}{j!}.$$

The k -th order simulation-based proxy ($k \geq 1$) is defined as

$$\mathcal{R}_{[k]}(\theta_0) := \arg \max_{\theta} \mathbb{E}_{Y_{1:n} \sim P_{\theta_0}^Y} \sum_{j=1}^k \frac{\kappa_j(\theta; Y_{1:n})}{j!}.$$

However, the practical utility of an higher-order MESLE is likely limited, because its estimator will involve high Monte Carlo variation.

S3.2 Bound on the Jensen bias $\ell(\theta; y) - \mu(\theta; y)$

The Jensen bias $B(\theta)$ can be upper bounded in the case where the simulated log-likelihood $\ell^S(\theta)$ has a sub-Gaussian tail.

Proposition S2. *Suppose that for some $C, C' > 0$,*

$$\mathbf{P}[\ell^S(\theta) - \mu(\theta) \geq t] \leq \frac{C'}{\sqrt{2\pi C}} e^{-\frac{t^2}{2C^2}}$$

for all $t \geq 0$. Then the Jensen bias satisfies

$$B(\theta) \leq \frac{C^2}{2} + \log(1 + C').$$

Proof of Proposition S2. We use the following result: for any random variable X with cumulative distribution function F ,

$$\mathbb{E} e^X \leq 1 + \int_0^\infty e^t (1 - F(t)) dt. \tag{S12}$$

This is because

$$\begin{aligned}
\mathbb{E} e^X &= \mathbb{E} e^X \mathbf{1}[X < 0] + \mathbb{E} e^X \mathbf{1}[X \geq 0] \\
&\leq \mathbb{P}[X < 0] + \mathbb{P}[X \geq 0] + \int_0^\infty (e^x - 1) F(dx) \\
&= 1 + \int_0^\infty \int_0^\infty e^t \mathbf{1}[t < x] dt F(dt) \\
&= 1 + \int_0^\infty e^t \int_0^\infty \mathbf{1}[x > t] F(dx) dt \\
&= 1 + \int_0^\infty e^t (1 - F(t)) dt.
\end{aligned}$$

Using (S12) for $X = \ell^S(\theta)$, we have

$$\begin{aligned}
\mathbb{E} e^{\ell^S(\theta)} &\leq 1 + \int_0^\infty e^t \frac{C'}{\sqrt{2\pi}C} e^{-\frac{t^2}{2C^2}} dt \\
&= 1 + \int_0^\infty \frac{C'}{\sqrt{2\pi}C} e^{-\frac{1}{2C^2}(t-C^2)^2} e^{\frac{C^2}{2}} dt \\
&\leq 1 + C' e^{\frac{C^2}{2}}.
\end{aligned}$$

Therefore, it follows that

$$\ell(\theta) = \log \mathbb{E} e^{\ell^S(\theta)} \leq \log(1 + C' e^{\frac{C^2}{2}}) \leq \log(e^{\frac{C^2}{2}} + C' e^{\frac{C^2}{2}}) = \frac{C^2}{2} + \log(1 + C').$$

□

We also have the following result. If the simulated log-likelihood for the i -th observation, $\ell_i^S(\theta; y_i)$, is almost surely at most $s_i(\theta)$ higher than $\mathbb{E} \ell_i^S(\theta)$, then the Jensen bias is upper bounded by $\sum_i s_i(\theta)$. This condition is satisfied, when the individual simulated log-likelihoods $\ell_i^S(\theta; y_i)$ are both upper and lower bounded, which may happen when the observation space is compact.

Proposition S3. *Suppose that $\ell_i^S(\theta; y_i) - \mu_i(\theta; y_i)$ is almost surely upper bounded by $s_i(\theta)$ for each $i \in 1:n$. Then we have*

$$B(\theta) \leq \sum_{i=1}^n s_i(\theta).$$

Proof of Proposition S3.

$$\ell(\theta) - \mu(\theta) = \log \mathbb{E} e^{\sum_i \{\ell_i^S(\theta; y_i) - \mu_i(\theta; y_i)\}} \leq \mathbb{E} e^{\sum_i s_i} = \sum_i s_i.$$

□

S3.3 Bound on the inference bias $\mathcal{R}(\theta_0) - \theta_0$

In the current section, we will construct a bound on the difference between θ_0 and $\mathcal{R}(\theta_0)$ using the upper bound on the Jensen bias developed in Section S3.1.

If the observations $Y_{1:n}$ are obtained under θ_0 , then the data-averaged log-likelihood $\mathbb{E}_{Y_{1:n} \sim P_{\theta_0}^Y} \ell(\theta; Y_{1:n})$ equals the negative cross entropy, denoted by $-H(\theta_0, \theta)$:

$$\mathbb{E}_{Y_{1:n} \sim P_{\theta_0}^Y} \ell(\theta; Y_{1:n}) = \int \{\log p_{\theta,n}^Y(y_{1:n})\} p_{\theta_0}^Y(y_{1:n}) dy_{1:n} =: -H(\theta_0, \theta).$$

We write $H(\theta_0, \theta_0) = H(\theta_0)$. The cross entropy $H(\theta_0, \theta)$ is minimized at $\theta = \theta_0$, because it is equal to $H(\theta_0) + D_{KL}(\theta_0 || \theta)$, where the Kullback-Leibler divergence $D_{KL}(\theta_0 || \theta)$ is minimized at $\theta = \theta_0$ [12].

On the other hand, by Definition 2, the data-averaged expected simulated log-likelihood $U(\theta_0, \theta)$ is maximized when θ equals the simulation-based proxy $\mathcal{R}(\theta_0) = \theta_*$. If we denote by $B(\theta; y_{1:n}) = \ell(\theta; y_{1:n}) - \mu(\theta; y_{1:n})$ the Jensen bias at θ given the observations $y_{1:n}$, we have

$$\mathbb{E}_{Y_{1:n} \sim P_{\theta_0}^Y} \mu(\theta; Y_{1:n}) \leq \mathbb{E}_{Y_{1:n} \sim P_{\theta_0}^Y} \ell(\theta; Y_{1:n}) \leq \mathbb{E}_{Y_{1:n} \sim P_{\theta_0}^Y} \mu(\theta; Y_{1:n}) + B(\theta; Y_{1:n}),$$

or

$$U(\theta_0, \theta) \leq -H(\theta_0, \theta) \leq U(\theta_0, \theta) + \mathbb{E}_{Y_{1:n} \sim P_{\theta_0}^Y} B(\theta; Y_{1:n}). \quad (\text{S13})$$

We consider a second order Taylor approximation to $-H(\theta_0, \theta)$ around $\theta = \theta_0$ and an approximation to $U(\theta_0, \theta)$ around $\theta = \theta_*$:

$$\begin{aligned} q_{-H}(\theta) &:= -H(\theta_0, \theta_0) - \frac{1}{2}(\theta - \theta_0)^\top \left[\frac{\partial^2}{\partial \theta^2} H(\theta_0, \theta) \right]_{\theta=\theta_0} (\theta - \theta_0), \\ q_U(\theta) &:= U(\theta_0, \theta_*) + \frac{1}{2}(\theta - \theta_*)^\top \left[\frac{\partial^2}{\partial \theta^2} U(\theta_0, \theta) \right]_{\theta=\theta_*} (\theta - \theta_*). \end{aligned}$$

The first order derivatives of $-H(\theta_0, \theta)$ and $U(\theta_0, \theta)$ evaluated at θ_0 and θ_* , respectively, are equal to zero because those points are the maximizers of the two functions. Note that the second derivative of H at θ_0 equals the Fisher information $\mathcal{I}(\theta_0)$,

$$\left[\frac{\partial^2}{\partial \theta^2} H(\theta_0, \theta) \right]_{\theta=\theta_0} = - \int \left[\frac{\partial^2}{\partial \theta^2} \log p_{\theta,n}^Y(y_{1:n}) \right]_{\theta=\theta_0} p_{\theta_0}^Y(y_{1:n}) dy_{1:n} = \mathcal{I}(\theta_0).$$

We restate our results from Section 2.5.

Proposition 2. *Suppose that the quadratic approximations $q_{-H}(\theta)$ and $q_U(\theta)$ given by (12)–(13) are ϵ -accurate on a δ -neighborhood of θ_* , that is,*

$$| -H(\theta_0, \theta) - q_{-H}(\theta) | \leq \epsilon, \quad | U(\theta_0, \theta) - q_U(\theta) | \leq \epsilon,$$

for every θ such that $\|\theta - \theta_*\| \leq \delta$. Suppose further that both the Fisher information $\mathcal{I}(\theta_0)$ and $\mathcal{J}(\theta_0, \theta_*)$ are positive definite and that

$$\bar{B} := \sup_{\theta; \|\theta - \theta_*\| \leq \delta} \mathbb{E}_{Y_{1:n} \sim P_{\theta_0}^Y} B(\theta; Y_{1:n})$$

is finite. If the smallest eigenvalue λ of $\mathcal{J}(\theta_0, \theta_*)$ satisfies $\lambda \delta^2 \geq 2(\bar{B} + 2\epsilon)$, then we have

$$\|\theta_0 - \theta_*\| \leq 2\delta^{-1} \lambda^{-1} (\bar{B} + 2\epsilon).$$

In fact, a somewhat stronger result can be established as follows: the true parameter θ_0 is located in the set

$$\theta_0 \in \{ \theta_* + tu; u \in \mathbb{R}^d, \|u\| = 1, |t| \leq 2(u^\top \mathcal{J}(\theta_0, \theta_*) u)^{-1} \delta^{-1} (\bar{B} + 2\epsilon) \}. \quad (\text{S14})$$

We note that (S14) implies our original result, $\|\theta_0 - \theta_*\| \leq 2\delta^{-1} \lambda^{-1} (\bar{B} + 2\epsilon)$, since $\lambda \|\theta_0 - \theta_*\|^2 \leq (\theta_0 - \theta_*)^\top \mathcal{J}(\theta_0, \theta_*) (\theta_0 - \theta_*)$. Additionally, we can obtain bounds for the Fisher information as

$$\mathcal{J}(\theta_0, \theta_*) - 2\delta^{-2} (\bar{B} + 2\epsilon) I_d \preceq \mathcal{I}(\theta_0) \preceq \mathcal{J}(\theta_0, \theta_*) + 2\delta^{-2} (\bar{B} + 2\epsilon) I_d,$$

where $A \preceq B$ indicates that $B - A$ is nonnegative definite and I_d denotes the $d \times d$ identity matrix. The proofs of Proposition 2 and these additional results are presented later in this section.

For large n , $\mathcal{J}(\theta_0, \theta_*)$ is approximately equal to the metamodel parameter c , because

$$-\frac{1}{2} \mathcal{J}(\theta_0, \theta_*) = \frac{1}{2} \left[\frac{\partial^2}{\partial \theta^2} \mathbb{E}_{Y_{1:n} \sim P_{\theta_0}^Y} \mu(\theta; Y_{1:n}) \right]_{\theta=\theta_*} \approx \frac{1}{2} \frac{\partial^2}{\partial \theta^2} \mu(\theta_*; y_{1:n}) = c(y_{1:n}).$$

Thus, $\mathcal{J}(\theta_0, \theta_*)$ can be approximately estimated by quadratic regression through the simulated log-likelihoods.

Proposition 3 provides a similar result for the MESLE. For given observation sequence $y_{1:n}$, consider second order Taylor approximations to $\ell(\theta; y_{1:n})$ and $\mu(\theta; y_{1:n})$:

$$\begin{aligned} q_\ell(\theta) &:= \ell(\theta_{MLE}) + \frac{1}{2}(\theta - \theta_{MLE})^\top \frac{\partial^2 \ell}{\partial \theta^2}(\theta_{MLE})(\theta - \theta_{MLE}), \\ q_\mu(\theta) &:= \mu(\theta_{MESLE}) + \frac{1}{2}(\theta - \theta_{MESLE})^\top \frac{\partial^2 \mu}{\partial \theta^2}(\theta_{MESLE})(\theta - \theta_{MESLE}). \end{aligned}$$

Proposition 3. *Suppose that for a given observation sequence $y_{1:n}$, the quadratic approximations $q_\ell(\theta)$ and $q_\mu(\theta)$ are ϵ -accurate,*

$$|\ell(\theta) - q_\ell(\theta)| \leq \epsilon, \quad |\mu(\theta) - q_\mu(\theta)| \leq \epsilon,$$

for every θ such that $\|\theta - \theta_{MESLE}\| \leq \delta$ for some $\epsilon, \delta > 0$. Suppose further that both $-\frac{\partial^2 \ell}{\partial \theta^2}(\theta_{MLE})$ and $-\frac{\partial^2 \mu}{\partial \theta^2}(\theta_{MESLE})$ are positive definite. Let

$$\bar{B}' := \sup_{\theta; \|\theta - \theta_{MESLE}\| \leq \delta} B(\theta; y_{1:n})$$

and assume that \bar{B}' is finite. If the smallest eigenvalue λ' of $-\frac{\partial^2 \mu}{\partial \theta^2}(\theta_{MESLE})$ satisfies $\lambda' \delta^2 \geq 2(\bar{B}' + 2\epsilon)$, then we have

$$\|\theta_{MLE} - \theta_{MESLE}\| \leq 2\delta^{-1} \lambda'^{-1} (\bar{B}' + 2\epsilon).$$

The conclusion of Proposition 3 is implied by a stronger result

$$\theta_{MLE} \in \left\{ \theta_{MESLE} + tu; u \in \mathbb{R}^d, \|u\| = 1, |t| \leq -2 \left(u^\top \frac{\partial^2 \mu}{\partial \theta^2}(\theta_{MESLE}) u \right)^{-1} \delta^{-1} (\bar{B}' + 2\epsilon) \right\}.$$

Moreover, we have

$$\frac{\partial^2 \mu}{\partial \theta^2}(\theta_{MESLE}) - 2\delta^{-2}(\bar{B}' + 2\epsilon)I_d \preceq \frac{\partial^2 \ell}{\partial \theta^2}(\theta_{MLE}) \preceq \frac{\partial^2 \mu}{\partial \theta^2}(\theta_{MESLE}) + 2\delta^{-2}(\bar{B}' + 2\epsilon)I_d.$$

Proof of Proposition 2. From Equation (S13), we have

$$U(\theta_0, \theta) \leq -H(\theta_0, \theta) \leq U(\theta_0, \theta) + \bar{B}$$

for θ satisfying $\|\theta - \theta_*\| \leq \delta$. Thus we have

$$\begin{aligned} q_{-H}(\theta) &\geq -H(\theta_0, \theta) - \epsilon \geq U(\theta_0, \theta) - \epsilon \geq q_U(\theta) - 2\epsilon, \\ q_{-H}(\theta) &\leq -H(\theta_0, \theta) + \epsilon \leq U(\theta_0, \theta) + \bar{B} + \epsilon \leq q_U(\theta) + \bar{B} + 2\epsilon. \end{aligned} \tag{S15}$$

Let

$$v = \frac{\theta_0 - \theta_*}{\|\theta_0 - \theta_*\|}$$

be a unit vector in the direction from θ_* to θ_0 . Define $r_U : [-\delta, \delta] \rightarrow \mathbb{R}$ and $r_{-H} : [-\delta, \delta] \rightarrow \mathbb{R}$ by

$$r_U(x) = q_U(\theta_* + xv) - q_U(\theta_*) = -\nu x^2$$

and

$$r_{-H}(x) = q_{-H}(\theta_* + xv) - q_{-H}(\theta_*) = -\alpha(x - \beta)^2 + \gamma.$$

Here,

$$2\nu = -\frac{d^2}{dx^2} r_U(x) = -v^\top \frac{\partial^2}{\partial \theta^2} q_U(\theta) v = v^\top \mathcal{J}(\theta_0, \theta_*) v \geq \lambda,$$

$$2\alpha = -\frac{d}{dx^2} r_{-H}(x) = -v^\top \frac{\partial^2}{\partial \theta^2} q_{-H}(\theta) v = v^\top \mathcal{I}(\theta_0) v.$$

Also, $\beta = \|\theta_0 - \theta_*\|$, because $r_{-H}(x)$ is maximized at $x = \beta$ and $q_{-H}(\theta)$ is maximized at $\theta = \theta_0$ by construction. From (S15), we have envelopes for $r_{-H}(x)$:

$$r_U(x) - 2\epsilon \leq r_{-H}(x) \leq r_U(x) + \bar{B} + 2\epsilon \quad (\text{S16})$$

for $|x| \leq \delta$. Additionally, we have

$$0 \leq -H(\theta_0, \theta_*) - U(\theta_0, \theta_*) \leq \gamma = -H(\theta_0) - U(\theta_0, \theta_*) \leq -H(\theta_0) - U(\theta_0, \theta_0) \leq \bar{B}.$$

We consider two separate cases. In the case $\alpha \leq \nu$, Equation (S16) implies that

$$r_{-H}(\delta) = -\alpha(x - \beta)^2 + \gamma \leq r_U(\delta) + \bar{B} + 2\epsilon = -\nu\delta^2 + \bar{B} + 2\epsilon.$$

Thus we have

$$(\delta - \beta)^2 \geq \alpha^{-1}(\nu\delta^2 - \bar{B} - 2\epsilon + \gamma), \quad (\text{S17})$$

or

$$\begin{aligned} \beta &\leq \delta - \sqrt{\alpha^{-1}(\nu\delta^2 - \bar{B} - 2\epsilon + \gamma)} \\ &\leq \delta - \sqrt{\delta^2 - \nu^{-1}(\bar{B} + 2\epsilon - \gamma)} = \delta - \delta\sqrt{1 - \delta^{-2}\nu^{-1}(\bar{B} + 2\epsilon - \gamma)}. \end{aligned}$$

Since $\nu\delta^2 \geq \frac{\lambda}{2}\delta^2 \geq \bar{B} + 2\epsilon \geq \bar{B} + 2\epsilon - \gamma$, the expression inside the square root symbol is nonnegative. Using the fact that $\sqrt{1-t} \geq 1-t$ for $0 \leq t \leq 1$, we obtain

$$\beta \leq \delta - \delta\{1 - \delta^{-2}\nu^{-1}(\bar{B} + 2\epsilon - \gamma)\} \leq \delta^{-1}\nu^{-1}(\bar{B} + 2\epsilon).$$

Now consider the case $\alpha > \nu$. Equation (S16) implies that

$$r_{-H}(-\delta) = -\alpha(-\delta - \beta)^2 + \gamma \geq r_U(-\delta) - 2\epsilon = -\nu(-\delta)^2 - 2\epsilon.$$

Thus we have

$$(\delta + \beta)^2 \leq \alpha^{-1}(\nu\delta^2 + \gamma + 2\epsilon), \quad (\text{S18})$$

or

$$\beta \leq \sqrt{\alpha^{-1}(\nu\delta^2 + \gamma + 2\epsilon)} - \delta \leq \sqrt{\delta^2 + \nu^{-1}(\gamma + 2\epsilon)} - \delta = \delta\sqrt{1 + \delta^{-2}\nu^{-1}(\gamma + 2\epsilon)} - \delta.$$

Using the fact that $\sqrt{1+t} \leq 1 + \frac{t}{2}$ for $t \geq 0$, we obtain

$$\beta \leq \delta\{1 + \frac{1}{2}\delta^{-2}\nu^{-1}(\gamma + 2\epsilon)\} - \delta \leq \delta^{-1}\nu^{-1}(\bar{B} + 2\epsilon).$$

In either case, we have

$$\beta = \|\theta_0 - \theta_*\| \leq \delta^{-1}\nu^{-1}(\bar{B} + 2\epsilon) = 2(v^\top \mathcal{J}(\theta_0, \theta_*)v)^{-1}\delta^{-1}(\bar{B} + 2\epsilon).$$

In other words, θ_0 is located in the set

$$\theta_0 \in \{\theta_* + tu; u \in \mathbb{R}^d, \|u\| = 1, |t| \leq 2(u^\top \mathcal{J}(\theta_0, \theta_*)u)^{-1}\delta^{-1}(\bar{B} + 2\epsilon)\}.$$

We now prove the bounds on the Fisher information $\mathcal{I}(\theta_0)$. Using (S17) again, we have

$$\alpha \geq (\delta - \beta)^{-2}(\nu\delta^2 - \bar{B} - 2\epsilon + \gamma) \geq \nu - \delta^{-2}(\bar{B} + 2\epsilon - \gamma) \geq \nu - \delta^{-2}(\bar{B} + 2\epsilon).$$

This implies that

$$\frac{1}{2}v^\top \mathcal{I}(\theta_0)v \geq \frac{1}{2}v^\top \mathcal{J}(\theta_0, \theta_*)v - \delta^{-2}(\bar{B} + 2\epsilon).$$

From (S18), we have

$$\alpha \leq (\delta + \beta)^{-2}(\nu\delta^2 + \gamma + 2\epsilon) \leq \nu + \delta^{-2}(\gamma + 2\epsilon) \leq \nu + \delta^{-2}(\bar{B} + 2\epsilon),$$

which implies that

$$\frac{1}{2}v^\top \mathcal{I}(\theta_0)v \leq \frac{1}{2}v^\top \mathcal{J}(\theta_0, \theta_*)v + \delta^{-2}(\bar{B} + 2\epsilon).$$

We can obtain the same results when we replace v by an arbitrary unit vector u . Hence, we have

$$\mathcal{J}(\theta_0, \theta_*) - 2\delta^{-2}(\bar{B} + 2\epsilon)I_d \preceq \mathcal{I}(\theta_0) \preceq \mathcal{J}(\theta_0, \theta_*) - 2\delta^{-2}(\bar{B} + 2\epsilon)I_d.$$

□

The proof of Proposition 3 follows similarly and is thus omitted.

S4 Mathematical details and proofs for Section 3

S4.1 Details and proofs for Section 3.1

The $MLLR_{A_0, \sigma_0^2}$ statistic for the test $H_0 : A = A_0, \sigma^2 = \sigma_0^2, H_1 : \text{not } H_0$ has the following distribution under the null hypothesis.

Proposition S4. *Under the normal, locally quadratic metamodel (Definition 3) and under the null hypothesis $A = A_0$ and $\sigma^2 = \sigma_0^2$, the metamodel log-likelihood ratio (16) has the following distribution:*

$$MLLR_{A_0, \sigma_0^2} \sim \text{SCL} \left(M, \frac{d^2 + 3d + 2}{2} \right).$$

Definition S2 (SCL distributions). Let $X_1 \sim \chi_k^2$ and $X_2 \sim \chi_{M-k}^2$ be independent random variables following the chi-squared distributions with k and $M - k$ degrees of freedom. Then the distribution of the random variable

$$-\frac{1}{2} \left\{ X_1 + X_2 - M \log \frac{X_2}{M} - M \right\} \quad (\text{S19})$$

will be called the $\text{SCL}(M, k)$ distribution.¹

The $-2 \cdot \text{SCL}(M, k)$ distribution converges to the chi-square distribution as M tends to infinity.

Proposition S5. *As M tends to infinity, we have*

$$-2 \cdot \text{SCL}(M, k) \xrightarrow{M \rightarrow \infty} \chi_{k+1}^2.$$

Propositions S4 and S5 show that our metamodel likelihood ratio test is asymptotically equivalent to Wilks' large-sample likelihood ratio test as the number of simulations M grows.

Lemma S2. *The sum of squared errors can be divided into the residual sum of squares and the squared error in fit as follows:*

$$\|\ell_{1:M}^S - \theta_{1:M}^{0:2} A_0\|_W^2 = \|\ell_{1:M}^S - \theta_{1:M}^{0:2} \hat{A}\|_W^2 + \|\theta_{1:M}^{0:2} \hat{A} - \theta_{1:M}^{0:2} A_0\|_W^2. \quad (\text{S20})$$

Furthermore, under the null hypothesis $A = A_0$ and $\sigma^2 = \sigma_0^2$ for the normal, locally quadratic metamodel, we have

$$\hat{\sigma}^2 \sim \frac{1}{M} \sigma_0^2 \chi_{M - \frac{d^2 + 3d + 2}{2}}^2 \quad \text{and} \quad \|\theta_{1:M}^{0:2} \hat{A} - \theta_{1:M}^{0:2} A_0\|_W^2 \sim \sigma_0^2 \chi_{\frac{d^2 + 3d + 2}{2}}^2,$$

and these two random variables are independent, provided that $\theta_{1:M}^{0:2}$ has rank $\frac{d^2 + 3d + 2}{2}$.

Proof of Lemma S2. The decomposition of the sum of squared errors given by (S20) is a common result in regression analysis, see e.g., Agresti [2, Section 2.2.5]. Define a random vector $\mathbf{Z} = (Z_1, \dots, Z_M)$ such that

$$\ell_{1:M}^S = \theta_{1:M}^{0:2} A_0 + \sigma_0 W^{-1/2} \mathbf{Z}.$$

¹This distribution is named SCL because it is the distribution of the Sum of a Chi-squared random variate and the Log of another chi-squared random variate.

For our normal, locally quadratic metamodel (Definition 3) under $H_0 : A = A_0$, $\sigma^2 = \sigma_0^2$, the M components of \mathbf{Z} are standard normal random variates and are independent of each other. We have

$$\begin{aligned}\hat{A} &= (\theta_{1:M}^{0:2 \top} W \theta_{1:M}^{0:2})^{-1} \theta_{1:M}^{0:2 \top} W \ell_{1:M}^S \\ &= (\theta_{1:M}^{0:2 \top} W \theta_{1:M}^{0:2})^{-1} \theta_{1:M}^{0:2 \top} W (\theta_{1:M}^{0:2} A_0 + \sigma_0 W^{-1/2} \mathbf{Z}) \\ &= A_0 + \sigma_0 (\theta_{1:M}^{0:2 \top} W \theta_{1:M}^{0:2})^{-1} \theta_{1:M}^{0:2 \top} W^{1/2} \mathbf{Z}.\end{aligned}\tag{S21}$$

Thus

$$\begin{aligned}\ell_{1:M}^S - \theta_{1:M}^{0:2} \hat{A} &= \theta_{1:M}^{0:2} A_0 + \sigma_0 W^{-1/2} \mathbf{Z} - \theta_{1:M}^{0:2} A_0 - \sigma_0 \theta_{1:M}^{0:2} (\theta_{1:M}^{0:2 \top} W \theta_{1:M}^{0:2})^{-1} \theta_{1:M}^{0:2 \top} W^{1/2} \mathbf{Z} \\ &= \sigma_0 W^{-1/2} (I - W^{1/2} \theta_{1:M}^{0:2} (\theta_{1:M}^{0:2 \top} W \theta_{1:M}^{0:2})^{-1} \theta_{1:M}^{0:2 \top} W^{1/2}) \mathbf{Z}.\end{aligned}$$

Let $H_w := W^{1/2} \theta_{1:M}^{0:2} (\theta_{1:M}^{0:2 \top} W \theta_{1:M}^{0:2})^{-1} \theta_{1:M}^{0:2 \top} W^{1/2}$. This matrix is an orthogonal projection matrix, that is, $H_w^\top = H_w$ and $H_w^2 = H_w$. It can be readily checked that $I - H_w$ is also an orthogonal projection matrix. The rank of H_w is $\frac{d^2+3d+2}{2}$ because we assume that $\theta_{1:M}^{0:2}$ has rank $\frac{d^2+3d+2}{2}$. The distribution of $\hat{\sigma}^2$ can be expressed as

$$\hat{\sigma}^2 = \frac{1}{M} \|\ell_{1:M}^S - \theta_{1:M}^{0:2} \hat{A}\|_W^2 = \frac{1}{M} \sigma_0^2 \mathbf{Z}^\top (I - H_w) \mathbf{Z} \sim \frac{1}{M} \sigma_0^2 \chi_{M - \frac{d^2+3d+2}{2}}^2,$$

because $I - H_w$ can be orthogonally diagonalizable with $M - \frac{d^2+3d+2}{2}$ eigenvalues equal to 1 and $\frac{d^2+3d+2}{2}$ eigenvalues equal to 0. One can also check that

$$\|\theta_{1:M}^{0:2} \hat{A} - \theta_{1:M}^{0:2} A_0\|_W^2 \stackrel{d}{=} \sigma_0^2 \mathbf{Z}^\top H_w \mathbf{Z} \sim \sigma_0^2 \chi_{\frac{d^2+3d+2}{2}}^2.$$

Two random variables $H_w \mathbf{Z}$ and $(I - H_w) \mathbf{Z}$ are uncorrelated, because $H_w(I - H_w) = 0$. Thus $\hat{\sigma}^2 = \frac{\sigma_0^2}{M} \mathbf{Z}^\top (I - H_w)(I - H_w) \mathbf{Z}$ and $\|\theta_{1:M}^{0:2} \hat{A} - \theta_{1:M}^{0:2} A_0\|_W^2 = \sigma_0^2 \mathbf{Z}^\top H_w H_w \mathbf{Z}$ are independent. \square

Proof of Proposition S4. Let

$$X_1 = \frac{\|\theta_{1:M}^{0:2} \hat{A} - \theta_{1:M}^{0:2} A_0\|_W^2}{\sigma_0^2}, \quad X_2 = \frac{\|\ell_{1:M}^S - \theta_{1:M}^{0:2} \hat{A}\|_W^2}{\sigma_0^2} = \frac{M \hat{\sigma}^2}{\sigma_0^2}.$$

By Lemma S2, we see that $X_1 \sim \chi_{\frac{d^2+3d+2}{2}}^2$, $X_2 \sim \chi_{M - \frac{d^2+3d+2}{2}}^2$ are independent and that $X_1 + X_2 = \|\ell_{1:M}^S - \theta_{1:M}^{0:2} \hat{A}\|_W^2$. The metamodel log likelihood ratio statistic can be expressed as

$$\begin{aligned}MLLR_{A_0, \sigma_0^2} &= \frac{M}{2} \log \frac{\hat{\sigma}^2}{\sigma_0^2} - \frac{\|\hat{\ell}_{1:M}^{SB} - \theta_{1:M}^{0:2} A_0\|_W^2}{2\sigma_0^2} + \frac{M}{2} \\ &= -\frac{X_1 + X_2}{2} + \frac{M}{2} \log \frac{X_2}{M} + \frac{M}{2} \\ &\sim \text{SCL}\left(M, \frac{d^2 + 3d + 2}{2}\right).\end{aligned}$$

\square

Proof of Proposition S5. Since $X_2 \sim \chi_{M-k}^2$ has the same distribution as that of the sum of $M-k$ independent squares of standard normal random variates, it can be readily seen by the central limit theorem that

$$\sqrt{M} \left(\frac{X_2}{M} - 1 \right) \xrightarrow{M \rightarrow \infty} \mathcal{N}(0, 2).$$

Using the Taylor expansion $\log(1 + \epsilon) = \epsilon - \frac{\epsilon^2}{2} + O(\epsilon^3)$, we see that

$$\log \frac{X_2}{M} = \frac{X_2}{M} - 1 - \frac{1}{2} \left(\frac{X_2}{M} - 1 \right)^2 + O_p \left(\frac{1}{\sqrt{M}^3} \right).$$

Therefore,

$$\begin{aligned} X_2 - M - M \log \frac{X_2}{M} &= X_2 - M - M \left[\frac{X_2}{M} - 1 - \frac{1}{2} \left(\frac{X_2}{M} - 1 \right)^2 + O_p \left(\frac{1}{\sqrt{M^3}} \right) \right] \\ &= \frac{M}{2} \left(\frac{X_2}{M} - 1 \right)^2 + O_p \left(\frac{1}{\sqrt{M}} \right) \\ &\xrightarrow{M \rightarrow \infty} \chi_1^2. \end{aligned}$$

Thus if $X_1 \sim \chi_k^2$ is independent of X_2 ,

$$-2 \cdot \text{SCL}(M, k) \stackrel{d}{=} X_1 + X_2 - M \log \frac{X_2}{M} - M \implies \chi_{k+1}^2.$$

□

S4.2 Details and proofs for Section 3.2

Proof of Proposition 4. For an arbitrary vector $\mathbf{v} = (\mathbf{v}_1^\top, \mathbf{v}_2^\top)^\top \in \mathbb{R}^{n_1+n_2}$ with $\mathbf{v}_1 \in \mathbb{R}^{n_1}$ and $\mathbf{v}_2 \in \mathbb{R}^{n_2}$ and a symmetric positive definite matrix $B = \begin{pmatrix} B_{11} & B_{12} \\ B_{12}^\top & B_{22} \end{pmatrix}$ with $B_{11} \in \mathbb{R}^{n_1 \times n_1}$ and $B_{22} \in \mathbb{R}^{n_2 \times n_2}$, the following holds:

$$\min_{\mathbf{v}_1} \mathbf{v}^\top B \mathbf{v} = \min_{\mathbf{v}_1} \begin{pmatrix} \mathbf{v}_1 \\ \mathbf{v}_2 \end{pmatrix}^\top \begin{pmatrix} B_{11} & B_{12} \\ B_{12}^\top & B_{22} \end{pmatrix} \begin{pmatrix} \mathbf{v}_1 \\ \mathbf{v}_2 \end{pmatrix} = \mathbf{v}_2^\top (B_{22} - B_{12}^\top B_{11}^{-1} B_{12}) \mathbf{v}_2.$$

From the fact that

$$U = \begin{pmatrix} u_{aa} & \mathbf{u}_{a,bc} \\ \mathbf{u}_{bc,a} & U_{bc,bc} \end{pmatrix} := \theta_{1:M}^{0:2}{}^\top W \theta_{1:M}^{0:2} = \left(\sum_{m=1}^M w_m \right) \cdot \begin{pmatrix} 1 & \bar{\theta} & \bar{\theta}^2 \\ \bar{\theta} & \bar{\theta}^2 & \bar{\theta}^3 \\ \bar{\theta}^2 & \bar{\theta}^3 & \bar{\theta}^4 \end{pmatrix},$$

it follows that

$$\begin{aligned} \min_{a_0} \|\theta_{1:M}^{0:2} \hat{A} - \theta_{1:M}^{0:2} A_0\|_W^2 &= \min_{a_0} (\hat{A} - A_0)^\top U (\hat{A} - A_0) \\ &= \begin{pmatrix} \hat{b} - b_0 \\ \text{vech}(\hat{c}) - \text{vech}(c_0) \end{pmatrix}^\top V \begin{pmatrix} \hat{b} - b_0 \\ \text{vech}(\hat{c}) - \text{vech}(c_0) \end{pmatrix} \end{aligned} \quad (\text{S22})$$

where

$$V := U_{bc,bc} - \mathbf{u}_{bc,a} u_{aa}^{-1} \mathbf{u}_{a,bc}.$$

We can find

$$\min_{-\frac{1}{2}c_0^{-1}b_0 = \theta_{H_0}} \begin{pmatrix} \hat{b} - b_0 \\ \text{vech}(\hat{c}) - \text{vech}(c_0) \end{pmatrix}^\top V \begin{pmatrix} \hat{b} - b_0 \\ \text{vech}(\hat{c}) - \text{vech}(c_0) \end{pmatrix}$$

using the method of Lagrange multiplier. Let

$$\mathcal{L} = \begin{pmatrix} \hat{b} - b_0 \\ \text{vech}(\hat{c}) - \text{vech}(c_0) \end{pmatrix}^\top V \begin{pmatrix} \hat{b} - b_0 \\ \text{vech}(\hat{c}) - \text{vech}(c_0) \end{pmatrix} + \lambda^\top (2\theta_{H_0, \text{mat}} \text{vech}(c_0) + b_0)$$

for $\lambda \in \mathbb{R}^d$. We find

$$\begin{aligned} \left(\frac{\partial \mathcal{L}}{\partial b_0} \right)^\top &= 2V_{bb}(b_0 - \hat{b}) - 2V_{bc}(\text{vech}(\hat{c}) - \text{vech}(c_0)) + \lambda, \\ \left(\frac{\partial \mathcal{L}}{\partial \text{vech}(c_0)} \right)^\top &= -2V_{cb}(\hat{b} - b_0) - 2V_{cc}(\text{vech}(\hat{c}) - \text{vech}(c_0)) + 2\theta_{H_0, \text{mat}}^\top \lambda. \end{aligned}$$

Equating both expression to zero gives

$$V_{cb}(b_0 - \hat{b}) + V_{cc}(\text{vech}(c_0) - \text{vech}(\hat{c})) = \theta_{H_0, \text{mat}}^\top \{2V_{bb}(b_0 - \hat{b}) + 2V_{bc}(\text{vech}(c_0) - \text{vech}(\hat{c}))\}.$$

Thus by writing

$$V_1 := V_{cb} - 2\theta_{H_0, \text{mat}}^\top V_{bb}, \quad V_2 := V_{cc} - 2\theta_{H_0, \text{mat}}^\top V_{bc},$$

we have

$$V_1(b_0 - \hat{b}) + V_2(\text{vech}(c_0) - \text{vech}(\hat{c})) = 0.$$

By using the constraint $2\theta_{H_0, \text{mat}} \text{vech}(c_0) + b_0 = 0$, we obtain

$$\begin{aligned} \text{vech}(c_0) &= (V_2 - 2V_1\theta_{H_0, \text{mat}})^{-1}(V_1\hat{b} + V_2\text{vech}(\hat{c})), \\ b_0 &= -2\theta_{H_0, \text{mat}}(V_2 - 2V_1\theta_{H_0, \text{mat}})^{-1}(V_1\hat{b} + V_2\text{vech}(\hat{c})). \end{aligned}$$

We will write

$$\begin{aligned} V_- &:= V_2 - 2V_1\theta_{H_0, \text{mat}} = V_{cc} - 2\theta_{H_0, \text{mat}}^\top V_{bc} - 2V_{cb}\theta_{H_0, \text{mat}} + 4\theta_{H_0, \text{mat}}^\top V_{bb}\theta_{H_0, \text{mat}} \\ &= \begin{pmatrix} -2\theta_{H_0, \text{mat}}^\top & I_{\frac{d^2+d}{2}} \end{pmatrix} \begin{pmatrix} V_{bb} & V_{bc} \\ V_{cb} & V_{cc} \end{pmatrix} \begin{pmatrix} -2\theta_{H_0, \text{mat}} \\ I_{\frac{d^2+d}{2}} \end{pmatrix}, \end{aligned}$$

We then have

$$\begin{aligned} \begin{pmatrix} b_0 \\ \text{vech}(c_0) \end{pmatrix} &= \begin{pmatrix} -2\theta_{H_0, \text{mat}} V_-^{-1} V_1 & -2\theta_{H_0, \text{mat}} V_-^{-1} V_2 \\ V_-^{-1} V_1 & V_-^{-1} V_2 \end{pmatrix} \begin{pmatrix} \hat{b} \\ \text{vech}(\hat{c}) \end{pmatrix} \\ &= \begin{pmatrix} -2\theta_{H_0, \text{mat}} \\ I_{\frac{d^2+d}{2}} \end{pmatrix} V_-^{-1} \begin{pmatrix} -2\theta_{H_0, \text{mat}}^\top & I_{\frac{d^2+d}{2}} \end{pmatrix} V \begin{pmatrix} \hat{b} \\ \text{vech}(\hat{c}) \end{pmatrix}. \end{aligned}$$

By plugging in this solution to the constrained optimization problem, we find

$$\begin{aligned} \min_{-\frac{1}{2}c_0^{-1}b_0 = \theta_{H_0}} & \begin{pmatrix} \hat{b} - b_0 \\ \text{vech}(\hat{c}) - \text{vech}(c_0) \end{pmatrix}^\top V \begin{pmatrix} \hat{b} - b_0 \\ \text{vech}(\hat{c}) - \text{vech}(c_0) \end{pmatrix} \\ &= \left\{ I_{\frac{d^2+3d}{2}} - \begin{pmatrix} -2\theta_{H_0, \text{mat}} \\ I_{\frac{d^2+d}{2}} \end{pmatrix} V_-^{-1} \begin{pmatrix} -2\theta_{H_0, \text{mat}}^\top & I_{\frac{d^2+d}{2}} \end{pmatrix} V \begin{pmatrix} \hat{b} \\ \text{vech}(\hat{c}) \end{pmatrix} \right\}^\top \\ & \quad \left\{ I_{\frac{d^2+3d}{2}} - \begin{pmatrix} -2\theta_{H_0, \text{mat}} \\ I_{\frac{d^2+d}{2}} \end{pmatrix} V_-^{-1} \begin{pmatrix} -2\theta_{H_0, \text{mat}}^\top & I_{\frac{d^2+d}{2}} \end{pmatrix} V \begin{pmatrix} \hat{b} \\ \text{vech}(\hat{c}) \end{pmatrix} \right\} \\ &= V - V \begin{pmatrix} -2\theta_{H_0, \text{mat}} \\ I_{\frac{d^2+d}{2}} \end{pmatrix} V_-^{-1} \begin{pmatrix} -2\theta_{H_0, \text{mat}}^\top & I_{\frac{d^2+d}{2}} \end{pmatrix} V. \end{aligned}$$

Using Lemma S3, we can express this constrained minimum as

$$\begin{pmatrix} I_d \\ 2\theta_{H_0, \text{mat}}^\top \end{pmatrix} \left\{ (I \quad 2\theta_{H_0, \text{mat}}) V^{-1} \begin{pmatrix} I \\ 2\theta_{H_0, \text{mat}}^\top \end{pmatrix} \right\}^{-1} (I_d \quad 2\theta_{H_0, \text{mat}}), \quad (\text{S23})$$

The $MLLR_{\theta_{H_0}}$ statistic is given by

$$\begin{aligned} MLLR_{\theta_{H_0}} &= \sup_{\sigma_0^2 > 0} \sup_{-\frac{1}{2}c_0^{-1}b_0 = \theta_{H_0}} \frac{M}{2} \log \frac{\hat{\sigma}^2}{\sigma_0^2} - \frac{M\hat{\sigma}^2}{2\sigma_0^2} - \frac{\|\theta_{1:M}^{0:2}\hat{A} - \theta_{1:M}^{0:2}A_0\|_W^2}{2\sigma_0^2} + \frac{M}{2} \\ &= \sup_{\sigma_0^2 > 0} \frac{M}{2} \log \frac{\hat{\sigma}^2}{\sigma_0^2} - \frac{M\hat{\sigma}^2}{2\sigma_0^2} - \frac{\xi}{2\sigma_0^2} + \frac{M}{2} \\ &= \frac{M}{2} \log \frac{\hat{\sigma}^2}{\hat{\sigma}^2 + M^{-1}\xi} = -\frac{M}{2} \log \left(\frac{\xi}{M\hat{\sigma}^2} + 1 \right). \end{aligned}$$

In the proof of Lemma S2, we showed that

$$\hat{A} = A_0 + \sigma_0(\theta_{1:M}^{0:2 \top} W \theta_{1:M}^{0:2})^{-1} \theta_{1:M}^{0:2 \top} W^{1/2} \mathbf{Z}$$

where $\mathbf{Z} \sim \mathcal{N}(0, I_M)$. Thus we have

$$\begin{aligned} \hat{b} + 2\hat{c}\theta_{H_0} &= (\mathbf{0}_d, I_d, 2\theta_{H_0, \text{mat}}) \hat{A} \\ &= \sigma_0 \cdot (\mathbf{0}_d, I_d, 2\theta_{H_0, \text{mat}}) U^{-1} \theta_{1:M}^{0:2 \top} W^{1/2} \mathbf{Z}, \end{aligned}$$

since we assume $(\mathbf{0}_d, I_d, 2\theta_{H_0, \text{mat}}) A_0 = b_0 + 2c_0\theta_{H_0} = 0$. Hence,

$$\hat{b} + 2\hat{c}\theta_{H_0} \sim \mathcal{N}\{0, \sigma_0^2 \cdot (\mathbf{0}_d, I_d, 2\theta_{H_0, \text{mat}}) U^{-1} (\mathbf{0}_d, I_d, 2\theta_{H_0, \text{mat}})^\top\}$$

Using the block matrix inversion formula [10], we see that when the first row and the first column of U^{-1} are removed, we obtain V^{-1} :

$$U^{-1} = \begin{pmatrix} * & * & * \\ * & V^{-1} & * \\ * & * & * \end{pmatrix}.$$

Thus

$$\hat{b} + 2\hat{c}\theta_{H_0} \sim \mathcal{N}\{0, \sigma_0^2 \cdot (I_d, 2\theta_{H_0, \text{mat}}) V^{-1} (I_d, 2\theta_{H_0, \text{mat}})^\top\}$$

Therefore, we have

$$\xi = (\hat{b} + 2\hat{c}\theta_{H_0})^\top \left\{ \begin{pmatrix} I_d \\ 2\theta_{H_0, \text{mat}}^\top \end{pmatrix}^\top V^{-1} \begin{pmatrix} I_d \\ 2\theta_{H_0, \text{mat}}^\top \end{pmatrix} \right\}^{-1} (\hat{b} + 2c_0\theta_{H_0}) \sim \sigma_0^2 \chi_d^2.$$

Furthermore, we showed in Lemma S2 that $M\hat{\sigma}^2 \sim \sigma_0^2 \chi_{M - \frac{d^2+3d+2}{2}}^2$ and that \hat{A} and $\hat{\sigma}^2$ are independent. It follows that

$$\frac{(M - \frac{d^2+3d+2}{2})\xi}{Md\hat{\sigma}^2} \sim F_{d, M - \frac{d^2+3d+2}{2}}.$$

□

Lemma S3. Let $V = \begin{pmatrix} V_{11} & V_{12} \\ V_{21} & V_{22} \end{pmatrix}$ be a block matrix with $V_{11} \in \mathbb{R}^{d_1 \times d_1}$ and $V_{22} \in \mathbb{R}^{d_2 \times d_2}$. If V and V_{11} are invertible, then for any matrix $B \in \mathbb{R}^{d_1 \times d_2}$, we have

$$\begin{aligned} \begin{pmatrix} I_{d_1} \\ B^\top \end{pmatrix} \left\{ (I_{d_1} \ B) V^{-1} \begin{pmatrix} I_{d_1} \\ B^\top \end{pmatrix} \right\}^{-1} (I_{d_1} \ B) \\ = V - V \begin{pmatrix} -B \\ I_{d_2} \end{pmatrix} \left\{ (-B^\top \ I_{d_2}) V \begin{pmatrix} -B \\ I_{d_2} \end{pmatrix} \right\}^{-1} (-B^\top \ I_{d_2}) V. \end{aligned} \quad (\text{S24})$$

Proof. Writing $V_{2|1} := V_{22} - V_{21}V_{11}^{-1}V_{12}$, we have, according to Lu and Shiou [10, Theorem 2.1], that

$$V^{-1} = \begin{pmatrix} V_{11}^{-1} + V_{11}^{-1}V_{12}V_{2|1}^{-1}V_{21}V_{11}^{-1} & -V_{11}^{-1}V_{12}V_{2|1}^{-1} \\ -V_{2|1}^{-1}V_{21}V_{11}^{-1} & V_{2|1}^{-1} \end{pmatrix}.$$

Thus we can write

$$(I_{d_1} \ B) V^{-1} \begin{pmatrix} I_{d_1} \\ B^\top \end{pmatrix} = V_{11}^{-1} + (I_{d_1} \ B) \begin{pmatrix} V_{11}^{-1}V_{12} \\ -I_{d_2} \end{pmatrix} V_{2|1}^{-1} (V_{21}V_{11}^{-1} \ -I_{d_2}) \begin{pmatrix} I_{d_1} \\ B^\top \end{pmatrix}$$

Using the Sherman-Morrison-Woodbury formula [14]

$$(A + BCD)^{-1} = A^{-1} - A^{-1}B(C^{-1} + DA^{-1}B)^{-1}DA^{-1},$$

we have

$$\begin{aligned}
& \left\{ V_{11}^{-1} + (I_{d_1} \quad B) \begin{pmatrix} V_{11}^{-1} V_{12} \\ -I_{d_2} \end{pmatrix} V_{2|1}^{-1} (V_{21} V_{11}^{-1} \quad -I_{d_1}) \begin{pmatrix} I_{d_1} \\ B^\top \end{pmatrix} \right\}^{-1} \\
&= V_{11} - V_{11} (V_{11}^{-1} V_{12} - B) \{ V_{2|1} + (V_{21} V_{11}^{-1} - B^\top) V_{11} (V_{11}^{-1} V_{12} - B) \}^{-1} (V_{21} V_{11}^{-1} - B^\top) V_{11} \\
&= V_{11} - (V_{12} - V_{11} B) \left\{ (-B^\top \quad I_{d_2}) V \begin{pmatrix} -B \\ I_{d_2} \end{pmatrix} \right\}^{-1} (V_{21} - B^\top V_{11}),
\end{aligned}$$

showing that the top-left matrix blocks for the left and the right hand sides of (S24) agree. To show that the bottom-left matrix blocks agree, we need to show that the bottom-left matrix block of the right hand side of (S24) is obtained by multiplying B^\top on the left of the top-left block. This can be checked by observing that

$$(-B^\top \quad I_{d_2}) \left[V - V \begin{pmatrix} -B \\ I_{d_2} \end{pmatrix} \left\{ (-B^\top \quad I_{d_2}) V \begin{pmatrix} -B \\ I_{d_2} \end{pmatrix} \right\}^{-1} (-B^\top \quad I_{d_2}) V \right] = 0.$$

The fact that the top-right and the bottom-right blocks agree on either side of (S24) can be shown by the fact that

$$\left[V - V \begin{pmatrix} -B \\ I_{d_2} \end{pmatrix} \left\{ (-B^\top \quad I_{d_2}) V \begin{pmatrix} -B \\ I_{d_2} \end{pmatrix} \right\}^{-1} (-B^\top \quad I_{d_2}) V \right] \begin{pmatrix} -B \\ I_{d_2} \end{pmatrix} = 0.$$

□

Proof of Corollary 1. Proposition 4 shows that for $d = 1$, $H_0 : \theta_{MESLE} = \theta_{H_0}$ is not rejected at level α if

$$\xi = \frac{M - 3}{M \hat{\sigma}^2} \frac{(\hat{b} + 2\hat{c}\theta_{H_0})^2 (V_{bb}V_{cc} - V_{bc}^2)}{V_{cc} - 4V_{bc}\theta_{H_0} + 4V_{bb}\theta_{H_0}^2} < F_{1, M-3, \alpha}.$$

Rearranging the terms, we see that a level $1 - \alpha$ confidence interval for θ_{MESLE} is given by

$$\begin{aligned}
& \{ \theta; [4(M - 3)\hat{c}^2 \det V - 4M\hat{\sigma}^2 F_{1, M-3, \alpha} V_{bb}] \theta^2 \\
& \quad + [4(M - 3)\hat{b}\hat{c} \det V + 4M\hat{\sigma}^2 F_{1, M-3, \alpha} V_{bc}] \theta \\
& \quad + (M - 3)\hat{b}^2 \det V - M\hat{\sigma}^2 F_{1, M-3, \alpha} V_{cc} < 0 \},
\end{aligned}$$

where $\det V = V_{bb}V_{cc} - V_{bc}^2$. □

S5 Mathematical details and proofs for Section 4

We have from Section 4 that

$$C\ell_{1:M}^S | \sigma^2 \sim \mathcal{N} \left(C\theta_{1:M}^{1:2} \begin{pmatrix} -2c\theta_* \\ \text{vech}(c) \end{pmatrix}, \sigma^2 C W^{-1} C^\top + C\theta_{1:M} n K_1 \theta_{1:M}^\top C^\top \right)$$

where $C = (-\mathbf{1}_{M-1}, I_{M-1})$. In fact, since we are concerned about relative values of $\ell^S(\theta_m)$, $m \in 1 : M$, we can use any $(M - 1) \times M$ matrix C whose rows are independent of each other and orthogonal to $(1, \dots, 1)$. It can be checked using the Sherman-Morrison-Woodbury formula $(A + BCD)^{-1} = A^{-1} - A^{-1}B(C^{-1} + DA^{-1}B)^{-1}DA^{-1}$ that

$$C^\top (CW^{-1}C^\top)^{-1}C = W - (\mathbf{1}_M^\top W \mathbf{1}_M)^{-1} W \mathbf{1}_M \mathbf{1}_M^\top W =: \bar{W}$$

[14]. We let

$$Q = (CW^{-1}C^\top + \sigma^{-2}C\theta_{1:M} n K_1 \theta_{1:M}^\top C^\top)^{-1}.$$

Then again by the Sherman-Morrison-Woodbury formula, we have

$$\begin{aligned}
Q &= (CW^{-1}C^\top)^{-1} \\
&\quad - (CW^{-1}C^\top)^{-1} C \theta_{1:M} \{ \sigma^2 n^{-1} K_1^{-1} + \theta_{1:M}^\top C^\top (CW^{-1}C^\top)^{-1} C \theta_{1:M} \}^{-1} \theta_{1:M}^\top C^\top (CW^{-1}C^\top)^{-1}.
\end{aligned}$$

If we let $P = C^\top QC$, we have

$$P = \bar{W} - \bar{W}\theta_{1:M}(\sigma^2 n^{-1} K_1^{-1} + \theta_{1:M}^\top \bar{W}\theta_{1:M})^{-1} \theta_{1:M}^\top \bar{W}.$$

We denote by \hat{Q} the matrix obtained by substituting $\hat{\sigma}^2$ for σ^2 and \hat{K}_1 for K_1 in the expression for Q :

$$\begin{aligned} \hat{Q} &= (CW^{-1}C^\top)^{-1} \\ &\quad - (CW^{-1}C^\top)^{-1} C\theta_{1:M} \{ \hat{\sigma}^2 n^{-1} \hat{K}_1^{-1} + \theta_{1:M}^\top C^\top (CW^{-1}C^\top)^{-1} C\theta_{1:M} \}^{-1} \theta_{1:M}^\top C^\top (CW^{-1}C^\top)^{-1}. \end{aligned}$$

Then we have $\hat{P} = C^\top \hat{Q} C$.

The log density function of (26) evaluated at $C\ell_{1:M}^S$, or the marginal metamodel log-likelihood, is given by

$$\begin{aligned} \log p_{\text{meta}}(C\hat{\ell}_{1:M}^S | \theta_*, c, \sigma^2) &= -\frac{M-1}{2} \log 2\pi - \frac{1}{2} \log \det(\sigma^2 Q^{-1}) \\ &\quad - \frac{1}{2\sigma^2} \left\| \ell_{1:M}^S - \theta_{1:M}^{1:2} \begin{pmatrix} -2c\theta_* \\ \text{vech}(c) \end{pmatrix} \right\|_{C^\top QC}^2 \end{aligned}$$

Using the matrix determinant lemma $\det(A + BCD) = \det(C^{-1} + DA^{-1}B) \det(A) \det(C)$, we see that

$$\begin{aligned} \det Q^{-1} &= \det \{ CW^{-1}C^\top + \sigma^{-2} (C\theta_{1:M}) n K_1 (C\theta_{1:M})^\top \} \\ &= \det \{ \sigma^2 n^{-1} K_1^{-1} + (C\theta_{1:M})^\top (CW^{-1}C^\top)^{-1} (C\theta_{1:M}) \} \det(\sigma^{-2} n K_1) \det(CW^{-1}C^\top) \\ &= \det \{ I_d + \sigma^{-2} n K_1 \theta_{1:M}^\top \bar{W} \theta_{1:M} \} \det(CW^{-1}C^\top). \end{aligned}$$

Therefore, we have

$$\begin{aligned} \log p_{\text{meta}}(C\ell_{1:M}^S | \theta_*, c, \sigma^2) &= \text{const.} - \frac{1}{2\sigma^2} \left\| \ell_{1:M}^S - \theta_{1:M}^{1:2} \begin{pmatrix} -2c\theta_* \\ \text{vech}(c) \end{pmatrix} \right\|_{C^\top QC}^2 \\ &\quad - \frac{M-1}{2} \log \sigma^2 - \frac{1}{2} \log \det(I_d + \sigma^{-2} n K_1 \theta_{1:M}^\top \bar{W} \theta_{1:M}). \quad (\text{S25}) \end{aligned}$$

We substitute $\hat{\sigma}^2$ for σ^2 and \hat{K}_1 for K_1 in the third term on the right hand side of the above equation and substitute \hat{P} for $P = C^\top QC$. The estimating equation for $\hat{\theta}_*$ and \hat{c} , namely Equation (27), is then obtained by a usual weighted least square estimate for

$$\min_{\theta_*, c} \left\| \ell_{1:M}^S - \theta_{1:M}^{1:2} \begin{pmatrix} -2c\theta_* \\ \text{vech}(c) \end{pmatrix} \right\|_{\hat{P}}^2.$$

Consider a test on θ_* , c , and σ^2 ,

$$H_0 : \theta_* = \theta_{*,0}, \quad c = c_0, \quad \sigma^2 = \sigma_0^2, \quad H_1 : \text{not } H_0$$

for some null values $\theta_{*,0}$, c_0 , and σ_0^2 . An approximate test for these hypotheses can be conducted by using the marginal metamodel log-likelihood (S25). The marginal metamodel log-likelihood ratio statistic for this test is given by

$$MLLR_{\theta_{*,0}, c_0, \sigma_0^2} = -\frac{1}{2\sigma_0^2} \left\| \ell_{1:M}^S - \theta_{1:M}^{1:2} \begin{pmatrix} -2c_0\theta_{*,0} \\ \text{vech}(c_0) \end{pmatrix} \right\|_{\hat{P}}^2 + \frac{M-1}{2} \log \frac{\hat{\sigma}_{2\text{nd}}^2}{\sigma_0^2} + \frac{M-1}{2}, \quad (\text{S26})$$

where $\hat{\sigma}_{2\text{nd}}^2$ is the second stage estimate given by (28). The distribution of the $MLLR_{\theta_{*,0}, c_0, \sigma_0^2}$ statistic under $H_0 : \theta_* = \theta_{*,0}, c = c_0, \sigma^2 = \sigma_0^2$ is given by Proposition S6 at the end of this section.

A test on the simulation-based proxy $H_0 : \theta_* = \theta_{*,0}$, $H_1 : \theta_* \neq \theta_{*,0}$ can be carried out by using the marginal metamodel log-likelihood ratio statistic obtained by taking the supremum of $MLLR_{\theta_{*,0}, c_0, \sigma_0^2}$ over c_0 and σ_0^2 :

$$MLLR_{\theta_{*,0}} = \sup_{c_0, \sigma_0^2} MLLR_{\theta_{*,0}, c_0, \sigma_0^2}. \quad (\text{S27})$$

Proof of Proposition 5. We consider the model

$$C\ell_{1:M}^S \sim \mathcal{N}\left(C\theta_{1:M}^{1:2} \begin{pmatrix} -2c\theta_* \\ \text{vech}(c) \end{pmatrix}, \sigma^2 \hat{Q}^{-1}\right),$$

where we use the plug-in estimate \hat{Q} for the variance. Define a random vector \mathbf{Z} such that

$$C\ell_{1:M}^S = C\theta_{1:M}^{1:2} \begin{pmatrix} -2c\theta_* \\ \text{vech}(c) \end{pmatrix} + \sigma \hat{Q}^{-1/2} \mathbf{Z}, \quad (\text{S28})$$

so that $\mathbf{Z} \sim \mathcal{N}(0, I_{M-1})$, approximately. We then have

$$\begin{aligned} & \left(I_{M-1} - \hat{Q}^{1/2} C \theta_{1:M}^{1:2} \{ \theta_{1:M}^{1:2}{}^\top C^\top \hat{Q} C \theta_{1:M}^{1:2} \}^{-1} \theta_{1:M}^{1:2} C^\top \hat{Q}^{1/2} \right) \hat{Q}^{1/2} C \ell_{1:M}^S \\ &= \left(I_{M-1} - \hat{Q}^{1/2} C \theta_{1:M}^{1:2} \{ \theta_{1:M}^{1:2}{}^\top C^\top \hat{Q} C \theta_{1:M}^{1:2} \}^{-1} \theta_{1:M}^{1:2} C^\top \hat{Q}^{1/2} \right) \sigma \mathbf{Z} \end{aligned} \quad (\text{S29})$$

From (27) and (S29), we have

$$\begin{aligned} \hat{\sigma}_{2\text{nd}}^2 &= \frac{1}{M-1} \left\| \hat{Q}^{1/2} C \ell_{1:M}^S - n \hat{Q}^{1/2} C \theta_{1:M}^{1:2} \begin{pmatrix} -2\hat{c}\hat{\theta}_* \\ \text{vech}(\hat{c}) \end{pmatrix} \right\|^2 \\ &= \frac{1}{M-1} \left\| \left(I_{M-1} - \hat{Q}^{1/2} C \theta_{1:M}^{1:2} \{ \theta_{1:M}^{1:2}{}^\top C^\top \hat{Q} C \theta_{1:M}^{1:2} \}^{-1} \theta_{1:M}^{1:2} C^\top \hat{Q}^{1/2} \right) \hat{Q}^{1/2} C \ell_{1:M}^S \right\|^2 \\ &= \frac{\sigma^2}{M-1} \mathbf{Z}^\top \left(I_{M-1} - \hat{Q}^{1/2} C \theta_{1:M}^{1:2} \{ \theta_{1:M}^{1:2}{}^\top C^\top \hat{Q} C \theta_{1:M}^{1:2} \}^{-1} \theta_{1:M}^{1:2} C^\top \hat{Q}^{1/2} \right) \mathbf{Z} \\ &\sim \frac{\sigma^2}{M-1} \chi_{M - \frac{d^2+3d+2}{2}}^2, \end{aligned}$$

since $\hat{Q}^{1/2} C \theta_{1:M}^{1:2} \in \mathbb{R}^{(M-1) \times \frac{d^2+3d}{2}}$ is a rank $\frac{d^2+3d}{2}$ matrix.

Now suppose that the null hypothesis $H_0 : \theta_* = \theta_{*,0}$ is true. Then by the usual results for weighted least squares regression, we have

$$\begin{aligned} & \inf_c \left\| \hat{Q}^{1/2} C \ell_{1:M}^S - \hat{Q}^{1:2} C \theta_{1:M}^{1:2} \begin{pmatrix} -2c\theta_{*,0} \\ \text{vech}(c) \end{pmatrix} \right\|^2 \\ &= \inf_{K_2} \left\| \hat{Q}^{1/2} C \ell_{1:M}^S - \hat{Q}^{1:2} C \theta_{1:M}^{1:2} \begin{pmatrix} -\theta_{*,0,\text{mat}} \\ -\frac{1}{2} I_{\frac{d^2+d}{2}} \end{pmatrix} n \text{vech}(K_2) \right\|^2 \\ &= \inf_{K_2} \left\| \ell_{1:M}^S - T(\theta_{*,0}) n \text{vech}(K_2) \right\|_{\hat{P}}^2 \\ &= \left\| \left(I_{M-1} - T(\theta_{*,0}) \{ T(\theta_{*,0})^\top \hat{P} T(\theta_{*,0}) \}^{-1} T(\theta_{*,0})^\top \hat{P} \right) \ell_{1:M}^S \right\|_{\hat{P}}^2 \\ &= \left\| \{ I_{M-1} - S(\theta_{*,0}) \hat{P} \} \ell_{1:M}^S \right\|_{\hat{P}}^2 \end{aligned}$$

Since the maximum of $-\frac{a}{x} - b \log x$ over $x > 0$ is obtained at $x = a/b$ for $a, b > 0$, we have

$$\begin{aligned} MLLR_{\theta_{*,0}} &= \sup_{\sigma_0^2} -\frac{1}{2\sigma_0^2} \left\| \{ I_{M-1} - S(\theta_{*,0}) \hat{P} \} \ell_{1:M}^S \right\|_{\hat{P}}^2 + \frac{M-1}{2} \log \frac{\hat{\sigma}_{2\text{nd}}^2}{\sigma_0^2} + \frac{M-1}{2} \\ &= -\frac{M-1}{2} + \frac{M-1}{2} \log \frac{(M-1) \hat{\sigma}_{2\text{nd}}^2}{\left\| \{ I_{M-1} - S(\theta_{*,0}) \hat{P} \} \ell_{1:M}^S \right\|_{\hat{P}}^2} + \frac{M-1}{2} \\ &= -\frac{M-1}{2} \log \frac{\left\| \{ I_{M-1} - S(\theta_{*,0}) \hat{P} \} \ell_{1:M}^S \right\|_{\hat{P}}^2}{(M-1) \hat{\sigma}_{2\text{nd}}^2}. \end{aligned}$$

Let

$$H := \hat{Q}^{1/2} C \theta_{1:M}^{1:2} (\theta_{1:M}^{1:2 \top} C^\top \hat{Q} C \theta_{1:M}^{1:2})^{-1} \theta_{1:M}^{1:2 \top} C^\top \hat{Q}^{1/2} \quad (\text{S30})$$

be a orthogonal projection matrix of rank $\frac{d^2+3d}{2}$ and

$$G := \hat{Q}^{1/2} C T(\theta_{*,0}) \left\{ T(\theta_{*,0})^\top \hat{P} T(\theta_{*,0}) \right\}^{-1} T(\theta_{*,0})^\top C^\top \hat{Q}^{1/2}$$

be another orthogonal projection matrix of rank $\frac{d^2+d}{2}$. We have $GH = HG = G$, that is, G is a nested orthogonal projection with respect to H . We have

$$(I - G) \hat{Q}^{1/2} C \ell_{1:M}^S = (I - G) \sigma \mathbf{Z}$$

due to (S29). Thus we obtain

$$\|(I - G) \hat{Q}^{1/2} C \ell_{1:M}^S\|^2 = \sigma^2 \mathbf{Z}^\top (I - G) \mathbf{Z} = (M - 1) \hat{\sigma}_{2\text{nd}}^2 + \sigma^2 \mathbf{Z}^\top (H - G) \mathbf{Z}. \quad (\text{S31})$$

Since $H - G$ is an orthogonal projection matrix with rank $\frac{d^2+3d}{2} - \frac{d^2+d}{2} = d$, we have

$$\|(I - G) \hat{Q}^{1/2} C \ell_{1:M}^S\|^2 - (M - 1) \hat{\sigma}_{2\text{nd}}^2 = \mathbf{Z}^\top (H - G) \mathbf{Z} \sim \sigma^2 \chi_d^2,$$

and since $(I - H)(H - G) = 0$, we have that the above display and $(M - 1) \hat{\sigma}_{2\text{nd}}^2 \sim \sigma^2 \chi_{M - \frac{d^2+3d+2}{2}}^2$ are independent. It follows that

$$\begin{aligned} \frac{\|\{I_{M-1} - S(\theta_{*,0}) \hat{P}\} \ell_{1:M}^S\|_{\hat{P}}^2}{(M - 1) \hat{\sigma}_{2\text{nd}}^2} - 1 &= \frac{\|(I - G) \hat{Q}^{1/2} C \ell_{1:M}^S\|^2}{(M - 1) \hat{\sigma}_{2\text{nd}}^2} - 1 \\ &= \frac{\sigma^2 \mathbf{Z}^\top (I - G) \mathbf{Z}}{\sigma^2 \mathbf{Z}^\top (I - H) \mathbf{Z}} - 1 \\ &= \frac{\mathbf{Z}^\top (H - G) \mathbf{Z}}{\mathbf{Z}^\top (I - H) \mathbf{Z}} \\ &\sim \frac{\chi_d^2}{\chi_{M - \frac{d^2+3d+2}{2}}^2} \\ &= \frac{d}{M - \frac{d^2+3d+2}{2}} F_{d, M - \frac{d^2+3d+2}{2}}. \end{aligned}$$

□

One might be concerned about the fact the test is based on the distribution (26) that is conditioned on σ^2 . However, since the distribution of the test statistic (29) under H_0 does not depend on the value of $\sigma^2(Y_{1:n})$, its marginal distribution over $\sigma^2(Y_{1:n})$ is the same. Therefore, the test is valid nonetheless. The same reasoning was used by Zellner [15] to consider multivariate t -distributed errors in linear regression.

Proof of Corollary 2. We have

$$\begin{aligned} &\|\{I_{M-1} - S(\theta_{*,0}) \hat{P}\} \ell_{1:M}^S\|_{\hat{P}}^2 \\ &= \ell_{1:M}^S \top \left(\hat{P} - \hat{P} S(\theta_{*,0}) \hat{P} \right) \ell_{1:M}^S \\ &= \|\ell_{1:M}^S\|_{\hat{P}}^2 - \ell_{1:M}^S \top \hat{P} \theta_{1:M}^{1:2} \begin{pmatrix} \theta_0 \\ -\frac{1}{2} \end{pmatrix} \left\{ \left(\theta_0, -\frac{1}{2} \right) \theta_{1:M}^{1:2 \top} \hat{P} \theta_{1:M}^{1:2} \begin{pmatrix} \theta_0 \\ -\frac{1}{2} \end{pmatrix} \right\}^{-1} \left(\theta_0, -\frac{1}{2} \right) \theta_{1:M}^{1:2 \top} \hat{P} \ell_{1:M}^S \\ &= \|\ell_{1:M}^S\|_{\hat{P}}^2 - \frac{(\zeta_1 \theta_0 - \frac{1}{2} \zeta_2)^2}{\rho_{11} \theta_0^2 - \rho_{12} \theta_0 + \frac{1}{4} \rho_{22}}. \end{aligned}$$

The null $H_0 : \theta = \theta_0$ is not rejected at an approximate significance level α if

$$\|\{I_{M-1} - S(\theta_{*,0}) \hat{P}\} \ell_{1:M}^S\|_{\hat{P}}^2 < (M - 1) \hat{\sigma}_{2\text{nd}}^2 \left(\frac{F_{1, M-3, \alpha}}{M - 3} + 1 \right).$$

This is equivalent to

$$\|\ell_{1:M}^S\|_{\hat{P}}^2 - (M-1)\hat{\sigma}_{2\text{nd}}^2 \left(\frac{F_{1,M-3,\alpha}}{M-3} + 1 \right) < \frac{(\zeta_1\theta_0 - \frac{1}{2}\zeta_2)^2}{\rho_{11}\theta_0^2 - \rho_{12}\theta_0 + \frac{1}{4}\rho_{22}}.$$

Denoting the left hand side of the above inequality by ζ_0 , we can rearrange the terms to obtain

$$(\zeta_0\rho_{11} - \zeta_1^2)\theta_0^2 + (\zeta_1\zeta_2 - \zeta_0\rho_{12})\theta_0 + \frac{1}{4}(\rho_{22}\zeta_0 - \zeta_2^2) < 0,$$

which gives an approximate level $1 - \alpha$ confidence interval for θ . \square

We conclude this section by giving the null distribution of the $MLLR_{\theta_*,0,c_0,\sigma_0^2}$ statistic as follows.

Proposition S6. *Suppose that Assumptions 1-6 hold. If $Q = \hat{Q}$, then the $MLLR_{\theta_*,0,c_0,\sigma_0^2}$ statistic under $H_0 : \theta_* = \theta_{*,0}, c = c_0, \sigma^2 = \sigma_0^2$ follows the $SCL(M-1, \frac{d^2+3d}{2})$ distribution.*

Proof of Proposition S6. From (S26) and (S28), we have

$$MLLR_{\theta_*,0,c_0,\sigma_0^2} = -\frac{1}{2}\|\mathbf{Z}\|^2 + \frac{M-1}{2} \log \frac{\mathbf{Z}^\top (I_{M-1} - H)\mathbf{Z}}{M-1} + \frac{M-1}{2}$$

where H is defined by (S30). In the proof of Proposition 5, we showed that

$$X_1 := \mathbf{Z}^\top H\mathbf{Z} \sim \chi_{\frac{d^2+3d}{2}}^2, \quad X_2 := \mathbf{Z}^\top (I_{M-1} - H)\mathbf{Z} \sim \chi_{M - \frac{d^2+3d+2}{2}}^2$$

and that X_1 and X_2 are independent. Therefore, the $MLLR_{\theta_*,0,c_0,\sigma_0^2}$ statistic follows the $SCL(M-1, \frac{d^2+3d}{2})$ distribution. \square

S6 Monte Carlo correction of the bias in the test on θ_*

Our hypothesis testing procedure for the simulation-based proxy uses a plug-in estimate \hat{K}_1 of K_1 . The estimation error in \hat{K}_1 introduces a bias in the test. This bias may be reduced by a Monte Carlo method that takes into account the variability in \hat{K}_1 , described as follows. The test statistic for the test on θ_* is given by (29),

$$\frac{M - \frac{d^2+3d+2}{2}}{d} \left\{ \frac{\|\{I_{M-1} - S(\theta_{*,0})\hat{P}\}\ell_{1:M}^S\|_{\hat{P}}^2}{(M-1)\hat{\sigma}_{2\text{nd}}^2} - 1 \right\}.$$

In order to obtain a Monte Carlo draw for the test statistic, we regard the estimated \hat{K}_1 , $\hat{\sigma}_{2\text{nd}}^2$, and $\hat{\theta}_*$ as if they are equal to the true values. We first create a Monte Carlo simulation for the vector $\ell_{1:M}^S$. From (S28), we see that a Monte Carlo simulation $\ell_{1:M,MC}^S$ can be obtained via

$$\hat{Q}^{1/2}C\ell_{1:M,MC}^S = \hat{Q}^{1/2}C\theta_{1:M}^{1:2} \begin{pmatrix} -2\hat{c}\hat{\theta}_* \\ \text{vech}(\hat{c}) \end{pmatrix} + \hat{\sigma}_{2\text{nd}}\mathbf{Z}_{MC}$$

where \mathbf{Z}_{MC} is a random draw from $\mathcal{N}(0, I_{M-1})$. Here $\hat{\theta}_*$ and $\text{vech}(\hat{c})$ are the point estimates obtained by (27). Since \hat{Q} is invertible and the left multiplication of $\ell_{1:M,MC}^S$ by C gives relative values with respect to $\ell_{1,MC}^S$, we can let without loss of generality

$$\ell_{1,MC}^S := 0, \quad \ell_{2:M,MC}^S = \hat{Q}^{-1/2} \left\{ \hat{Q}^{1/2}C\theta_{1:M}^{1:2} \begin{pmatrix} -2\hat{c}\hat{\theta}_* \\ \text{vech}(\hat{c}) \end{pmatrix} + \hat{\sigma}_{2\text{nd}}\mathbf{Z}_{MC} \right\}.$$

A Monte Carlo draw for the first stage estimate of σ^2 is given by

$$\sigma_{MC}^2 := \frac{1}{M} \|(I - \theta_{1:M}^{0:2} \{\theta_{1:M}^{0:2}{}^\top W \theta_{1:M}^{0:2}\}^{-1} \theta_{1:M}^{0:2}{}^\top W)\ell_{1:M,MC}^S\|^2.$$

Denote by τ_1 and τ_2 the first and the second term on the right hand side of (22), which is used to obtain an estimate \hat{K}_1 . If $Y_{1:n}$ are iid and τ_1 is estimated by the sample variance of the n estimated slopes of the fitted quadratic polynomial, a Monte Carlo draw $\tau_{1,MC}$ can be obtained by a draw from the Wishart distribution $\mathcal{W}_d(\frac{1}{\nu}\tau_1, \nu)$ where the degrees of freedom is equal to $\nu = n - 1$. If τ_1 is estimated by using n_b batch estimates, a Monte Carlo draw is obtained from $\mathcal{W}_d(\frac{1}{\nu}\tau_1, \nu)$ with $\nu = n_b - 1$. A Monte Carlo draw for τ_2 is obtained by

$$\tau_{2,MC} = \frac{1}{n}(\mathbf{0}_d, I_d, 2\theta_{\text{mat}})(\theta_{1:M}^{0:2 \top} W \theta_{1:M}^{0:2})^{-1}(\mathbf{0}_d, I_d, 2\theta_{\text{mat}})^\top \hat{\sigma}_{MC}^2$$

(see (23).) A Monte Carlo draw for \hat{K}_1 is then obtained by

$$\hat{K}_{1,MC} = \tau_{1,MC} - \tau_{2,MC}.$$

A Monte Carlo replicate for \hat{Q} is given by

$$\hat{Q}_{MC} := \{CW^{-1}C^\top + \sigma_{MC}^{-2}C\theta_{1:M}n\hat{K}_{1,MC}\theta_{1:M}^\top C^\top\}^{-1}.$$

We let $\hat{P}_{MC} := C^\top \hat{Q}_{MC} C$. A Monte Carlo draw for the second stage estimate $\hat{\sigma}_{2\text{nd}}^2$ is obtained by

$$\hat{\sigma}_{2\text{nd},MC}^2 = \frac{1}{M-1} \left\| \ell_{1:M,MC}^S - \theta_{1:M}^{1:2} \left\{ \theta_{1:M}^{1:2 \top} \hat{P}_{MC} \theta_{1:M}^{1:2} \right\}^{-1} \theta_{1:M}^{1:2 \top} \hat{P}_{MC} \ell_{1:M,MC}^S \right\|_{\hat{P}_{MC}}^2.$$

If we write

$$S(\hat{\theta}_*) = T(\hat{\theta}_*) \{T(\hat{\theta}_*)^\top \hat{P}_{MC} T(\hat{\theta}_*)\}^{-1} T(\hat{\theta}_*)^\top$$

where $T(\hat{\theta}_*) = \theta_{1:M}^{1:2} \begin{pmatrix} \hat{\theta}_{*,\text{mat}} \\ -\frac{1}{2} I_{\frac{d^2+d}{2}} \end{pmatrix}$, a Monte Carlo draw for the test statistic is then given by

$$\frac{M - \frac{d^2+3d+2}{2}}{d} \left\{ \frac{\| \{I_{M-1} - S(\hat{\theta}_*) \hat{P}_{MC}\} \ell_{1:M,MC}^S \|_{\hat{P}_{MC}}^2}{(M-1)\hat{\sigma}_{2\text{nd},MC}^2} - 1 \right\}.$$

A Monte Carlo corrected p-value for the hypothesis test on θ_* can be found by using the empirical distribution of the replicated Monte Carlo draws in place of the $F_{d, M - \frac{d^2+3d+2}{2}}$ distribution in (29).

S7 Additional numerical results

S7.1 Additional figures for the gamma-Poisson example in Section 5.1

Here we provide additional figures for the gamma-Poisson example considered in Section 5.1. Figure S-1 shows the distributions of the p-value for the hypothesis test $H_0 : \lambda_{\text{MESLE}} = \lambda_{\text{MESLE},0}$, $H_1 : \lambda_{\text{MESLE}} \neq \lambda_{\text{MESLE},0}$ for varied null values $\lambda_{\text{MESLE},0}$. The distribution of the p-value when the null value $\lambda_{\text{MESLE},0}$ equals the exact MESLE is close to the uniform distribution, indicating that our estimation and uncertainty quantification method for the MESLE has little bias. The other two plots in Figure S-1 show that the p-values are skewed toward zero when the null value is not equal to the exact MESLE, indicating that the power is greater than the significance level.

Figure S-2 shows the distribution of the p-value for the test on the third order term in the Taylor expansion of $\mu(\theta; y_{1:n})$ mentioned at the end of Section 4. The distribution of the p-value is close to uniform, indicating that the quadratic approximation of $\mu(\theta; y_{1:n})$ was adequate. If the simulation points were taken from a wider range, this distribution would be skewed toward zero.

Figure S-3 shows the distributions of the p-values for hypothesis tests for the simulation-based proxy, $H_0 : \lambda_* = \lambda_{*,0}$, $H_1 : \lambda_* \neq \lambda_{*,0}$ for varied null values $\lambda_{*,0}$. The left plot shows that the proportion of the replications where the p-value is between 0 and 0.05 is somewhat greater than what would be expected under the uniform distribution, implying the presence of some bias in the test. For $\lambda_{*,0} = 0.9$, the p-values are skewed toward zero, indicating a reasonably high power. The empirical probability of rejecting the null hypothesis shown in Figure 5 was minimized at $\lambda_{*,0} = 1.025$. For this null value, the distribution of the p-value was close to uniform, as shown by the right plot of S-3. Although this implies a bias in estimating the true value of $\lambda_0 = 1$, the magnitude (≈ 0.025) is not large.

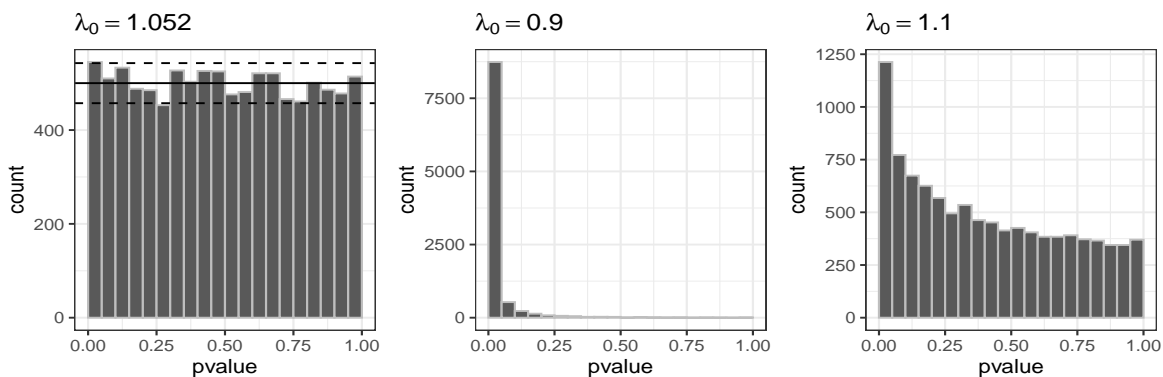


Figure S-1: The distribution of the p-value for the test on the MESLE for varied null values. The horizontal lines on the left plot show the expected counts under the uniform distribution (solid) and 95% confidence bounds (dashed).

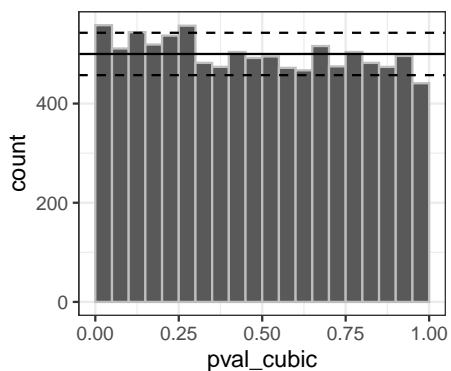


Figure S-2: The distribution of the p-value for the test on the cubic coefficient for the expected simulated log-likelihood.

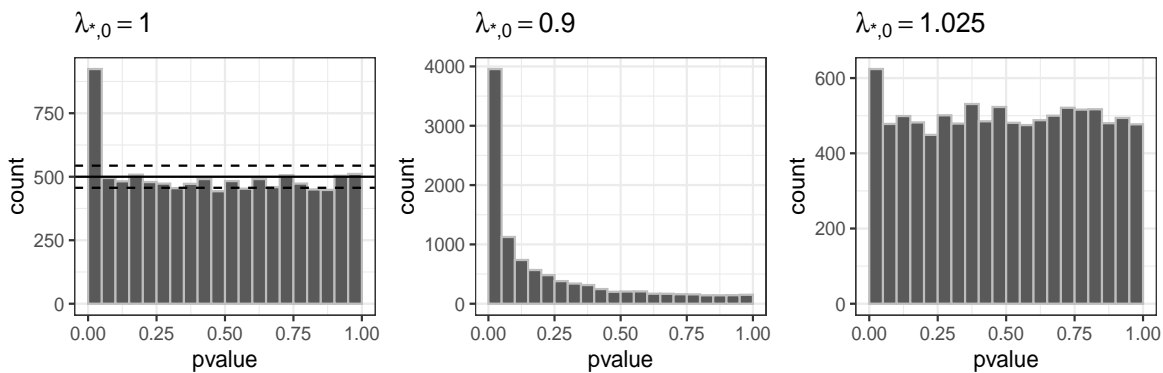


Figure S-3: Distribution of the p-values for the test on the simulation-based proxy λ_* for varied null values $\lambda_{*,0}$.

S7.2 Normal processes with normally distributed observations

Here we show numerical results for an example not considered in the main text. Example S2 describes a normal process $X_{1:n} \stackrel{iid}{\sim} \mathcal{N}(\theta, I_2)$ observed with $\mathcal{N}(0, I_2)$ -distributed noises. The mean parameter $\theta \in \mathbb{R}^2$ is estimated using simulations. We generated $n = 1000$ observations at $\theta_0 = (1, 1)$. The MESLE is given by the sample mean of observations, $\theta_{MESLE} = \bar{y} = \frac{1}{n} \sum_{i=1}^n y_i \in \mathbb{R}^2$. Simulations are carried out at $(\theta_1, \theta_2) = (1 \pm 0.02 \times k_1, 1 \pm 0.02 \times k_2)$ where $k_1, k_2 \in 0:10$.

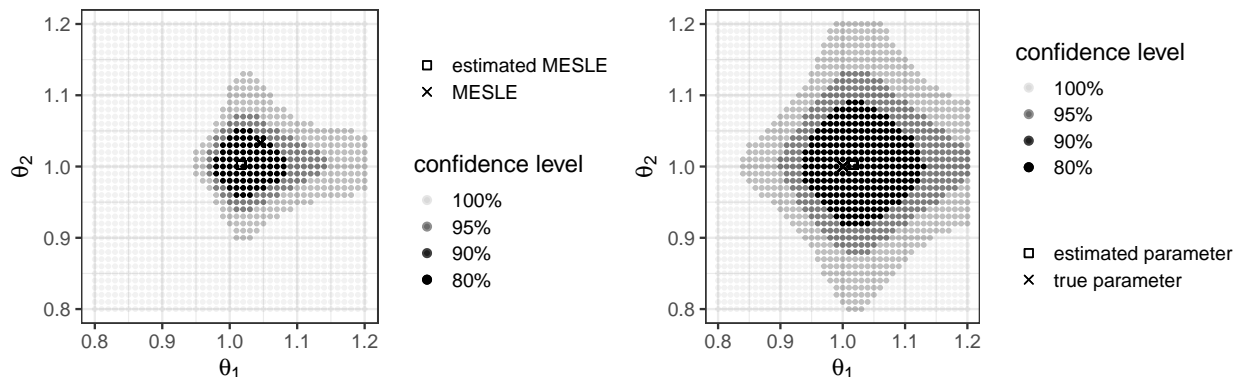


Figure S-4: Left: Constructed confidence regions for θ_{MESLE} . Right: Constructed confidence regions for θ_* .

Tests on the MESLE, $H_0 : \theta_{MESLE} = \theta_{MESLE,0}$, $H_1 : \theta_{MESLE} \neq \theta_{MESLE,0}$ were carried out. A $100(1-\alpha)\%$ confidence region for θ_{MESLE} can be obtained by collecting all null values for which the p-value is greater than α . The left plot in Figure S-4 shows the constructed confidence regions for θ_{MESLE} . Similarly, tests on the simulation-based parameter proxy $H_0 : \theta_* = \theta_{*,0}$, $H_1 : \theta_* \neq \theta_{*,0}$ were conducted, and confidence regions were constructed. The constructed confidence regions for θ_* are shown in the right plot of Figure S-4.

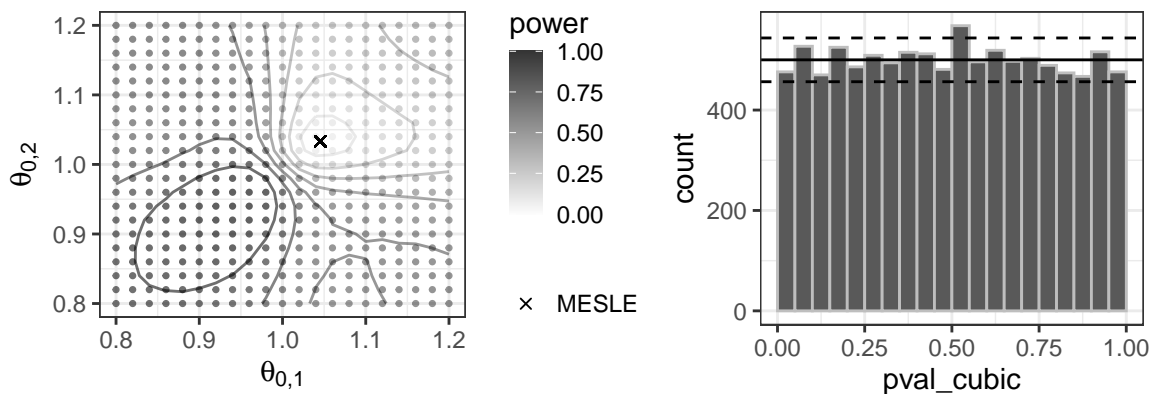


Figure S-5: Left: Probability of rejecting $H_0 : \theta_{MESLE} = \theta_{MESLE,0}$ at a 5% significance level, where the contours show the level sets. Right: Distribution of p-values for the test on the cubic coefficient for the expected simulated log-likelihood function.

We replicated hypothesis test $H_0 : \theta_{MESLE} = \theta_{MESLE,0}$ for varied null values 10000 times. The left plot of Figure S-5 shows the probabilities of rejecting the null hypothesis for varied null values $\theta_{MESLE,0}$. The right plot of Figure S-5 shows the distribution of the p-values for the test on significance of the third-order term in the Taylor expansion of $\mu(\theta)$. The distribution of the p-values for the cubic test is close to uniform, implying that the range of simulation points were suitably chosen.

We carried out hypothesis tests on the simulation-based proxy, which is the same as the true parameter value $\theta = (1, 1)$ for this example. For each of 10000 replications, a new set of observations were generated under $\theta = (1, 1)$. The distribution of the p-value under the true null hypothesis $H_0 : \theta_* = \theta_{*,0} = (1, 1)$ is

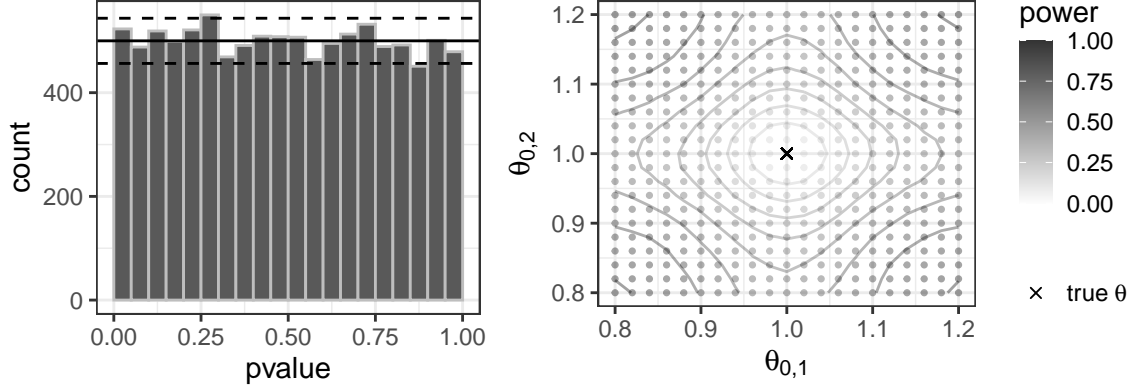


Figure S-6: Left: Distribution of the p-value for the test on the simulation-based proxy under a true null hypothesis, $H_0 : \theta_* = (1, 1)$. Right: Probability of rejecting the null hypothesis at a 5% significance level for varied null values. The contours show the level sets.

shown in the left plot of Figure S-6. The distribution was close to uniform, implying that our test had little bias. The estimated probabilities of rejecting the null hypotheses at a 5% significance level for varied null values are shown in the right plot of Figure S-6.

S7.3 Additional details and figures for the compartment model for the population dynamics of measles transmission in Section 5.3

We provide additional information about the SEIR model considered in Section 5.3 and additional numerical results. The population size at time t , $N(t)$, which is assumed to be known, is equal to the sum of $S(t)$, $E(t)$, $I(t)$, and $R(t)$, the compartment sizes at t . The compartment sizes evolve over time according to the stochastic equations (S32). The evolution of compartment sizes is described by the following stochastic equation:

$$\begin{aligned}
 dS(t) &= - \left\{ \left(\frac{R_0 s(t) (I(t) + \iota)^\alpha}{N(t)} + \mu \right) S(t) dt + dW_{SE}(t) + dW_{SD}(t) \right\} + db(t) \\
 dE(t) &= \left\{ \frac{R_0 s(t) (I + \iota)^\alpha}{N(t)} S(t) dt + dW_{SE}(t) \right\} - \{ (\gamma_{EI} + \mu) E(t) dt + dW_{EI}(t) + dW_{ED}(t) \} \\
 dI(t) &= \{ \gamma_{EI} dt + dW_{EI}(t) \} - \{ (\gamma_{IR} + \mu) I(t) dt + dW_{IR}(t) + dW_{ID}(t) \}.
 \end{aligned} \tag{S32}$$

Here $b(t)$ is the cumulative number of entry into the S compartment (i.e., births), R_0 the basic reproduction number, $s(t)$ the seasonal fluctuation of the transmission rate, ι the number of infectious individuals visiting the population, α a mixing parameter, which is close to the unity, μ the mortality rate, γ_{EI} and γ_{IR} the rates of progression from E to I and from I to R respectively, W_{**} the cumulative stochastic noises for transitions between compartments, where D signifies mortality. Each noise process $W_{**}(t)$ is modelled by a Poisson process subordinated by a gamma process, and its rate depends on the current compartment sizes. A fraction of cumulative transitions from I to R each week is assumed to be reported and recorded, with mean reporting rate ρ and inflated variance relative to the binomial distribution. The variation inflation parameter is denoted by ψ .

In addition to the basic reproduction number R_0 (Figure 8), we carried out parameter inference for α , a mixing parameter, and γ_{EI} and γ_{IR} the rates of progression from E to I and from I to R respectively. Partial observations of the compartment sizes are given by weekly reported case numbers, which are random fractions of weekly aggregate transitions from the infectious to the recovered compartment.

Unbiased likelihood estimate for the observed data sequence were obtained for varied parameters using the bootstrap particle filter via the R package `pomp`. The package vignette (<https://kingaa.github.io/pomp/vignettes/He2010.html>) describes steps for analyzing the observed data for London.

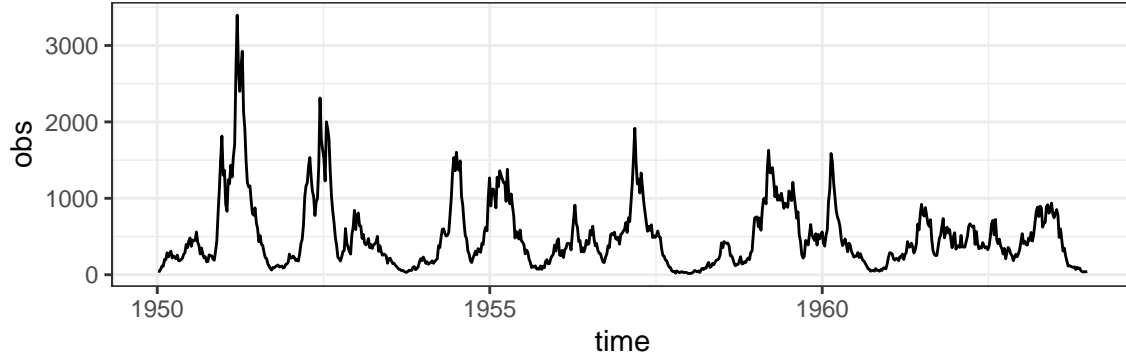


Figure S-7: A sequence of weekly reported measles cases generated by simulating the stochastic SEIR process for the chosen parameter vector.

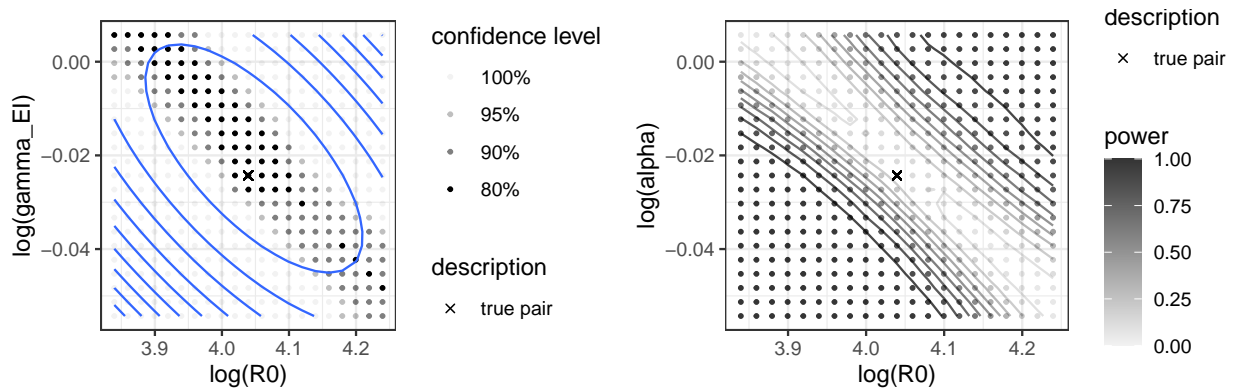


Figure S-8: Left: Constructed confidence regions for R_0 and α . The contours show the level sets of the estimated expected simulated log-likelihood, $\hat{\mu}(\theta; y_{1:n})$. Right: Probabilities of rejecting the null hypothesis for varying null values at a 5% significance level. The contours show the level sets of the estimated rejection probabilities.

We simulated the SEIR model at a suitably chosen parameter vector and generated a sequence of weekly reported cases data. Since all considered parameters had positivity constraints, they were estimated on the log scale. The left plot of Figure 8 shows the simulated log-likelihoods for varying $\log(R_0)$, and the constructed 90% and 95% confidence intervals. Simulations were carried out at $M = 100$ points uniformly placed between the exact value ± 0.1 on the log scale. We replicated hypothesis tests for R_0 1000 times. The right plot of Figure 8 shows the probability of rejecting the null hypothesis at a 5% significance level for varying null values for $\log(R_0)$. The power at the true parameter value, indicated by the vertical dashed line, is about 10%, which is somewhat higher than the significance level, implying that there is a bias in our hypothesis test method. However, the rejection probability is closest to the significance level near the true parameter value.

Next we carried out hypothesis tests for pairs of the parameters among R_0 , α , γ_{EI} , and γ_{IR} . The constructed two dimensional confidence regions visualize the joint parameter inference. We note that all two dimensional slices of the mean function $\mu(\theta; y_{1:n})$ fully describe the local dependence of $\mu(\theta; y_{1:n})$ on the four parameters, because the mean function in our metamodel is locally quadratic. The left plot of Figure S-8 shows the constructed 80%, 90%, and 95% confidence regions for R_0 and α by marking the points where the p-value was higher than 20%, 10%, and 5%, respectively for the test on the pair of simulation-based proxy. Simulations were carried out at $M = 400$ points uniformly placed on the rectangle centered at the true value pair and having widths 0.2 for $\log(R_0)$ and 0.03 for $\log(\alpha)$. The elliptic contours on the plot show the level sets of the estimated expected simulation log-likelihood, $\hat{\mu}(\theta; y_{1:n})$. The p-value for the test on the

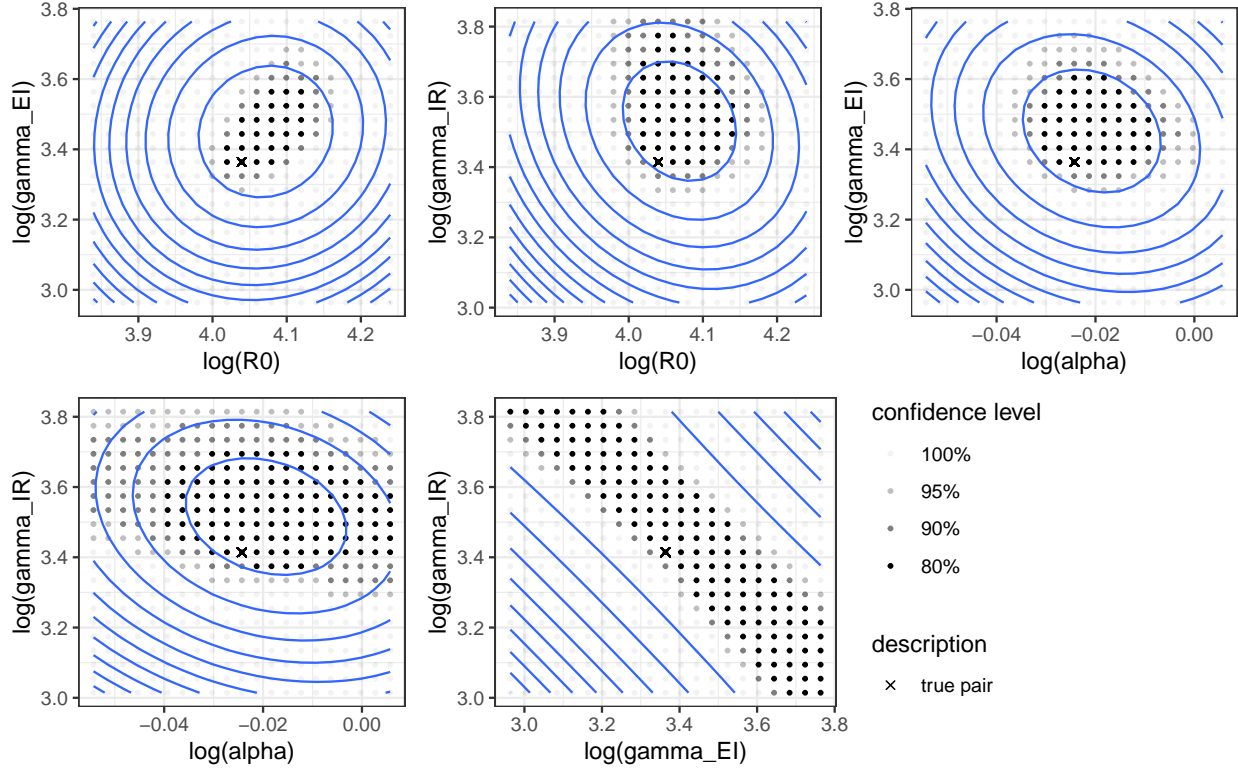


Figure S-9: Constructed confidence regions for pairs of parameters for the SEIR model. The contours show the level sets of the estimated expected simulated log-likelihood, $\hat{\mu}(\theta; y_{1:n})$.

significance of the cubic term in the expected simulated log-likelihood was 0.56, implying that the simulation points were appropriately chosen. These results show that R_0 and α are hardly identifiable jointly, unless a much longer observation sequence is analyzed. The statistical power could increase with more simulations (i.e., larger M) or with a greater range for simulation points. However, when we used simulation points from a wider range, the p-value for the test on the cubic coefficient in the mean function dropped close to zero, implying an increase in the bias in the test. Figure S-9 shows the constructed confidence regions for other pairs of parameters. These results show that all pairs except (α, R_0) and $(\gamma_{EI}, \gamma_{IR})$ can be jointly identified. The right plot of Figure S-8 shows the estimated probabilities of rejecting the null hypothesis for varying null values of the pair $\log(R_0)$ and $\log(\alpha)$ at a 5% significance level when the tests were repeated 1000 times.

S8 Additional information on Section 6

S8.1 Justification of the fact that the Monte Carlo standard error for pseudo-marginal MCMC is $\mathcal{O}((\log M)^{-1/4})$

We justify below the claim made in Section 6 that the standard error of the estimates obtained by pseudo-marginal MCMC scales as $\mathcal{O}((\log M)^{-1/4})$ where M is the length of the constructed Markov chain. Suppose that initial state of the chain is denoted by θ_1 and subsequent proposed values are denoted by $\theta_2, \dots, \theta_M$. For simplicity, we will suppose that the acceptance probability for θ' given a current state θ is approximately given by

$$\min \left(1, \frac{\hat{L}(\theta'; y_{1:n})}{\hat{L}(\theta; y_{1:n})} \right) = \exp[-\{\ell^S(\theta) - \ell^S(\theta')\}_+] \quad \text{where } a_+ := \max(a, 0)$$

by assuming that the log ratio $\left| \frac{h(\theta')_q(\theta|\theta')}{h(\theta)_q(\theta'|\theta)} \right|$ is small compared to the difference in ℓ^S . We suppose that $\ell^S(\theta) = \log \hat{L}(\theta; y_{1:n})$ is normally distributed such that we can write

$$\ell^S(\theta_m) = \mu(\theta_m) + \sigma Z_m, \quad Z_m \stackrel{iid}{\sim} \mathcal{N}(0, 1), \quad m \in 1:M$$

and that $\mu(\theta) = \text{const.} + (\theta - \theta_{MESLE})^\top c(\theta - \theta_{MESLE})$.

A candidate θ_m has a high chance to be accepted if $\mu(\theta_m) + \sigma Z_m$ is relatively large among other values. Denote the ordered simulation-based random variates Z_1, \dots, Z_M by $Z_{(1)} \geq Z_{(2)} \geq \dots \geq Z_{(M)}$ and the corresponding parameter values by $\theta_{(1)}, \dots, \theta_{(M)}$. In order to obtain an approximate lower bound on the Monte Carlo standard error for parameter estimator derived from pseudo-marginal MCMC, we consider the case where the second largest random error $\sigma Z_{(2)}$ is obtained at θ_{MESLE} —that is, we assume $\theta_{(2)} = \theta_{MESLE}$. The proposal $\theta_{(1)}$ will be accepted with probability one, provided that

$$\mu(\theta_{(1)}) + \sigma Z_{(1)} \geq \mu(\theta_{(2)}) + \sigma Z_{(2)},$$

or

$$Z_{(1)} - Z_{(2)} \geq \sigma^{-1} \{ \mu(\theta_{(2)}) - \mu(\theta_{(1)}) \} = \sigma^{-1} (\theta_{(1)} - \theta_{(2)})^\top c(\theta_{(1)} - \theta_{(2)}). \quad (\text{S33})$$

Denoting the cdf for the standard normal distribution by $\Phi(x)$, we use the result

$$1 - \Phi(x) = \frac{1}{\sqrt{2\pi}} \left(\frac{1}{x} + O\left(\frac{1}{x^3}\right) \right) e^{-x^2/2} \quad (\text{S34})$$

[1]. For $0 < \epsilon < 1$, denote by x_ϵ the value satisfying $1 - \Phi(x_\epsilon) = \epsilon$. We approximate $Z_{(1)}$ by $x_{1/M}$ and $Z_{(2)}$ by $x_{2/M}$. Using (S34), we can approximate

$$Z_{(1)} \approx x_{1/M} \approx \sqrt{W\left(\frac{M^2}{2\pi}\right)}, \quad Z_{(2)} \approx x_{2/M} \approx \sqrt{W\left(\frac{M^2}{8\pi}\right)}$$

where $W(t)$ is the Lambert W function satisfying $W(t) \exp\{W(t)\} = t$ [13]. Since $W(t) = \log t - \log \log t + O(\log \log t / \log t)$ for large t [8], we approximate

$$\begin{aligned} Z_{(1)} - Z_{(2)} &\approx \sqrt{W\left(\frac{M^2}{2\pi}\right)} - \sqrt{W\left(\frac{M^2}{8\pi}\right)} \approx \sqrt{2 \log M - \log 2\pi} - \sqrt{2 \log M - \log 8\pi} \\ &\approx \sqrt{2 \log M} \left\{ 1 - \frac{\log 2\pi}{4 \log M} - \left(1 - \frac{\log 8\pi}{4 \log M} \right) \right\} = O((\log M)^{-1/2}). \end{aligned}$$

Hence, from (S33) we have

$$\|\theta_{(1)} - \theta_{MESLE}\| = \|c\|^{-1/2} \sigma^{1/2} (\log(M))^{-1/4} = O((\log M)^{-1/4}).$$

S8.2 Justification of the fact that the variance of Equation 35 scales as $O(k/\log J)$

When the likelihood is estimated using the particle filter with J particles, Equation S8.2 in Section 6 shows that ℓ_i^S can be approximated as

$$\ell_i^S \approx \max_{j \in 1:J} \log g_i(y_i | X_i^j) - \log J,$$

provided that the dimension k of y_i is at least moderately large. In this section, we numerically demonstrate that the variance of ℓ_i^S scales as $O(k/\log J)$, given that $\log g_i(y_i | X_i^j)$ is approximately normally distributed. This normality assumption is reasonable if $\log g_i(y_i | X_i^j)$ is given by the sum of the log measurement densities for the k components of y_i .

Figure S-10 shows the inverse of the variance of $\max_{j \in 1:J} Z_j$, where Z_j are iid standard normal random variables. This result shows that $\text{Var}(\max_{j \in 1:J} Z_j)$ scales inversely proportional to $\log J$. Thus, given that the variance of $\log g_i(y_i | X_i^j)$ increases linearly with k , the variance of ℓ_i^S scales as $O(k/\log J)$.

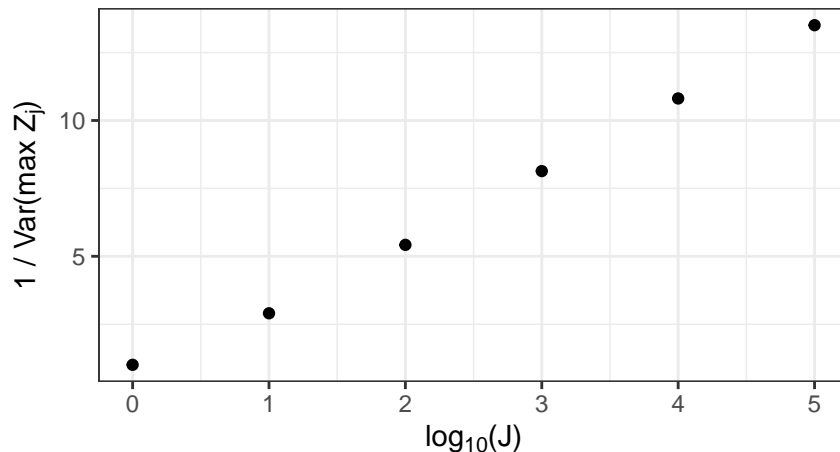


Figure S-10: The inverse of the variance of $\max_{j \in 1:J} Z_j$ for J varying across 1, 10, 10^2 , 10^3 , 10^4 , and 10^5 .

S9 Additional information on Section 7

S9.1 Additional information on Section 7.1

Section 7.1 introduces an algorithm that automatically adjusts the weights of the simulation points for bias reduction. This algorithm aims balance using as many points as possible for efficient parameter estimation with narrowing the range of parameter values used for simulation to ensure that quadratic approximation introduces little bias. The weights are adjusted by multiplying a discount factor given by

$$\exp\left(-\frac{q_2(\hat{\theta}_{MESLE}) - q_2(\theta)}{g}\right)$$

for parameter value θ . However, the value of g can sometimes decrease to a point where there are insufficient effective number of simulation points for parameter estimation. In order for cubic regression to be numerically stable, the effective sample size (ESS) should satisfy

$$\text{ESS} := \frac{(\sum_{m=1}^M w_m^{adj})^2}{\sum_{m=1}^M w_m^{adj^2}} \gtrsim \frac{(d+1)(d+2)(d+3)}{6}, \quad (\text{S35})$$

where $(d+1)(d+2)(d+3)/6$ is the total number of scalar parameters being estimated in cubic regression (d is the dimension of the parameter vector). If this condition is not satisfied, g is increased to a level where the ESS grows above the required threshold. Note that the effective sample size defined in (S35) differs from the ESS defined in (33) in Section 6 to compare the efficiency of our method with that of pseudo-marginal MCMC. Algorithm 1 summarizes the modified procedure taking into account the ESS for weight adjustments.

In the `sbim` package, adding the option `autoAdjust=TRUE` in the functions `ht()` and `ci()` enables automatic weight adjustments as described in Algorithm 1.

S9.2 Additional information on Section 7.2

Section 7.2 introduces an algorithm that proposes the next simulation point by minimizing the Monte Carlo variation in parameter estimation (Algorithm 5). Suppose that a new simulation is carried out at θ_{M+1} and that \hat{A}_{M+1} denotes the coefficients of the new quadratic polynomial fitted to $(\theta_m, \ell^S(\theta_m))$ with weights w_m^{adj} , $m \in 1:M+1$, where the adjusted weight for the new point is given by

$$w_{M+1}^{adj} = w_{M+1} \cdot \exp\left(-\frac{(\hat{b}^\top \hat{\theta}_{MESLE} + \hat{\theta}_{MESLE}^\top \hat{c} \hat{\theta}_{MESLE}) - (\hat{b}^\top \theta_{M+1} + \theta_{M+1}^\top \hat{c} \theta_{M+1})}{g}\right).$$

Algorithm 1 Automatic weight adjustments for bias reduction (with the consideration of effective sample size)

```

1: Fit a quadratic polynomial to  $(\theta_m, \ell^S(\theta_m))$  with weights  $w_m, m \in 1 : M$ , to obtain a first-stage quadratic
   approximation  $q_2(\theta) = \hat{a} + \hat{b}^\top \theta + \theta^\top \hat{c} \theta$ 
2: Let  $\hat{\theta}_{MESLE} = -\frac{1}{2} \hat{c}^{-1} \hat{b} = \arg \max_{\theta} q_2(\theta)$  be the estimated MESLE
3: Let  $g \leftarrow \infty$ 
4: Let ExitUponSufficientESS  $\leftarrow$  FALSE
5: loop
6:   Weight adjustments:  $w_m^{adj} = w_m \cdot \exp(-\{q_2(\hat{\theta}_{MESLE}) - q_2(\theta_m)\}/g)$ 
7:   Compute effective sample size:  $ESS = (\sum_{m=1}^M w_m^{adj})^2 / (\sum_{m=1}^M w_m^{adj^2})$ 
8:   if  $ESS < (d+1)(d+2)(d+3)/6$  then ▷ numerically instable cubic regression
9:     Let ExitUponSufficientESS  $\leftarrow$  TRUE
10:    Let  $g \leftarrow 1.5g$ 
11:    Go to the next iteration
12:  end if
13:  if ExitUponSufficientESS then
14:    Break from loop
15:  end if
16:  Update  $q_2$  and  $\hat{\theta}_{MESLE}$  using the adjusted weights
17:  Fit a cubic polynomial to  $(\theta_m, \ell^S(\theta_m))$  with weights  $w_m^{adj}, m \in 1 : M$ 
18:  Let  $p_{cubic}$  be the p-value for the significance of the cubic term
19:  if  $p_{cubic} < 0.01$  then ▷ cubic term is significant, decrease  $g$ 
20:    if  $g = \infty$  then
21:      Let  $g \leftarrow q_2(\hat{\theta}_{MESLE}) - \min_{m \in 1 : M} q_2(\theta_m)$ 
22:    else
23:      Let  $g \leftarrow g/1.8$ 
24:    end if
25:  else if  $p_{cubic} > 0.3$  then ▷ cubic term is not significant, increase  $g$  for efficiency
26:    Let  $g \leftarrow 1.3 \cdot g$ 
27:  else
28:    Break from loop
29:  end if
30: end loop

```

The value of g is determined using Algorithm 4. The variance of these updated set of coefficients is given by

$$\text{Var}(\hat{A}_{M+1}) = \sigma^2 \{ \theta_{1:M}^{0:2 \top} W^{adj} \theta_{1:M}^{0:2} + w_{M+1}^{adj} \theta_{M+1}^{0:2} \theta_{M+1}^{0:2 \top} \}^{-1}.$$

After the addition of the $(M+1)$ th simulation point, the Monte Carlo variance of the estimated MESLE is approximated by $\sigma^2 V_{M+1}(\theta_{M+1})$, where

$$V_{M+1}(\theta_{M+1}) := \left(\frac{\partial \hat{\theta}_{MESLE}}{\partial \hat{A}} \right) \{ \theta_{1:M}^{0:2 \top} W^{adj} \theta_{1:M}^{0:2} + w_{M+1}^{adj} \theta_{M+1}^{0:2} \theta_{M+1}^{0:2 \top} \}^{-1} \left(\frac{\partial \hat{\theta}_{MESLE}}{\partial \hat{A}} \right)^\top.$$

Since

$$\frac{\partial \hat{\theta}_{MESLE}}{\partial \hat{A}} = -\frac{1}{2} \frac{\partial \hat{c}^{-1} \hat{b}}{\partial (\hat{a}, \hat{b}, \text{vech}(\hat{c}))}$$

only depends on \hat{b} and \hat{c} , the matrix V_{M+1} depends on θ_{M+1} only through the middle term. In order to quantify the total amount of Monte Carlo variation in the parameter estimate, we consider a scaled total variation (STV) measure defined by

$$\text{STV}(\theta_{M+1}) := \text{Tr}\{-\hat{c}^{-1} V_{M+1}(\theta_{M+1})\}$$

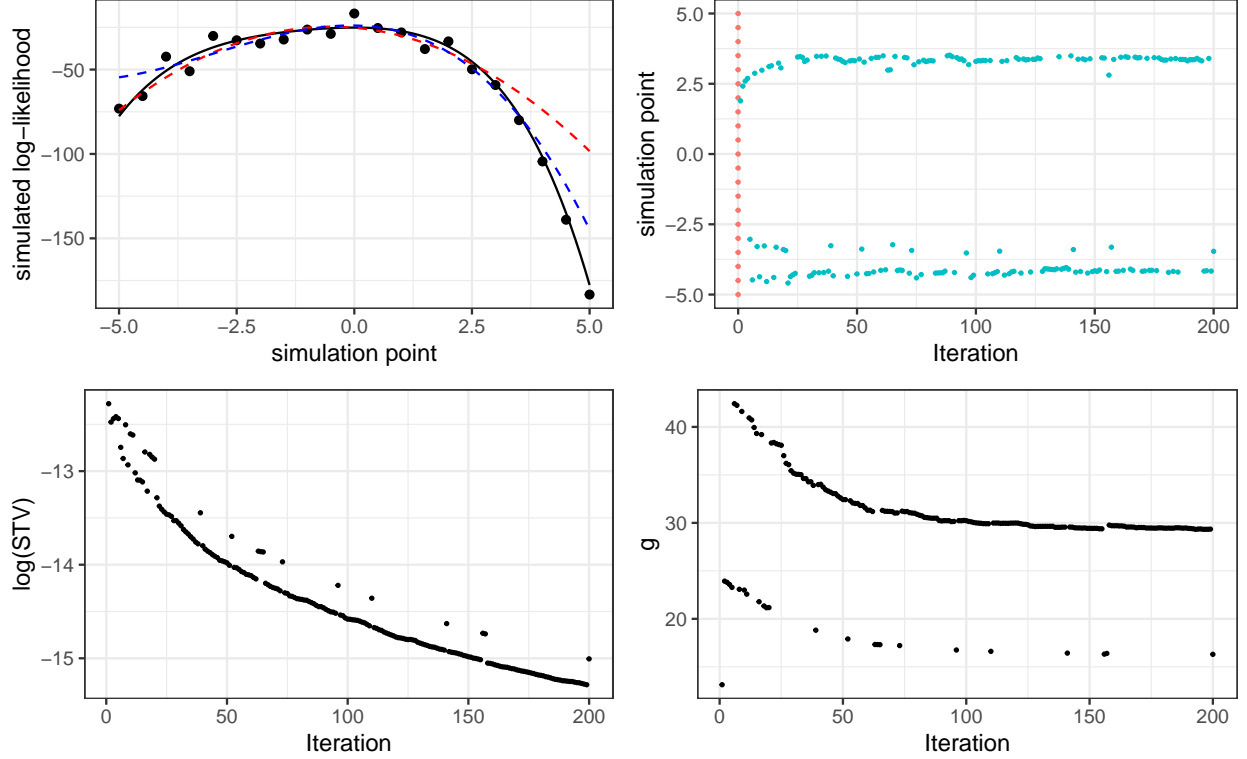


Figure S-11: Top left: Simulated log-likelihoods for initial points for Example S7. The black curve indicates the expected simulation log-likelihood function, $\mu(\theta)$. The red and blue dashed curves show the fitted quadratic and cubic polynomials, respectively. Top right: Simulation points iteratively proposed by Algorithm 5. The initial simulation points are indicated by red dots. Bottom left: Logarithms of scaled total variation (STV) over iterations. Bottom right: Tuned values of g over iterations.

where $-\hat{c}$ is the curvature of the fitted quadratic function before the addition of the new simulation point. The multiplication by $-\hat{c}^{-1}$ ensures that the estimation scales of the parameter components are taken into account when summing the Monte Carlo variances.

The optimization of STV can be rapidly performed using the Broyden–Fletcher–Goldfarb–Shanno (BFGS) algorithm, which uses the gradients of the objective function [7]. Writing

$$\Omega = \theta_{1:M}^{0:2 \top} W^{adj} \theta_{1:M}^{0:2} + w_{M+1}^{adj} \theta_{M+1}^{0:2} \theta_{M+1}^{0:2 \top},$$

we can express the derivative of STV with respect to the i -th component of θ_{M+1} by

$$\frac{\partial \text{STV}}{\partial \theta_{M+1,(i)}} = \text{Tr} \left\{ \hat{c}^{-1} \left(\frac{\partial \hat{\theta}_{\text{MESLE}}}{\partial \hat{A}} \right) \Omega^{-1} \frac{\partial \Omega}{\partial \theta_{M+1,(i)}} \Omega^{-1} \left(\frac{\partial \hat{\theta}_{\text{MESLE}}}{\partial \hat{A}} \right)^\top \right\}$$

where

$$\frac{\partial \Omega}{\partial \theta_{M+1,(i)}} = w_{M+1}^{adj} g^{-1} (\hat{b} + 2\hat{c}\theta_{M+1})_{(i)} \theta_{M+1}^{0:2} \theta_{M+1}^{0:2 \top} + w_{M+1}^{adj} \frac{\partial \theta_{M+1}^{0:2}}{\partial \theta_{M+1,(i)}} \theta_{M+1}^{0:2 \top} + w_{M+1}^{adj} \theta_{M+1}^{0:2} \frac{\partial \theta_{M+1}^{0:2 \top}}{\partial \theta_{M+1,(i)}}.$$

Example S7. We generate simulated log-likelihoods from an artificial metamodel

$$\ell^S(\theta) = -(\theta - 0.2)^2 + \min(4, 0.2 \times \theta^3) - 0.1 \times (\theta + 1)^4 + \mathcal{N}(0, \sigma^2), \quad \theta \in \mathbb{R}$$

with $\sigma = 5$. Initially, simulations are carried out regular intervals of 0.5 over the range $[-5, 5]$.

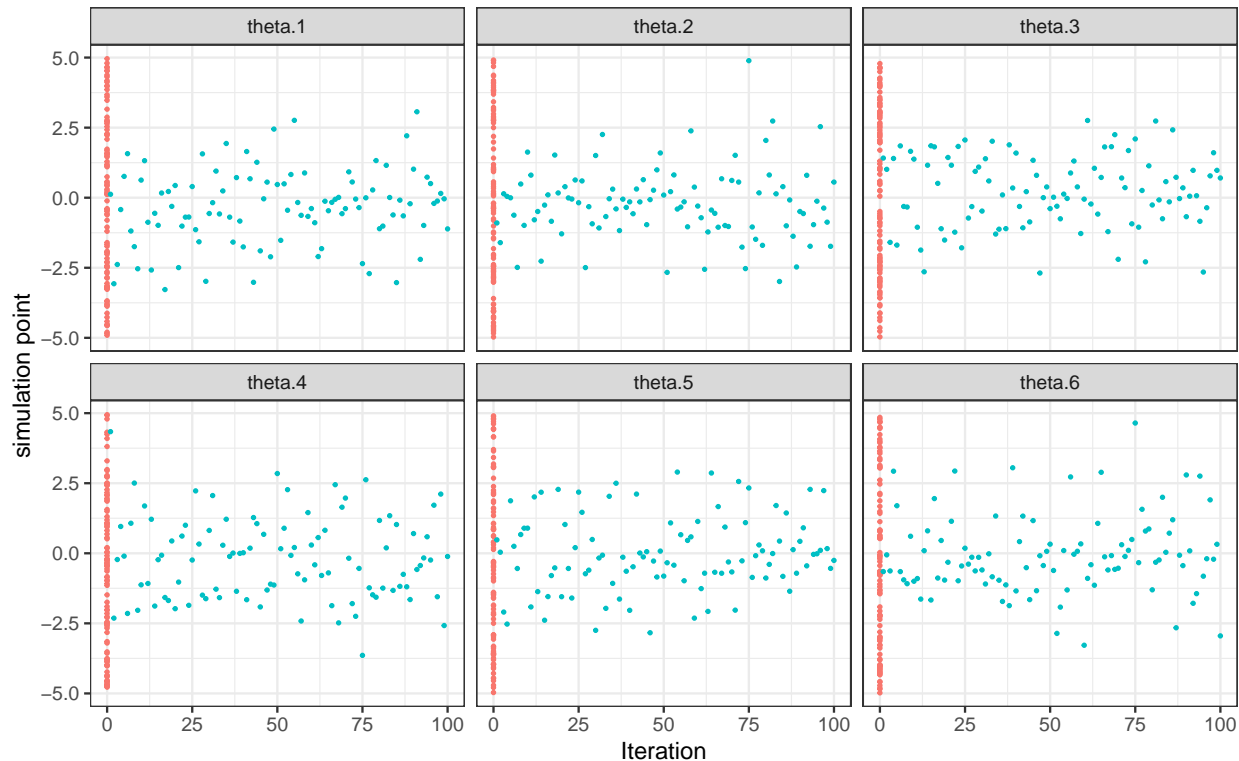


Figure S-12: Proposed simulation points for each of the $d = 6$ components for Example S8 using Algorithm 5. Red dots indicate the initial simulation points.

The simulated log-likelihoods for these initial points are shown in the top left plot of Figure S-11. The quadratic approximation (red dashed curve) deviates significantly from the cubic approximation (blue dashed curve) for $|\theta| \gtrsim 3$. The top right plot of Figure S-11 displays the proposed simulation points after Algorithm 5 is applied iteratively two hundred times. The proposed points alternate between two values, approximately -3 and 3. These results suggest that near-optimal points tend to be positioned as far as possible from the estimated MESLE while still ensuring sufficient accuracy in the quadratic approximation. Optimization of $\log(\text{STV})$ was carried out using the automatically tuned value for g . However, for comparison across iterations, the bottom left plot of Figure S-11 shows $\log(\text{STV})$ values evaluated at the proposed points using a fixed value of $g = 20$. These STV values generally decrease, indicating that the algorithm effectively reduces uncertainty in parameter estimation. Occasionally, STV takes a relative large values, which is due to the small tuned values for g in those instances. The tuned values of g are shown in the bottom right panel of Figure S-11. The fact that g consistently drops suggests that as more simulation points are added, the cubic term becomes increasingly significant. Consequently, to preserve the fidelity of the quadratic approximation, the effective range of parameter values for inference shrinks.

We next considered a metamodel with a six-dimensional parameter space.

Example S8. Simulated log-likelihoods are generated from a metamodel

$$\ell^S(\theta) = -(\theta - \theta_0)^\top c(\theta - \theta_0) - 0.1 \times \sum_{i=1}^6 \theta_{(i)}^4 + \mathcal{N}(0, \sigma^2).$$

Here θ_0 is a random draw from $\mathcal{N}(0, 0.5^2 I_6)$, $c = U\Lambda U^\top$ where U is a random draw from $SO(6)$ and Λ is a diagonal matrix with diagonal entries independently drawn from $\text{Uniform}(0,1)$, and $\sigma = 5$. Simulated log-likelihoods are initially obtained at one hundred randomly selected points θ_m with $\theta_{m,(i)} \stackrel{iid}{\sim} \text{Uniform}(-5, 5)$. Subsequent simulation points are proposed using Algorithm 5 with fixed weight adjustment parameter $g = 20$.

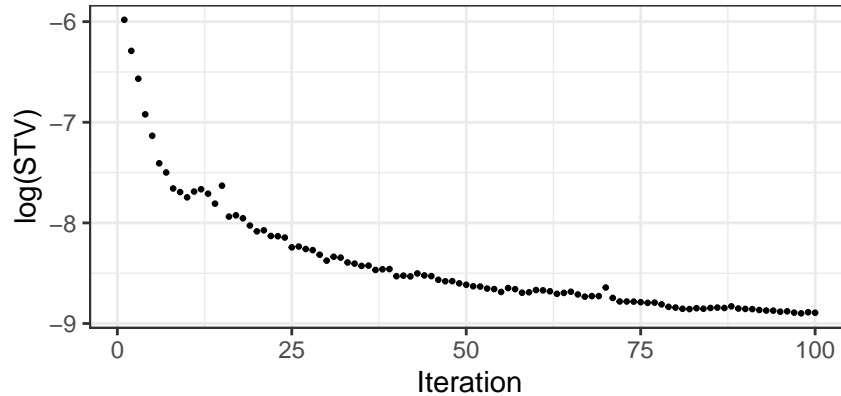


Figure S-13: Logarithms of STV at the proposed points for Example S8.

Figure S-12 shows the iteratively proposed simulation points. At each iteration, the optimization started from a randomly selected point, with each entry independently drawn from $\text{Uniform}(-5, 5)$. All six entries of the proposed points approximately fall between -2.5 and 2.5 . We repeated this experiment using starting points whose entries were randomly drawn from $\text{Uniform}(-1, 1)$. The proposed points exhibited the same pattern, with a similar range of $[-2.5, 2.5]$ (figure not shown). These results suggest that the simulation points are the minimizers of $\log(\text{STV})$ and are largely independent of the initial values used for optimization. Figure S-13 shows the $\log(\text{STV})$ values at the proposed points. The decreasing values of $\log(\text{STV})$ indicate that Algorithm 5 successfully selects points for efficient parameter estimation.

Supplementary References

- [1] M. Abramowitz and I. A. Stegun. *Handbook of Mathematical Functions with Formulas, Graphs, and Mathematical Tables. National Bureau of Standards Applied Mathematics Series 55. Tenth Printing.* National Bureau of Standards (DOC), Washington, D.C., 1972.
- [2] A. Agresti. *Foundations of linear and generalized linear models.* John Wiley & Sons, 2015.
- [3] L. V. Ahlfors. *Complex analysis.* McGraw-Hill, second edition, 1966.
- [4] J. Bérard, P. Del Moral, and A. Doucet. A lognormal central limit theorem for particle approximations of normalizing constants. *Electron. J. Probab.*, 19(94):1–28, 2014.
- [5] K. L. Chung. *A course in probability theory.* Academic press, third edition, 2001.
- [6] P. Doukhan, P. Massart, and E. Rio. The functional central limit theorem for strongly mixing processes. *Ann. Inst. Henri Poincaré Probab. Stat.*, 30(1):63–82, 1994.
- [7] R. Fletcher. *Practical methods of optimization.* John Wiley & Sons, second edition, 1987.
- [8] A. Hoorfar and M. Hassani. Inequalities on the lambert w function and hyperpower function. *J. Inequal. Pure and Appl. Math.*, 9(2):5–9, 2008.
- [9] M. Kendall and A. Stuart. *The advanced theory of statistics. Vol. 1: Distribution theory.* MacMillan Publishing, New York, 4th edition, 1977.
- [10] T.-T. Lu and S.-H. Shiou. Inverses of 2×2 block matrices. *Comput. Math. Appl.*, 43(1-2):119–129, 2002.
- [11] E. Lukacs. *Characteristic functions, Griffin's Statistical Monographs & Courses, No. 5.* Griffin: London, 1960.

- [12] K. P. Murphy. *Machine learning: a probabilistic perspective*. MIT press, 2012.
- [13] E. W. Weisstein. Lambert w-function. From MathWorld—A Wolfram Web Resource, 2024. Last visited on 5/21/2024.
- [14] M. A. Woodbury. Inverting modified matrices. Statistical Research Group, Memo. Rep., no. 42, Princeton University, Princeton, N. J., 1950.
- [15] A. Zellner. Bayesian and non-Bayesian analysis of the regression model with multivariate student-t error terms. *J. Amer. Statist. Assoc.*, 71(354):400–405, 1976.